Research in Conservation

1989

5

Glen R. Cass
James R. Druzik
Daniel Grosjean
William W. Nazaroff
Paul M. Whitmore
Cynthia L Wittman

Protection of Works of Art From Atmospheric Ozone

THE GETTY CONSERVATION INSTITUTE

Protection of Works of Art From Atmospheric Ozone

Research in Conservation

1989

5

Glen R. Cass
James R. Druzik
Daniel Grosjean
William W. Nazaroff
Paul M. Whitmore
Cynthia L Wittman

Protection of Works of Art From Atmospheric Ozone

THE GETTY CONSERVATION INSTITUTE

Printed in the United States of America.

Library of Congress Cataloging-in-Publication Data

Protection of works of art from atmospheric ozone.

(Research in Conservation; 5)
Includes bibliographical references.
1. Painting—Deterioration. 2. Painting—Effect of atmospheric ozone on. 3. Painting—Conservation and restoration. I. Cass, Glen Rowan. II. Series.
ND1638.P7 1989 751.6'2 89-16985
ISBN 0-89236-126-3

The Getty Conservation Institute

The Getty Conservation Institute (GCI), an operating Program of the J. Paul Getty Trust, was created in 1982 to enhance the quality of conservation practice in the world today. Based on the belief that the best approach to conservation is interdisciplinary, the Institute brings together the knowledge of conservators, scientists, and art historians. Through a combination of in-house activities and collaborative ventures with other organizations, the Institute plays a catalytic role that contributes substantially to the conservation of our cultural heritage. The Institute aims to further scientific research, to increase conservation training opportunities, and to strengthen communication among specialists.

Research in Conservation

This reference series is born from the concern and efforts of the Getty Conservation Institute to publish and make available the findings of research conducted by the GCI and its individual and institutional research partners, as well as state-of-the-art reviews of conservation literature. Each volume will cover a separate topic of current interest and concern to conservators.

Contents

The Authors

Glen R. Cass

Glen R. Cass received his Ph.D. in environmental engineering in 1978 from the California Institute of Technology, where he is presently Associate Professor of Environmental Engineering. Current research interests center on control of air pollution problems, including the problem of protection of works of art from damage due to atmospheric ozone.

James R. Druzik

James R. Druzik has a Bachelor's degree in chemistry and is currently a Conservation Scientist at the Getty Conservation Institute, where he coordinates extramural research. His research interests have related to all aspects of the museum environment, but center on the characterization and control of museum air pollution and materials damage. He and Dr. Cass have been research collaborators since 1982.

Daniel Grosjean

Daniel Grosjean holds a Ph.D. in physical organic chemistry and is currently president of DGA, a research-oriented environmental consulting company in Ventura, California, which he founded in 1983. Since 1979 he has also held an appointment as Visiting Associate, Department of Chemical Engineering, California Institute of Technology. Research interests include experimental studies in atmospheric chemistry and art conservation chemistry, with emphasis on reactive organic compounds.

William W. Nazaroff

William W. Nazaroff received his Ph.D. in environmental engineering science at the California Institute of Technology. He is currently Assistant Professor of Civil Engineering, University of California at Berkeley. He is interested in the experimental and theoretical aspects of indoor air quality, including the behavior of small particles, photo-oxidants, and control of radon exposure indoors.

Paul M. Whitmore

Paul M. Whitmore received his Ph.D. in physical chemistry from the University of California at Berkeley in 1982. In 1984 he joined the staff of the Environmental Quality Laboratory at the California Institute of Technology, and in 1986 he became Assistant Conservation Scientist at the Center for Conservation and Technical Studies, Harvard University Art Museums. Currently he is director of the Research Center on the Materials of the Artist and Conservator, Mellon Institute, Pittsburgh.

Cynthia Wittman

Cynthia Wittman received a Bachelor's degree in chemistry from Caltech in 1988. She is currently pursuing graduate studies in chemical research.

Foreword

This report, "Protection of Works of Art from Atmospheric Ozone," is the first in a planned series of reports on various aspects of the Getty Conservation Institute's research in environmental issues in museums. In order to put this research in context, I would like to outline the overall environmental program of the Scientific Program of the GCI.

The control of the environment in buildings that house cultural collections has long been recognized as the best measure to insure the preservation of the objects in our care. Addressing this concern, Gary Thomson's book *The Museum Environment* has become one of the best-sellers in the museum field; many museums have implemented recommendations in this book and in other professional literature. Nonetheless, HVAC (heating, ventilation, and air conditioning) systems with air purification units are still found in only a small fraction of museums worldwide, and levels of illumination also frequently exceed internationally recommended levels. For the former, costs of installation, operation, and maintenance are often prohibitive; for the latter, architectural and other display considerations are often overriding factors. The concerns of the conservators in this area are sometimes considered to be exaggerated, and the scientific literature does not provide enough information about the environmentally caused deterioration of all the different materials encountered in today's museums and collections.

In 1984, having recognized that many problems still remained to be addressed, the Scientific Program of the GCI embarked on a major program of environmental research within the museum shell. Considering the magnitude of this undertaking and the variety of expertise and technology required, it was decided to contract major areas to various research groups and to undertake only part of the research in the GCI laboratories. The following areas were identified as requiring attention: outdoor-generated air pollution infiltrating collections, indoor-generated air pollution from construction materials and consumer products, and microenvironmental studies that deal with all nonpollution issues.

In the microenvironment the targeted issues are: humidity control and monitoring, low-cost sealed display cases, storage and display under inert gas atmospheres, microbiological and insect control, and selected issues in exhibition lighting. In separate but related areas,

research in environmental engineering and energy conservation within the HVAC plant is being conducted.

The air pollution research, regardless of source or origin, was subdivided into: (1) surveys of pollutant concentrations in buildings containing cultural and natural history collections, including discussions of pollutant fate over time, (2) assessments of potential materials damage and estimations of potential long-term risks, and (3) monitoring and control strategies.

Museum surveys are accompanied by simultaneous outdoor measurements and a full recording of the specifics of the building and its ventilation strategy. Mathematical models have been developed for the indoor-outdoor relationship of pollutants found in photochemical smog and for airborne particulates. Surveys of the following outdoor- and indoor-generated air pollutants are now complete, in progress, or in the planning stages: ozone (O_3), peroxyacetyl nitrate (PAN), nitrogen oxides (NO, NO_2), nitric acid (HNO_3), hydrochloric acid (HCl), chloro-hydrocarbons (Cl-HC), carbonyls (R_2O), carboxylic acids (RCO_2H), hydrogen sulfide (H_2S), sulfur dioxide (SO_2), total reduced sulfur (TRS), soil dust, sulfates, nitrates, and elemental and organic carbon. Some of these pollutants were included not because they pose a documented risk to collections, but because either they fit into a chemical series with other species having known materials effects, or evidence exists for damage to objects outdoors and indoor concentrations are unknown.

It is an impossible task to measure the potential for damage of all pollutants to all types of materials encountered in the world's museums within a reasonable time. Therefore a selection of the specific substrates to be studied had to be made. The following substrates have been or are being studied, or are under consideration for future research: organic colorants on paper and silk for ozone, organic colorants on paper and deacidified papers for nitrogen oxides and sulfur dioxide, metals for carbonyls and carboxylic acids, organic colorants for nitric acid, and metals for hydrogen sulfide. Expanding this matrix is under consideration. It is felt, however, that these materials are encountered so frequently in all types of museums that they can serve as representative examples of the risks to which our collections are exposed (e.g., the effects on natural organic colorants on paper can also suggest probable effects on some textile dyes, and paper is an appropriate model for all cellulose- and lignin-based materials).

Most museums, libraries, and collections cannot afford the expense of sophisticated air quality measurements in their buildings, nor the installation, operation, and maintenance of high-technology air-handling systems. Therefore a project was initiated aiming at the devel-

opment of simple, low-cost, yet sensitive and selective monitors for the major pollutants. The first target is formaldehyde, a widely found indoor-generated pollutant. As far as control measures are concerned, an attempt is being made to provide museums and collections with a variety of solutions in terms of cost and control efficiency. In addition to the mitigation measures described in this report, another project in progress deals with the use of sorbents to remove pollutants from display cases.

The results of these projects are being published in scientific and conservation journals, in the GCI publication series *Research in Conservation,* and as limited-distribution GCI reports. A more detailed report on GCFs overall environmental research program, its findings to date, and its future goals is available from the GCI.

The following report on ozone is a summary of the full 284-page report of the Environmental Quality Laboratory, California Institute of Technology, Pasadena (see Cass et al. 1988), on this three-year project. The results have also been published or submitted for publication in the form of 11 papers in the literature. The executive-summary format has been chosen to provide museum professionals, collectors, architects, and administrators with essential information that can be absorbed without specialized scientific training. For those interested in the specific technical and scientific details, the full report is available from the authors or the GCI. The journal articles are referenced in this report (Drisko et al. 1985/86, Whitmore et al. 1987, Whitmore and Cass 1988, Grosjean et al. 1987, Grosjean et al. 1988a, 1988b, 1989, Whitmore and Cass 1989, Nazaroff and Cass 1988, Druzik et al. 1989, Wittman et al. 1989, Cass et al. 1989). The chapter on mathematical modeling of indoor pollutant concentration, briefly described in Chapter 4 of this report, has been appended unabridged from the original report since it constitutes one of the major findings and is a valuable tool for the planning of ventilation systems for buildings.

Frank D. Preusser
Program Director, Scientific Research
Getty Conservation Institute

Chapter I Ozone and the Fading of Artists' Pigments

Introduction

Air pollution has been suspected as a possible cause of damage to museum collections for at least one hundred years. As early as 1888, concern over pollution in the London atmosphere led to a systematic investigation of whether direct exposure to the combustion exhaust from a burning gas jet would cause artists' pigments to fade (Brommelle 1964). Since that time, a number of studies have examined the effects of sulfur oxides air pollutants on leather, paper, calcareous stone, textiles, and a few pigments (Baer and Banks 1985). Much less has been said about the effects of photochemically generated air pollutants such as ozone, which is found in Los Angeles, Athens, and other cities that experience intense solar radiation in the presence of high pollutant emission densities.

Ozone (O_3) is one of the most powerful oxidants found in nature. High levels of atmospheric ozone in outdoor urban atmospheres are known to be caused by the combined interaction of sunlight, oxygen, oxides of nitrogen, and hydrocarbons (Seinfeld 1975). Many effects of ozone on materials have been reviewed by Jaffe (1967) and by the Committee on Preservation of Historical Records (under the National Research Council 1986), and ozone-caused damage has been reported for rubber (Newton 1945), exterior paint binders (Campbell et al. 1974), and textile fibers (Kerr et al. 1969). Ozone attack on cellulose has been investigated by Katai and Schuerch (1966). Within the textile industry, ozone has been implicated in the fading of anthraquinone dyes on nylon and cellulose acetate (Salvin and Walker 1955, Salvin 1969, Beloin 1973, Lebensaft and Salvin 1972, Haylock and Rush 1976).

In the early 1980s, a pilot study was conducted to determine whether artists' pigments were affected by exposure to ozone at the concentrations found in urban atmospheres. In the first exploratory test, seventeen artists' watercolor pigment samples and two Japanese woodblock prints were exposed to 0.40 ppm ozone in a controlled test chamber for three months (Shaver et al. 1983). A second study followed in which the ozone-fastness of 27 modern organic watercolor pigments was examined (Drisko et al. 1985/86). It was found that several pigments applied on paper faded in the absence of light when exposed to an atmosphere containing ozone at the concentrations found in photochemical smog. Alizarin-based watercolors containing 1,2-dihydroxyanthraquinone lake pigments were shown to be particularly sensitive to ozone

damage, as were the yellow pigments used in the Japanese woodblock prints tested. Indoor-outdoor ozone measurements made at that time in an art gallery in Pasadena, California, confirmed that ozone concentrations half as high as those outdoors can be found in art galleries that lack a chemically protected air conditioning system. The identification of ozone-sensitive artists' pigments together with the existence of high ozone levels inside at least one museum argued that further investigation was warranted of the hazard to works of art posed by exposure to photochemically generated air pollutants.

Objectives and Approach

The objective of the present research is to provide a comprehensive assessment of the effect of ozone on the fading of artists' pigments and to determine methods to protect works of art from damage due to atmospheric ozone. In Chapter 2 of this research summary, the ozone-induced fading of traditional natural organic artists' pigments is described, based on pigment samples obtained from the Forbes collection at Harvard and elsewhere. In Chapter 3 the mechanisms of the ozone reaction with alizarin lakes, indigos, curcumin, and the triphenylmethanes are discussed based on gas chromatographic/mass spectrometric analysis of the ozone-colorant reaction products. It is shown that the reaction products observed during the exposure experiments are consistent with ozone-caused destruction of the colorants.

Whether photochemical oxidants pose a hazard by fading works of art depends in part on whether the high concentrations of O_3 and NO_2 found in outdoor air are transferred to the indoor atmospheres of museums and galleries. In Chapter 4 of this summary, a mathematical model is described that predicts the concentration of chemically reactive air pollutants in indoor air based on outdoor pollutant levels and building design variables. This model was tested by application to the Virginia Steele Scott Gallery of the Huntington Library in San Marino, California. Close agreement was found between computed and observed indoor O_3 and NO_2 levels. A survey of indoor/outdoor ozone concentration relationships in eleven museums, galleries, historical society houses, and libraries in Southern California is also presented. Advice is offered on how to estimate ozone concentrations in untested buildings, based on analogy to the various buildings and ventilation system types studied here.

The protection of works of art from damage due to atmospheric ozone is discussed in Chapter 5. Several categories of control measures are evaluated using laboratory and field experiments, including:

a. eliminating pollutants from indoor atmospheres by redesigning building ventilation systems
b. constructing display cases to protect the works
c. framing paintings, prints, and watercolors behind glass
d. using ozone-resistant pigments
e. applying binders or coatings, when appropriate, to protect the pigments

While advanced air purification systems indeed can be used to protect museum collections from ozone damage, a number of inexpensive protective measures are also identified that are quite effective.

The present report serves as a summary of the major findings of this research effort and is written as an index to the contents of the complete project final report (Cass et al. 1988).

Chapter 2

Ozone Fading of Natural Organic Colorants

In order to assess the effect of atmospheric ozone on the colorfastness of traditional organic colorants, a controlled laboratory exposure experiment was conducted. More than 50 samples of traditional natural organic pigments from the Forbes collection at Harvard and elsewhere were applied to watercolor paper and then exposed to 0.40 ppm ozone at 22 °C and 50% RH, in the absence of light, for twelve weeks. This ozone concentration is typical of that found in the Los Angeles atmosphere during a heavy smog episode, and the total ozone dose delivered to the samples is equivalent to about four years of exposure to outdoor air in Los Angeles, or to about eight years inside a typical air conditioned building in that city (Shaver et al. 1983). The complete list of the natural organic colorants tested is shown in Table 2.1, along with the Color Index designation for each. Also shown are the number of examples of each colorant tested. These multiple samples represent various shades, manufacturers, or dates of manufacture for a single coloring agent.

The ozone exposure apparatus used is illustrated in Figure 2.1. A dry airstream was pumped at a rate of 2.5 1pm through a series of filters to remove existing pollutants. The airstream then was split in half. One half of the flow was saturated with water vapor while the other dry airstream was irradiated by ultraviolet light from mercury vapor lamps housed in commercial ozone generators (Ultra Violet Products SOG-2). The ozonated air and humidified air were mixed and then admitted to the exposure chamber through a perforated Teflon tube. The ozone concentration inside the chamber was measured continuously with a UV photometric ozone monitor (Dasibi, model 1003 AH), and a computer interfaced to the ozone monitor automatically collected and stored the hourly average ozone concentrations during the course of the exposure.

Color changes that occurred as a result of the ozone exposure experiment were quantified in several ways. Diffuse reflectance spectra were measured at intervals during the experiment using a Diano Match-Scan II reflectance spectrophotometer. Chromaticity coordinates and color differences (using the CIE 1976 L*a*b* formula) were calculated for the CIE Illuminant C (Billmeyer and Saltzman 1981). Munsell color notations were subsequently calculated from these chromaticity coordinates (American Society for Testing and Materials 1980).

Table 2.1. Traditional natural organic colorants tested. Also shown are the Color Index designations and the number of examples of each colorant.

Colorant	Color Index Designation	Number of Samples Tested
Weld Lake	Natural Yellow 2	1
Curcumin	Natural Yellow 3	1
Saffron	Natural Yellow 6	5
Quercitron Lake	Natural Yellow 9	2
Persian Berries Lake	Natural Yellow 14	3
Gamboge	Natural Yellow 24	5
Cochineal Lake	Natural Red 4	4
Madder Lake	Natural Red 9	13
Lac Lake	Natural Red 25	6
Litmus	Natural Red 28	1
Dragon's Blood	Natural Red 31	2
Indigo	Natural Blue 1	6
Van Dyke Brown	Natural Brown 8	1
Sepia	Natural Brown 9	1
Bitumen	Natural Black 6	3
Indian Yellow	None	2

Figure 2.1. Ozone exposure apparatus.

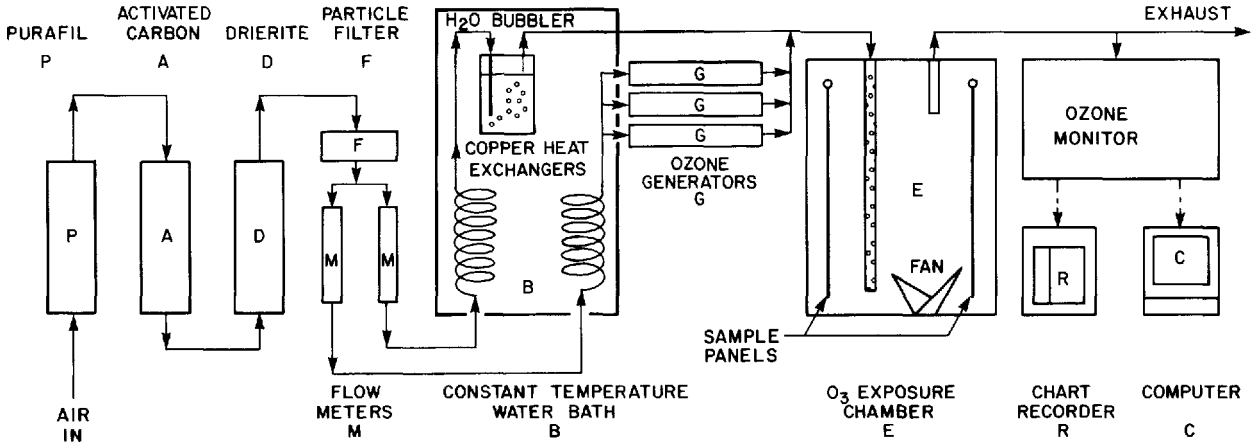

Almost all of the organic colorants tested showed some fading after ozone exposure. This ozone-induced fading can be quantified in several ways. Figure 2.2 shows the change in the reflectance spectrum of indigo on paper during 12 weeks of exposure to 0.40 ppm ozone. As the colorant is consumed by reaction with ozone, the reflectance of the sample increases, and the sample fades from its initial bluish-gray appearance toward a lighter shade of gray. A single parameter that represents the total color difference between samples before and after the ozone exposure experiments can be calculated from these reflectance spectra. In this work the CIE 1976 L*a*b* formula was used to determine the color difference, ΔE, of a colorant system before and after a given ozone dose, thus providing an approximate indicator of the magnitude or extent of the total color change caused by ozone reaction. (On average, a ΔE value less than 0.5 is not perceptible, and a ΔE value less than 1 is usually considered a good color match.) A color difference of $\Delta E = 14.20$ was calculated between the unexposed indigo/paper sample shown in Figure 2.2 before the experiment, versus the condition of the same sample at the end of the 12-week exposure. Clearly, indigo applied on watercolor paper fades severely when exposed to atmospheric ozone under conditions similar to those of this experiment.

Ozone-induced fading such as that seen for indigo is in fact a general property of most of the traditional natural organic colorants tested. As seen in Figure 2.3, the majority of the pigments tested faded perceptibly during the course of the experiments. Curcumin, dragon's blood, indigo, and madder lake are found to be very ozone fugitive, changing by $\Delta E > 9$ after 12 weeks at 0.40 ppm ozone. Lac lake, Persian berries lake, saffron, cochineal lake, bitumen, gamboge, and weld lake are reactive with ozone, having faded by between $\Delta E = 3$-8 over the 12 week experiment. Indian yellow, litmus, and quercitron lake fall in a borderline category, where slight fading in the range $\Delta E = 1$-3 was observed. Van Dyke brown and sepia showed no definite color change over the 12 weeks and thus appear to be more stable than is true for the other colorants.

Figure 2.2. Reflectance spectrum of the indigo/ paper system at several stages during its exposure to 0.40 ppm ozone at 22 °C, 50% RH, in the absence of light.

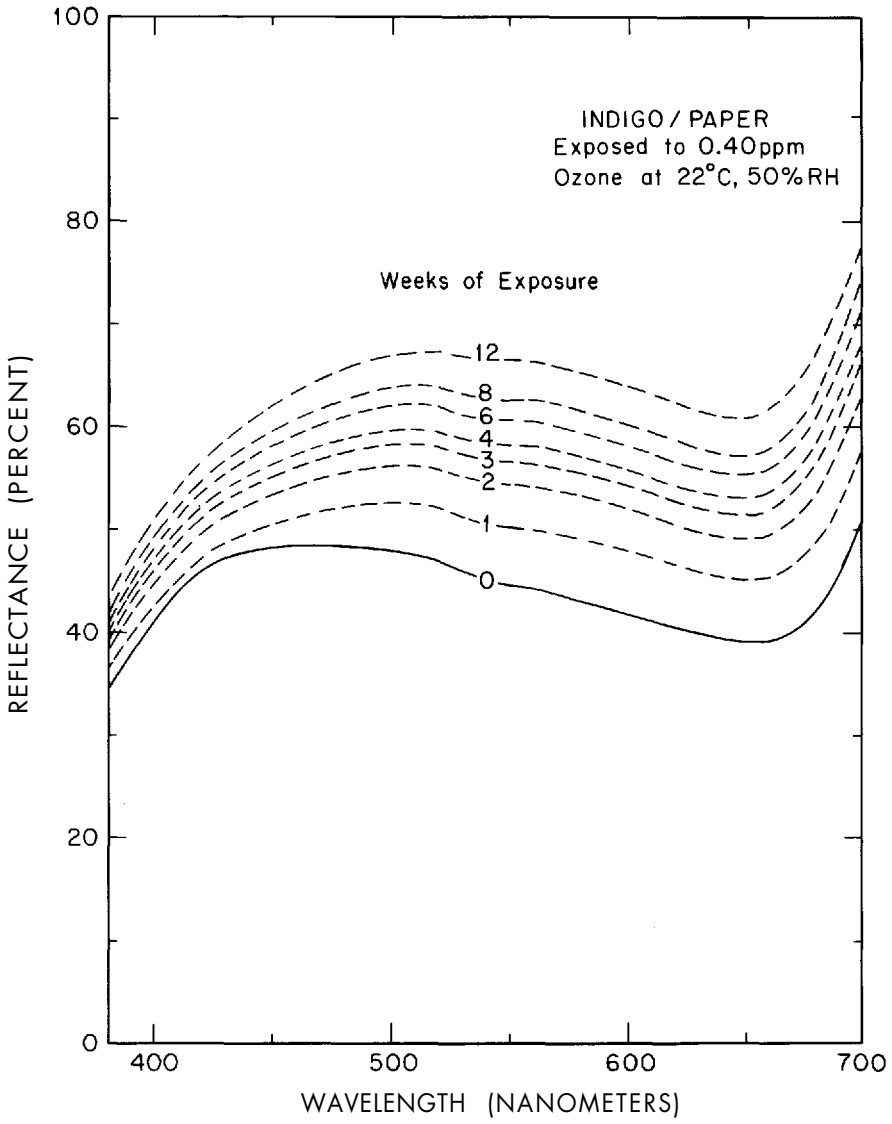

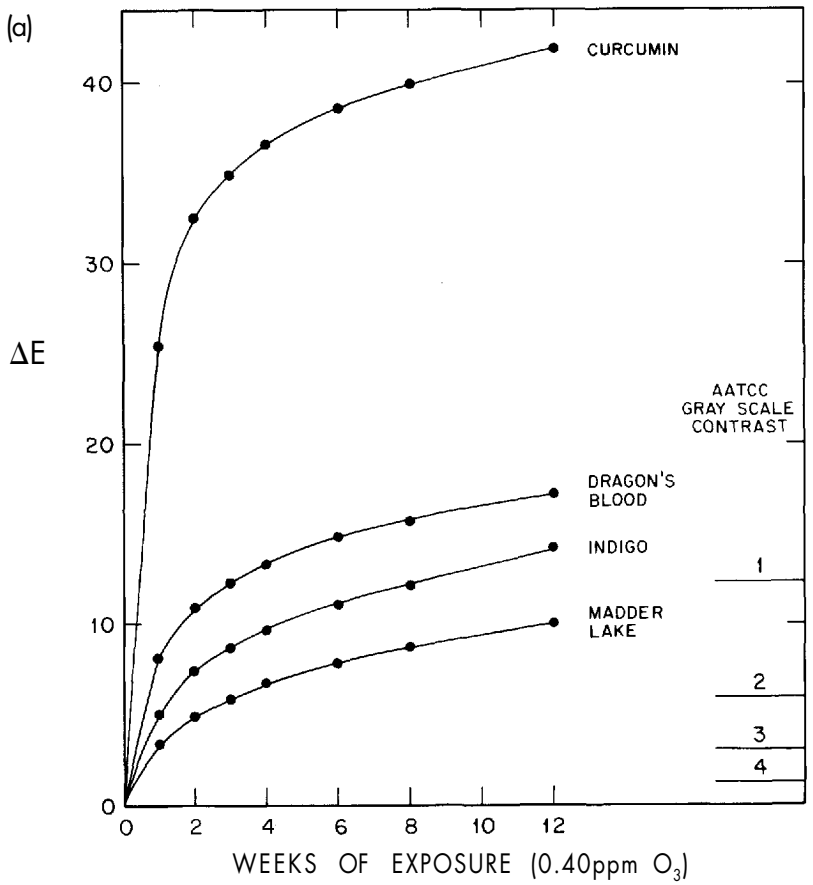

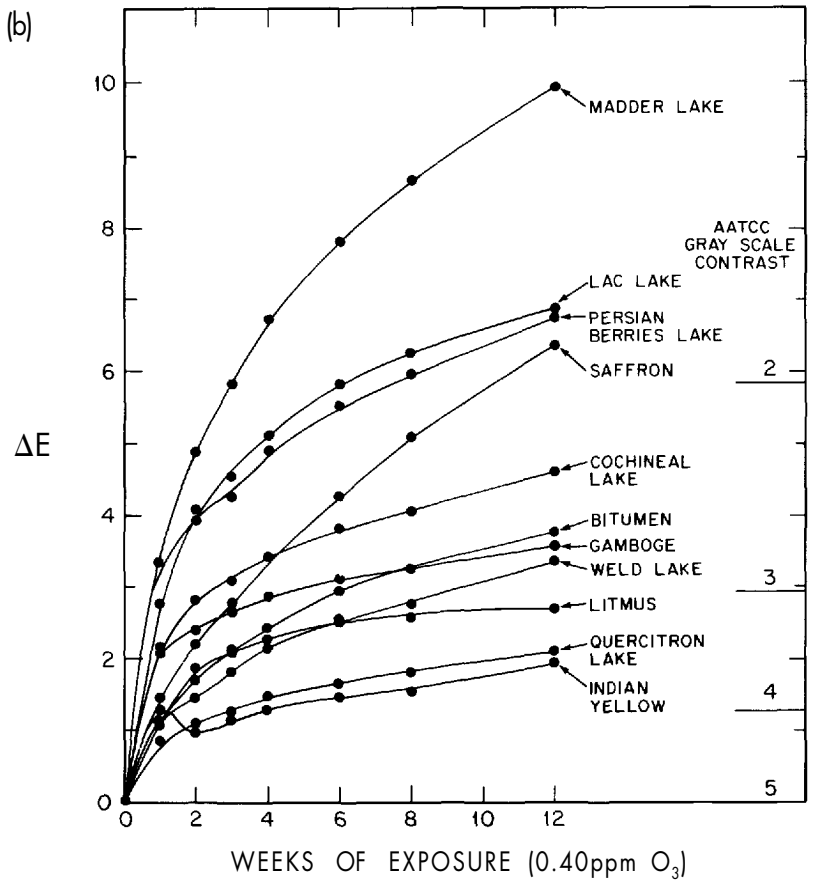

Figure 2.3. Plot of the observed color changes of natural colorant/ paper systems during exposure to 0.40 ppm ozone at 22 °C, 50% RH, in the absence of light. Color differences, ΔE, were calculated for CIE Illuminant C using the CIE 1976 L*a*b* equation. Measured color differences for the AATCC Gray Scale are also indicated for reference. Color changes are shown for (a) very reactive, and (b) moderately reactive colorant systems (note different scales for vertical axes).

The colorfastness of several traditional Japanese colorants upon exposure to atmospheric ozone also was tested in an identical chamber-exposure experiment. Samples, in the form of colorants applied to paper, dyes on silk cloth, and colorants on a nineteenth-century Japanese woodblock print were exposed to an atmosphere containing 0.40 ppm ozone at 22 °C and 50% RH, in the absence of light, for 12 weeks. Color differences, calculated from the measured diffuse reflectance spectra, were used to assess the rate and extent of the ozone fading. Of the colorants applied to paper, orpiment was the only inorganic pigment that showed severe color loss after ozone exposure. Several organic colorants on paper also reacted, including the widely used plant colorants *ai* (indigo) and *ukon* (turmeric). The woodblock print, produced using the plant-derived colorants *beni* (safflower), *ai* (indigo), *shio* (gamboge), and *aigami* (dayflower) showed significant ozone fading only in the blue and green areas, both of which contain *ai.* The Japanese dyed silk cloths included in this experiment are described in Table 2.2. These cloths differed both in mordant and in depth of shade. Because of this, the exposure of these textiles to ozone, rather than providing a measure of the relative ozone sensitivities of the colorants, should be viewed only as a survey of the fading hazard for this type of material.

Table 2.3 shows the color changes for the Japanese dyed silk cloths that faded to a measurable extent upon exposure to ozone. Not surprisingly, among the textiles that reacted were those dyed with *ai* (indigo), alone or in combination with one of the yellow plant dyes. Also showing evidence of ozone-caused fading were the purple *shikon,* the red-orange *akane,* and several yellow plant dyes. Although some of these color changes were relatively slight, and the color differences for materials not listed in Table 2.3 were even smaller ($\Delta E < 2$), these results nevertheless suggest that prolonged exposure of traditional Japanese dyed textiles to atmospheric ozone presents a risk of damage to their colorants.

It is concluded that a large number of traditional organic artists' pigments, if applied without protective binders and coatings, will fade when exposed to an atmosphere containing ozone. The same is true of many Japanese silk cloths that have been dyed by traditional methods. The total ozone dose administered to the samples in these experiments is equivalent to that which would be encountered within about four years outdoors or about eight years in a typical air-conditioned indoor environment. The results of this exposure study suggest that the risk of ozone damage to a wide range of works of art and artifacts is significant, and that protection of these objects from prolonged ozone exposure would be a prudent precaution.

Table 2.2. Natural colorant/mordant combinations for silk cloths tested.

Color	Natural dye	Mordant
Yellow	*Enju* (Japanese pagoda tree)	Al
	Kariyasu (Anthroxon hispidus)	Al
	Kariyasu (Anthraxon hispidus)	Cu
	Kihada (Japanese yellow wood)	Al
	Kuchi nashi (Jasmine)	Al
	Ukon (Turmeric)	Al
	Ukon (Turmeric)	Acetic acid
	Woren (Coptis joponica)	None
	Yamahaji (Rhus succedanea)	Al
	Yoma-momo (Myrico rubra)	Al
	Zumi (Malus toringo)	Al
	Shio (Orpiment, As_2S_3)	None
Red	*Seiyo akane* (Western madder)	Al
	Akane (Japanese madder)	Al
	Enji (Cochineal)	Sn
	Shiko (Lac)	Al
	Suo (Caesalpinia soppon L.)	Al
	Beni (Safflower)	None
Blue	*Ai* (Indigo)	None
Green	*Ai + enju*	Al
	Ai + kariyasu	Al
	Ai + kihada	Al
Violet	*Shikon (Lithospermum)*	Al

Table 2.3. Observed color change of dyed silk cloths under CIE Illuminant C after exposure to 0.40 ppm ozone.[a] Munsell notation (hue, value/chroma) calculated from tristimulus values.

Dye/mordant	Weeks of Exposure	X	Y	Z	Munsell	ΔE
Akone/Al	0	26.15	29.68	15.21	2.0YR6.0/7.6	
	12	40.82	34.38	18.33	2.7YR6.4/7.3	4.36
Al	0	7.37	7.22	16.93	5.1PB3.1/4.7	
	12	8.70	8.76	20.08	4.1PB3.4/5.0	3.78
Ai + enju/Al	0	29.25	34.84	12.95	3.0GY6.4/6.6	
	12	32.92	38.64	14.03	2.6GY6.7/6.9	4.11
Ai + kariyasu/Al	0	9.19	10.99	11.73	6.7G3.8/2.4	
	12	12.08	14.68	13.78	2.3G4.4/2.9	7.74
Ai + kihada/Al	0	11.89	14.38	8.16	5.6GY4.3/4.0	
	12	17.45	20.62	9.10	3.1GY5.1/5.0	12.95
Shikon/Al	0	9.23	8.01	12.75	7.3P3.3/2.8	
	12	12.25	10.76	16.69	7.5P3.8/3.0	5.17
Kuchinashi/Al	0	31.27	28.76	5.81	0.1Y5.9/9.2	
	12	34.97	32.14	6.04	0.1Y6.2/9.8	4.98
Yamohaji/Al	0	45.80	46.01	26.44	2.2Y7.2/4.8	
	12	48.87	49.21	28.65	2.3Y7.4/4.8	2.06
Yama-momo/Al	0	30.79	30.60	19.00	1.4Y6.0/3.9	
	12	33.51	33.24	21.05	1.1Y6.3/3.9	2.21
Zumi/Al	0	37.87	37.89	16.42	2.6Y6.6/6.0	
	12	40.87	41.10	18.27	2.8Y6.9/6.0	2.40

a. All dyed cloth samples listed in Table 2.2 were tested. Results are given here only for those samples showing a noticeable color change (ΔE > 2) after ozone exposure.

Chapter 3

Ozone as the Cause of Observed Fading Phenomena

As a result of the chamber ozone exposure experiments described in Chapter 2 and the findings of Shaver et al. (1983) and Drisko et al. (1985/86), several families of artists' colorants were identified as being particularly ozone-sensitive. Four colorant families were selected for detailed examination to confirm that the chemical reaction products of the ozone-colorant interaction were indeed consistent with ozone being the cause of the observed fading phenomena.

The colorants alizarin, alizarin crimson (a calcium-aluminum lake pigment), indigo, dibromoindigo, colorants containing thioindigo and tetrachlorothioindigo, curcumin (l,7-bis(4-hydroxy-3-methoxy-phenyl)-l,6-heptadiene-3,5-dione), the triphenylmethane cationic dye Basic Violet 14, and other closely related compounds were deposited on silica gel, cellulose, and Teflon substrates and exposed in the dark to ozone in purified air (~0.4 ppm O_3 for 95 days and ~10 ppm O_3 for 18-80 hours). Exposed and control samples were analyzed by mass spectrometry.

In all cases, the reaction products observed were consistent with the proposition that reaction with ozone is indeed the cause of the observed fading. Alizarin crimson reacted with ozone on all substrates, yielding phthalic acid (major product), benzoic acid (minor product), and other unidentified products. Important substrate-specific effects were observed, with alizarin dye on silica gel and the alizarin lake pigment samples being far more reactive toward ozone than alizarin dye deposited on cellulose, Teflon, or watercolor paper. A chemical mechanism responsible for the fading of these alizarin-related colorants by ozone is suggested in Figure 3.1, which is consistent with the products' distribution, the observed reactivity sequence, and the observed substrate-specific effects. Under the conditions employed, indigo and dibromo-indigo were entirely consumed; the major reaction products were isatin and isatoic anhydride from indigo and bromoisatin and bromoisatoic anhydride from dibromoindigo. The mechanism of the ozone reaction with indigo is shown in Figure 3.2. Thioindigo and its chloro-derivative also reacted with ozone, though at a slower rate; the corresponding substituted isatins and anhydrides were tentatively identified as reaction products. The major products of the ozone-curcumin reaction shown in Figure 3.3 included vanillin (4-hydroxy-3-methoxy benzaldehyde) and vanillic acid (4-hydroxy-3-methoxy benzoic acid). Basic Violet 14 reacted

to form methyldiaminobenzophenone and other products, as shown in Figure 3.4.

These products and the corresponding loss of chromophore (i.e., fading) are consistent with a reaction mechanism involving electrophilic addition of ozone onto the olefinic bonds of the indigos, curcumin, and triphenylmethane-derived colorants studied. At least in the case of dibromoindigo, the ozone-indigo reaction products are distinctly different from those produced by the light-induced fading of the same colorant (Hibbert 1927, Weber 1933).

Figure 3.1. Reaction of ozone with the 9,10-dihydroxy tautomeric form of alizarin.

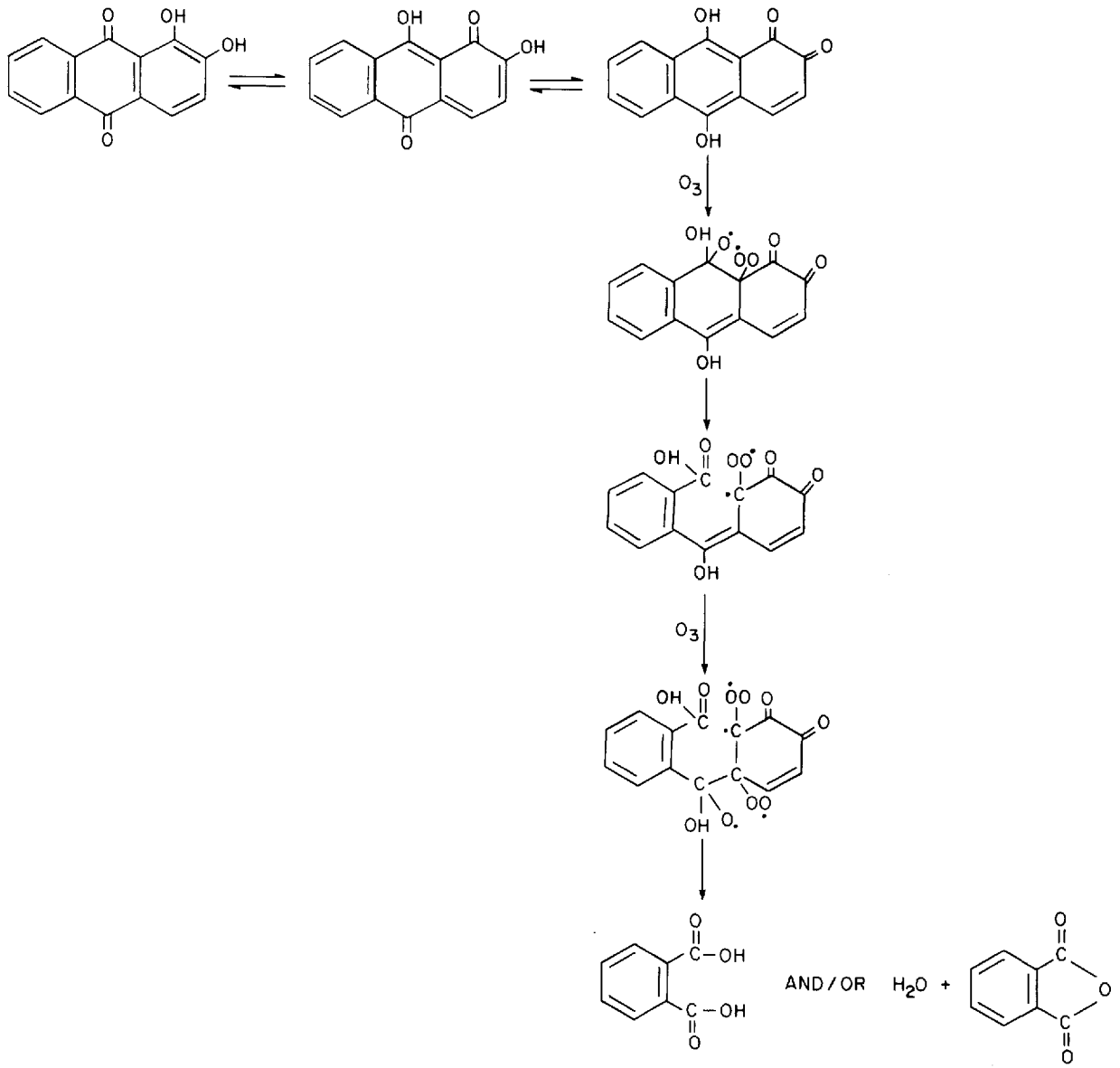

Figure 3.2. Mechanism of the ozone-indigo reaction.

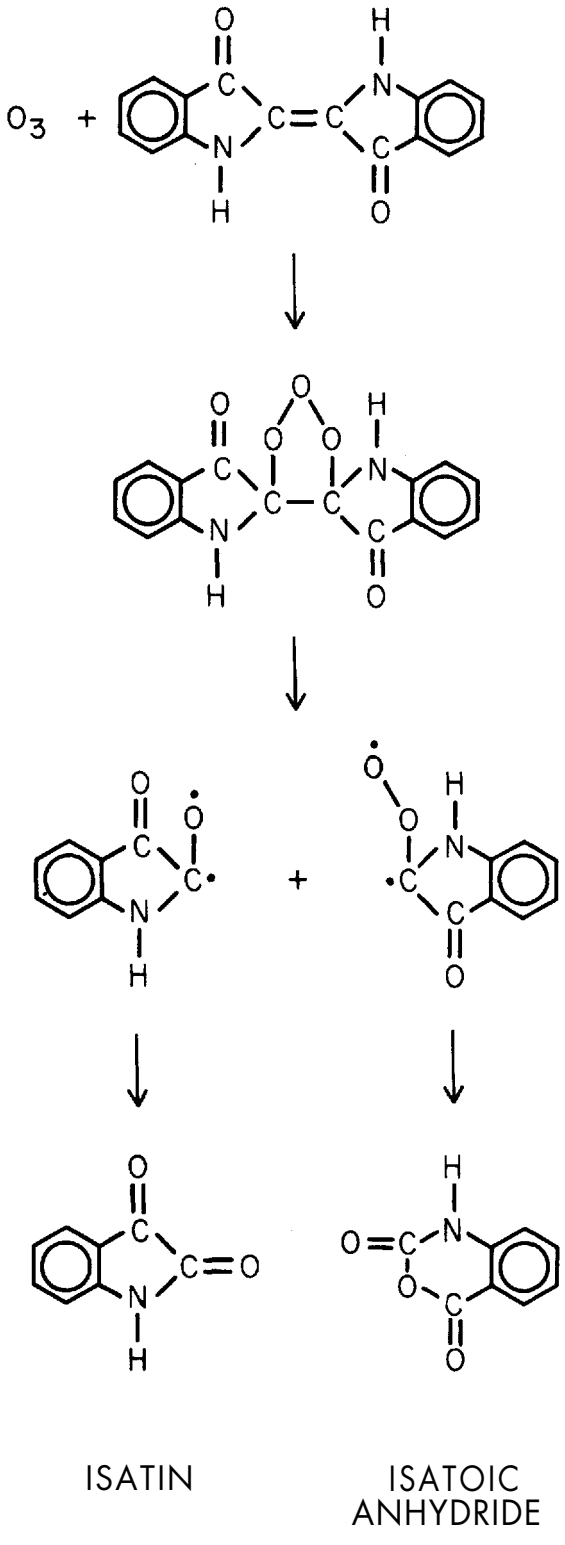

Figure 3.3. Tentative mechanism for the ozone-curcumin reaction.

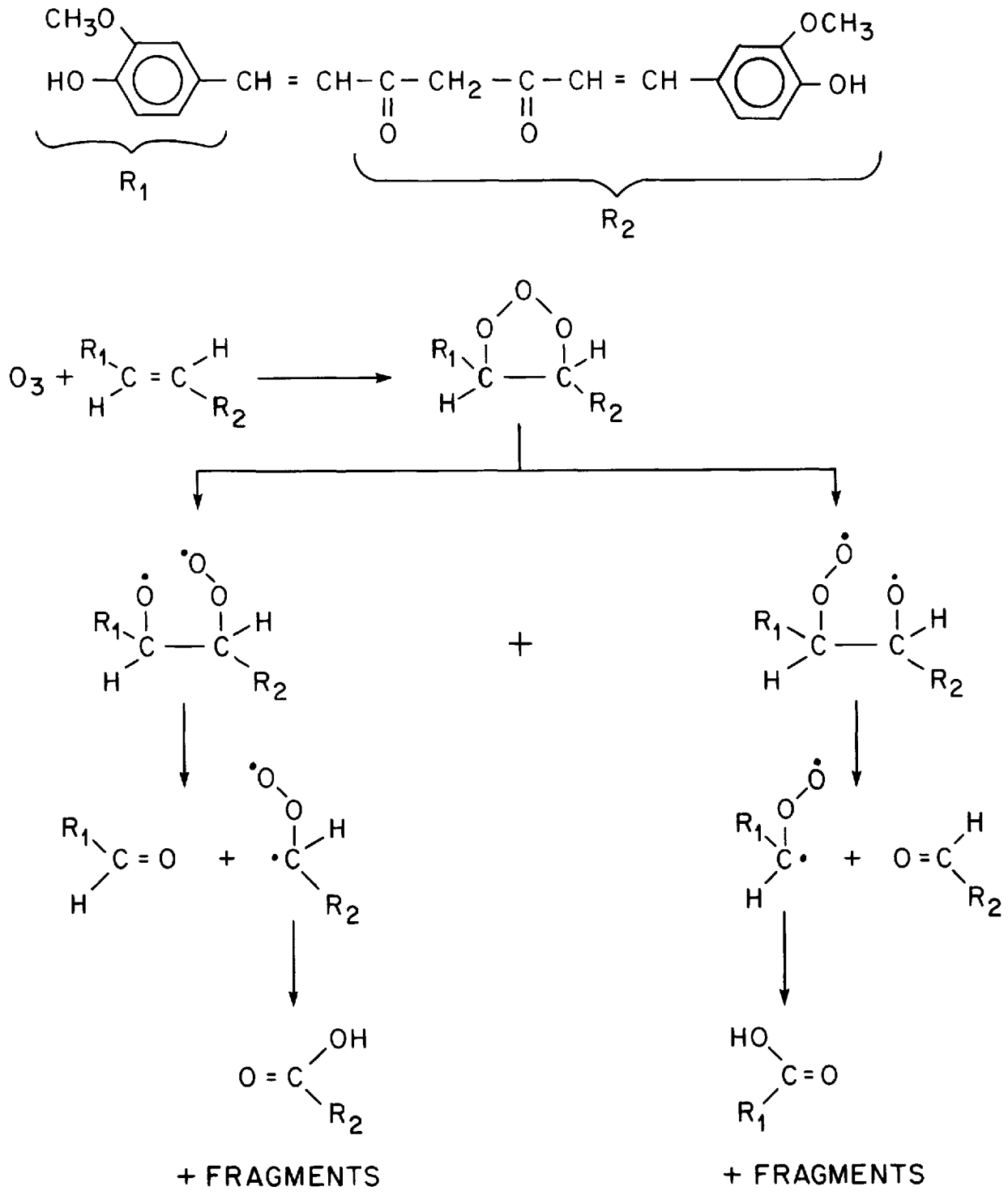

Figure 3.4. Tentative mechanism for the ozone-Basic Violet 14 reaction.

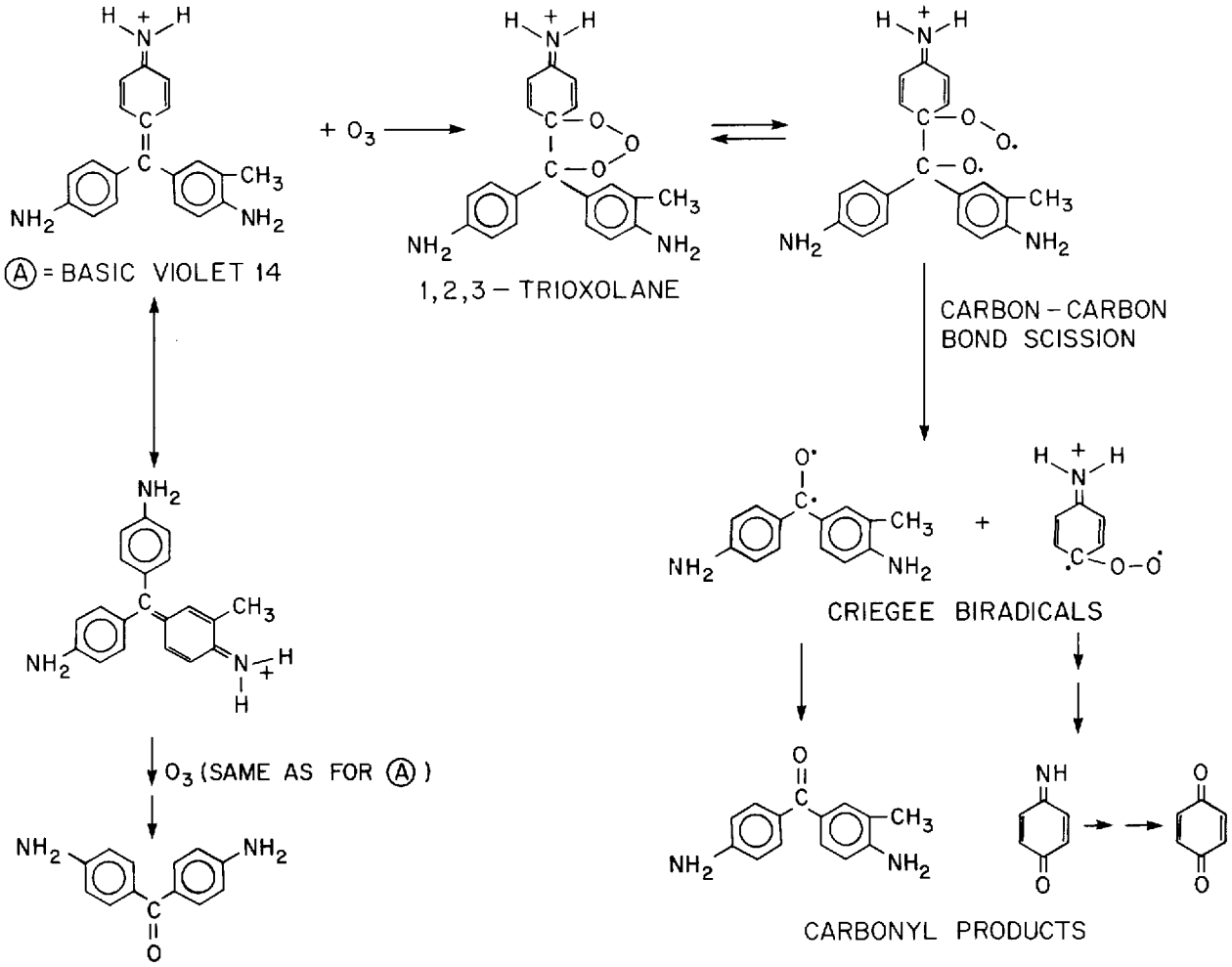

Chapter 4

Measurements and Model Predictions of Ozone and Other Pollutant Concentrations

Whether ozone poses a hazard to museum collections depends in part on whether the high ozone concentrations found outdoors are transferred to the indoor atmosphere of museums. In order to address this question, a computer-based model for predicting the indoor concentration of photochemically generated air pollutants was developed as a tool for studying the effect of building design on indoor pollutant exposure.

The model is structured to represent the ventilation system of a typical museum facility, as shown in Figure 4.1. Outdoor air that is completely described in terms of ozone, hydrocarbons, oxides of nitrogen, and their reaction products found in the outdoor atmosphere, is brought into the building through the mechanical ventilation system. Activated carbon filters, if present, are simulated as pollutant-removal devices. The air then passes to the inside of the museum facility, which is represented as a series of adjacent rooms or chambers, with the possibility of air exchange between those rooms. Inside each chamber, a 57-step chemical mechanism that describes the possible chemical reactions among pollutants acts to modify pollutant concentrations over time as a function of indoor lighting levels. Indoor emissions sources, such as the evaporation of hydrocarbon solvents from a conservation laboratory into the rest of the building, can be simulated. Loss of pollutants by reaction with building surfaces, including the collections, is also computed. Air can be recirculated from indoor spaces back to the mechanical ventilation system, with or without additional chemical filtration. Infiltration of untreated air from outdoors through open doors and windows or through cracks in the building shell is captured, as is exhaust from the building, back to the outdoor atmosphere. The indoor air quality model is described in detail in the Appendix to this report.

The indoor air quality model first was tested by comparison to experimental data taken at the Virginia Steele Scott Gallery on the Huntington Library grounds in San Marino, California. Figure 4.2 shows a floor plan of the west gallery of the Scott building and the ventilation flow rates, taken from the architectural plans and engineering specifications. The conditioned volume of the west gallery is 2530 m^3 and the surface area is 3060 m^2. In the gallery areas, rooms 101 and 102, which constitute 86% of the conditioned volume, the floors are oak plank, and the walls are painted plaster and plywood. The ceiling consists of plaster-veneer coffered beams and plastic diffusers. Above room

101 are skylights; fluorescent lamps behind the diffusers provide background lighting to room 102. The lighting in both rooms is supplemented by track lamps. Floor coverings in the other rooms are granite or ceramic tile, or linoleum-type flooring. Walls and ceilings are, for the most part, gypsum drywall.

Figure 4.1. Schematic representation of the ventilation components of the multichamber indoor air quality model.

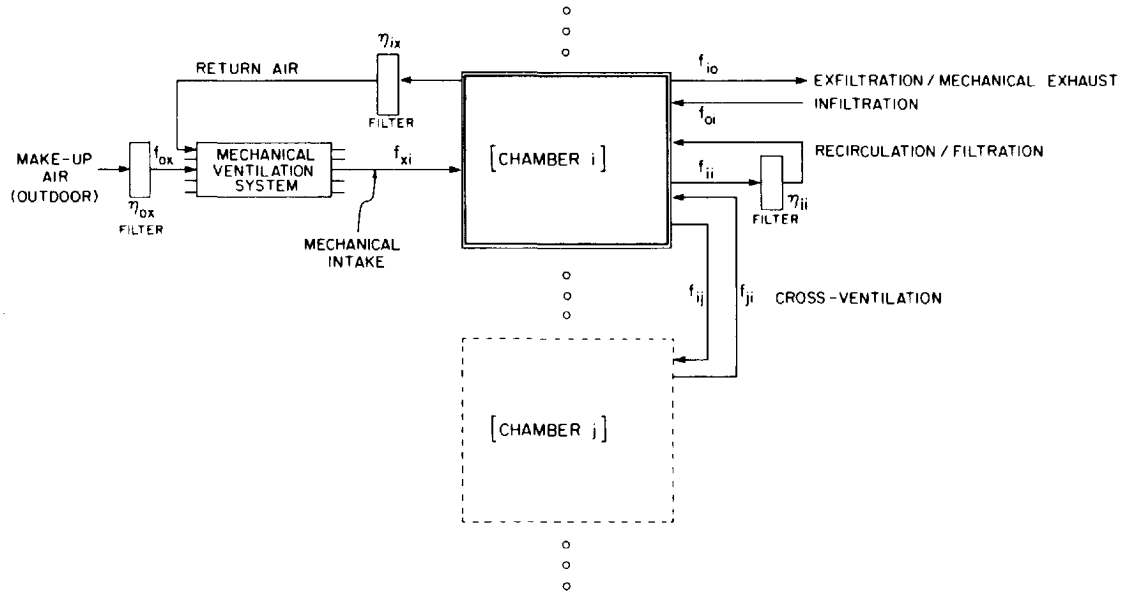

The ventilation system is designed to maintain a temperature of 70 ± 1 °F and a relative humidity of 50 ± 3% RH in the galleries. The only pollutant-removal devices in the ventilation system at the time of our tests were strainer mat-type filters (U.L. Class 2, Farr 30/30), designed to remove coarse particulate matter. When the internal recirculation fan is on, the total air flow rate through the mechanical ventilation system is 345 m^3 min^{-1} . The outdoor make-up air flow rate assumes two values: 85 m^3 min^{-1} during the day and 14m^3 min^{-1} at night. The daytime setting was maintained from approximately 7 a.m. to 6 p.m. during the study period. In each room, supply and return registers are located on the ceiling, raising the possibility of ventilation "short-circuiting," which would lead to a smaller effective ventilation rate than suggested by the flow rate data. However, the relatively low outdoor-air exchange rate (0.3-2.0 h^{-1}) and the absence of rapid fluctuations in monitored pollutant concentrations, combined with the relatively large recirculation rate (8 h^{-1}), suggests that convection was sufficient to effect rapid mixing during the daytime. On the other hand, the indoor data show fluctuations in pollutant concentrations at night that could be the result of incomplete mixing.

Monitoring Experiment

For a 10-day period beginning on October 30,1984, O_3, NO, and NO_2 concentrations were monitored inside and outside the Scott Gallery. Ozone concentrations were measured with a pair of UV photometric ozone monitors (Dasibi models 1003-AH and 1003-PC). A pair of chemiluminescent NO_x monitors (Thermo Electron Corporation, model 14 B/E) was used to measure NO and NO_2. NO2 values measured by this method include contributions from other nitrogen-containing species such as HNO_3 and PAN (Winer et al. 1974). The symbol NO_2* will be used to signify measurement data for this group of species, determined as NO_x - NO by the monitors. The NO_x monitors were calibrated daily against zero air and a known supply of 0.4 ppm NO in nitrogen. Data from all instruments were continuously registered on strip-chart recorders. Pollutant concentration values averaged over 12-minute intervals throughout the experiment were extracted from the strip-chart records.

On two days during the monitoring period, November 4-5, peak outdoor O_3concentrations exceeded 0.120 ppm in the presence of NO_x levels in excess of 0.200 ppm. Because of the relatively high pollution levels, tests of model performance were conducted for those days.

A comparison of measured and simulated ozone concentrations is presented in Figure 4.3. Model results are shown for both the base case and for a case where the chemical mechanism in the model is turned off. The full kinetic model is slightly better in predicting indoor ozone concentrations, particularly during the morning hours when the presence of a significant nitric oxide (NO) concentration constitutes a substantial sink for ozone. The reaction of ozone with the interior building surfaces (including the collection) is the dominant factor behind the difference between indoor and outdoor ozone concentrations within this particular building during the November 4-5, 1984 experiment (the base case). Indoor chemical reaction is, however, a significant net sink for ozone.

Comparisons between measurements and simulations for oxides of nitrogen are presented in Figure 4.4. At most times the measured NO_x and NO_2* concentrations are seen to lie between the results for the base case and for a "low NO_2 wall loss" simulation in which the NO_2 loss rate to building surfaces is set to zero. The nitric oxide concentration, on the other hand, is underpredicted at most times by both simulations, supporting Yamanaka's (1984) inference that NO_2 is converted to NO at indoor surfaces. The "low NO_2 wall loss" case predicts a total NO_x concentration that is closer to the measured value (5% high) than is the result for the base-case simulation (14% low).

Figure 4.2. Floor plan of the west wing of the Virginia Steele Scott Gallery, San Marino, California. Daytime/(night-time) ventilation flow rates are given in units of m^3 min^{-1}. Air sampling locations for the validation experiment are indicated by "x."

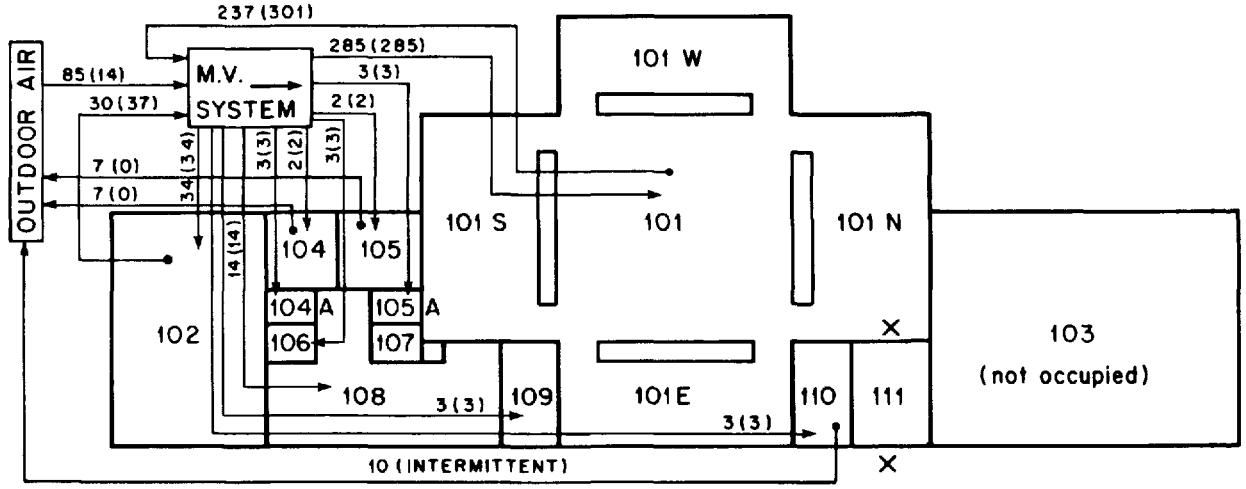

Figure 4.3. Comparison of modeled and measured ozone concentrations for a two-day period.

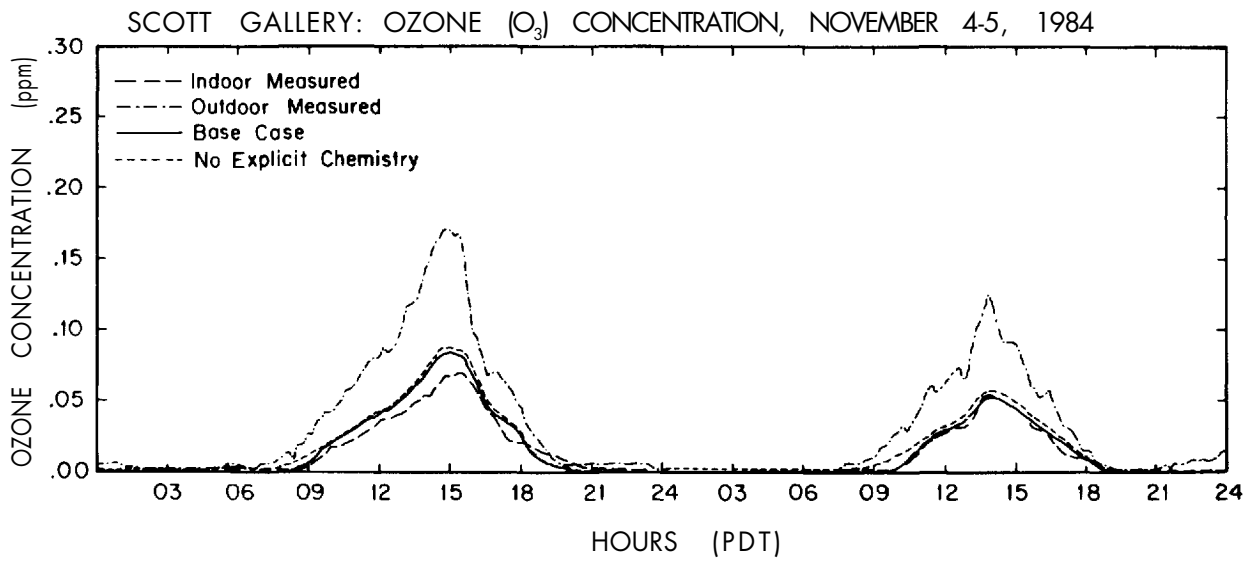

Figure 4.4. Comparison of modeled and measured concentrations of (a) nitric oxide, (b) nitrogen dioxide (NO_2^*, measured as NO_x-NO), and (c) total oxides of nitrogen for a two-day period. In the case of nitric oxide, the "base case" and "low (NO_2) wall loss" simulations produce essentially equivalent results.

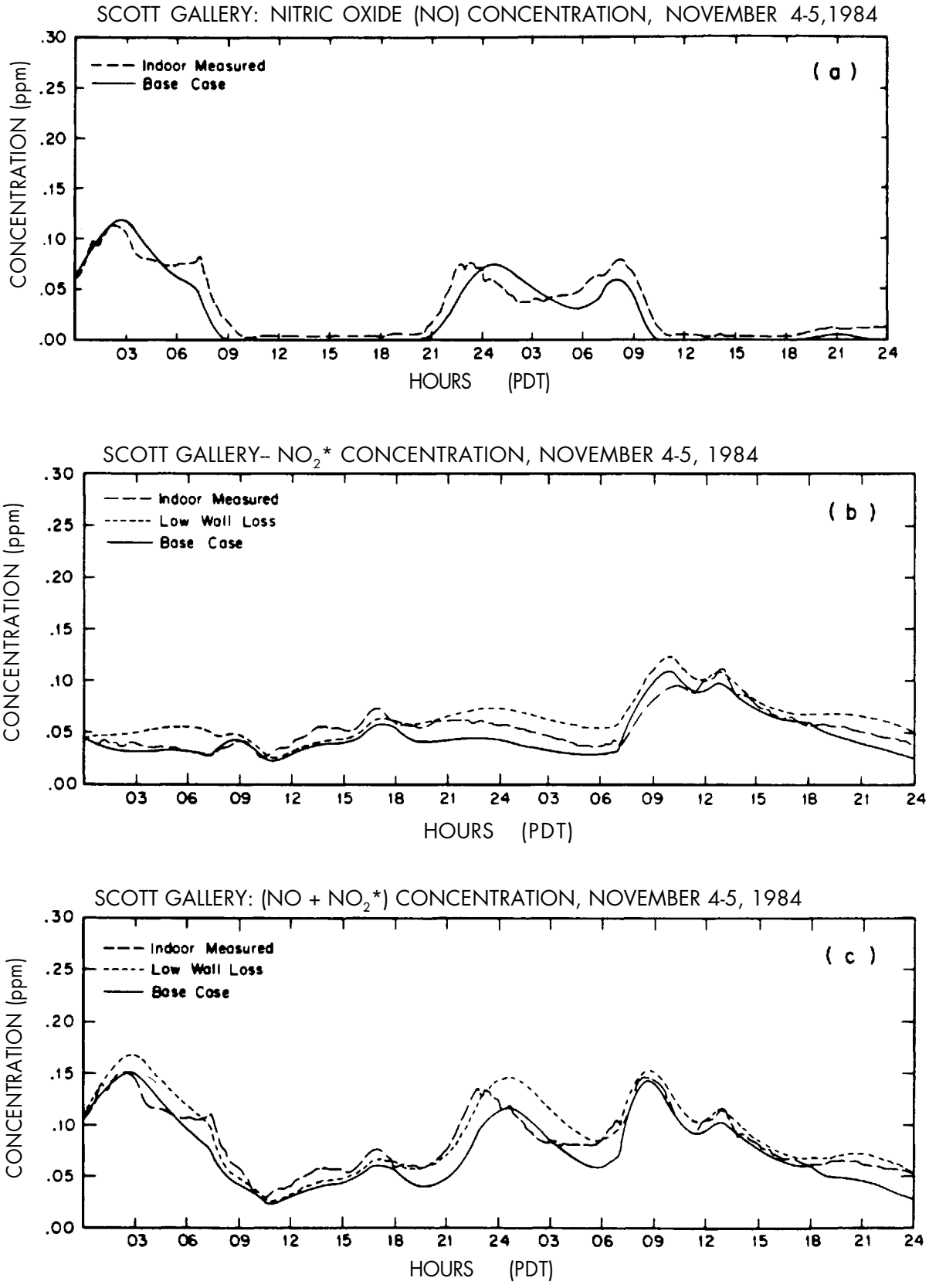

Four additional cases were selected to examine how changes in building design or operation could influence indoor pollutant concentrations through chemical reaction. The "multichamber" case addresses the magnitude of errors that result when it is assumed that this building may be represented as a single well-mixed chamber. The case with an "indoor hydrocarbon source" could represent a situation in which fumes from an underground parking garage enter the building, or a case in which solvents are used in the building. The "indoor oxides of nitrogen (NO_x) source" considers the effect of operating combustion appliances, like those possibly found in a museum restaurant kitchen. The "glass-walled building" case considers the effects of increased photolytic reaction rates and reduced wall loss rates that would result if the walls of the Scott Gallery had been made of glass through which outdoor sunlight could enter the building. Several of the findings are noteworthy (Fig. 4.5).

Comparing the average concentrations for the base case and no chemistry simulations, we see that several nitrogen-containing species—HNO_2, HNO_3, HNO_4, NO_3 and N_2O_5—are produced at substantial net rates by chemical reaction indoors.

The results of the multichamber simulation indicate that the treatment of this building as a single chamber is a reasonable approximation. Concentration variations among chambers are approximately 10% or less, owing to the relatively high rate of recirculation through the mechanical ventilation system.

The two cases for which an indoor pollutant source is postulated show that such sources may either increase or decrease the concentration of species not directly emitted. For example, the hydrocarbon source leads to substantial reduction in the indoor concentration of O_3 and NO, but markedly increased concentrations of HNO_2, HNO_4, HCHO, and H_2O_2, among others. The indoor combustion source likewise leads to a consumption of O_3, but increased production of HNO_2 and HNO_3.

In the case of the glass-walled building, indoor concentrations of several key species—including O_3, HNO_2, HNO_3, PAN, and H_2O_2—are increased markedly over the base case values, and in fact exceed the outdoor levels. In this case, homogeneous chemical reactions are greatly enhanced by the combined effects of increased lighting, leading to higher photolysis rates, and reduced wall loss, leading in turn to higher concentrations of reactive species. In summary, it is possible for a museum facility constructed largely with glass walls to act as an indoor smog chamber. A more detailed description of this model is presented in Appendix A.

Figure 4.5. Average measured and modeled pollutant concentrations for the Scott Gallery, November 4-5, 1984.

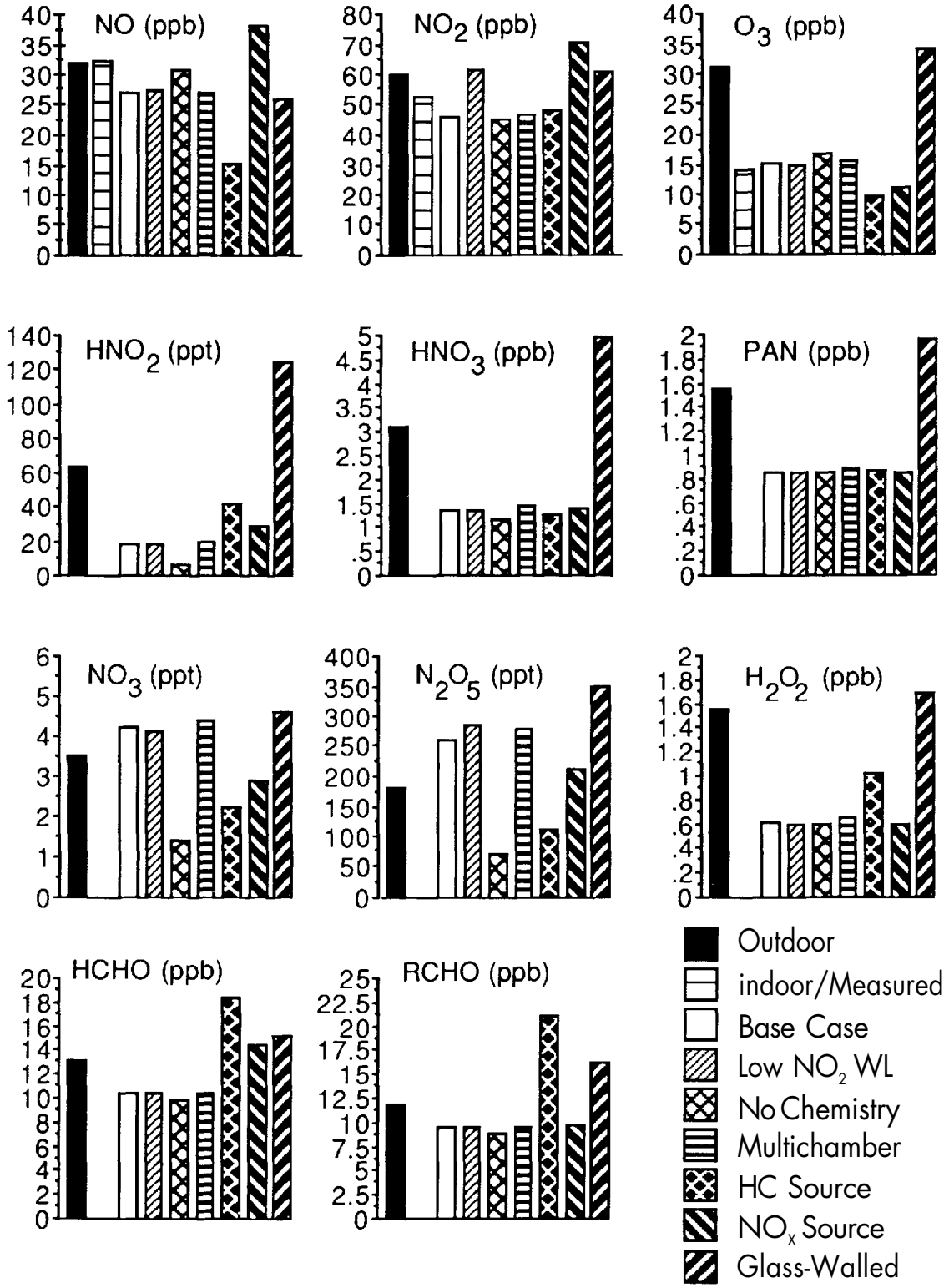

Ozone Concentrations Inside Southern California Museums

During the summers of 1984 and 1985, a program of simultaneous indoor and outdoor ozone measurements was conducted over a period of thirty-eight days at eleven institutions housing cultural properties. The purpose of these experiments was twofold: to gather data on the indoor ozone levels in buildings of varying construction, and to provide a database that could be used to test thoroughly the ability of the indoor ozone air-quality model just described to account for the indoor ozone levels observed.

The sites were picked to represent a wide range of building types in the Los Angeles area and 100 miles to the south in San Diego, California. Represented in this group were six art museums, two historical society houses, a museum library, and two college art galleries (Table 4.1). The blueprints of each facility were examined to determine the volume, surface area, and materials of construction used in each building. Each building's ventilation system was documented. Whenever possible, the senior building engineer was consulted to determine the air exchange rates at which he was actually running the air handling system. A hot-wire anemometer was used to measure air flow into and out of ventilation ducts, doors, and windows at each site. In stagnant areas, air-exchange rates were evaluated from standard engineering estimates for air infiltration. From this information, the air-exchange rates and retention times for ozone destruction by reaction with building surfaces could be determined. The physical dimensions, air-exchange rates, and interior surface characteristics of those buildings not equipped with activated-carbon ozone-removal systems at the time of this study are given in Table 4.2.

Table 4.1. Indoor/outdoor ozone measurement sites.

Site	Use	HVAC Type	Date	Comments
Pasadena Historical Society, Pasadena	1	1	7/03 to 7/05 1984	a
Southwest Museum, Los Angeles	2	1	7/11 to 7/12 1984	b
Southwest Museum Library, Los Angeles	3	3	7/13 to 7/15 1984	c
Virginia Steele Scott Gallery, San Marino	4	2	7/25 to 7/26 1984	d
Huntington Art Gallery, San Marino	4	3	7/27 to 7/29 1984	e
Montgomery Gallery, Claremont	5	2	7/30 to 7/31 1984	
Lang Gallery, Claremont	5	1	8/01 to 80/21984	a
Villa Montezuma, San Diego	1	1	8/07 to 8/08 1984	f
Junipero Serra Museum, San Diego	2	1	8/09 to 8/10 1984	f
Los Angeles County Museum of Art, Los Angeles	4	3	6/28 to 6/30 1985	
J. Paul Getty Museum, Malibu	4	3	7/02 to 7/15 1985	g

Use:

1. Historical society
2. Archaeological museum
3. Museum library
4. Art museum
5. College art gallery

HVAC type:

1. Not air conditioned. The Southwest Museum has a partial forced-ventilation system (see text).
2. Modern heating, ventilation, and air conditioning plant without activated-carbon filtration. The Scott Gallery was retrofitted with an activated-carbon filtration system following the completion of the present study.
3. Modern air conditioned plant with activated-carbon filtration.

Comments:

a. Observed during worst- and best-case situations and during normal operations.

b. Normal operation.

c. Normal operation, and with the building "buttoned up."

d. New structure completed within the year prior to this study.

e. Old structure retrofitted for complete environmental control.

f. Sites outside of Los Angeles County.

g. Located near the ocean and northwest of downtown Los Angeles. Usually assumed to be upwind of major air pollution sources.

Table 4.2. Building characteristics of selected museums and galleries in Southern California.

Institution	Surface Area[a] (ft^2)	(m^2)	Building Volume (ft^3)	(m^3)	Surface to Volume Ratio (ft^{-1})	(m^{-1})	Outdoor air Exchange Rate (hr^{-1})
Southwest Museum upper floor galleries in direct line with exhaust fans	22,399	2,081	101,915	2,886	0.22	0.72	5.5[b]
Junipero Serra Museum	12,922	1,200	43,000	1,218	0.30	0.98	—[c]
Pasadena Historical Society Museum	30,272	2,812	105,285	2,981	0.29	0.94	0.06[d]-2.2[e,f]
Lang Gallery	13,062	1,213	42,405	1,201	0.31	1.01	0.0[d]-0.99[e]
Villa Montezuma	16,608	1,543	34,282	971	0.48	1.59	1.8-2.6
Scott Gallery east wing + west wing	43,033	3,998	177,343	5,022	0.24	0.80	1.6
Montgomery Gallery	23,964	2,226	83,475	2,364	0.29	0.94	1.6

a. Estimated surface area includes area of walls, floors, and ceilings.

b. Based on measured exhaust rate divided into the volume of those upper floor galleries that are in a direct line between the open windows and the exhaust fans. This is a realistic ventilation estimate for the location of our ozone monitor. For purposes of comparison, the estimated air exchange rate is about 3.2 hr^{-1} if the exhaust air flow is divided by the volume of the entire building.

c. Not possible to measure flow because many open windows are far above ground level.

d. When building is closed. The value 0.0 indicates that the air exchange rate through building openings was too small to measure with a hot wire anemometer.

e. With doors and windows open. This condition is normal during the daytime in the summer at the Lang Gallery.

f. Under "normal operating conditions," the air exchange rate at the Pasadena Historical Museum is about 0.5 air exchanges per hour.

Results

These sites fell into three distinct groups: not air conditioned (Pasadena Historical Society Museum, Southwest Museum, Lang Gallery, Villa Montezuma, and Junipero Serra Museum); air conditioned but without an activated-carbon air filtration system (Virginia Steele Scott Gallery and Montgomery Gallery); and air conditioned with activated-carbon filters (Southwest Museum Library, Huntington Art Gallery, Los Angeles County Museum of Art, and the J. Paul Getty Museum).

Buildings that operate without conventional air conditioning are arrayed in a distribution between two extremes: those with rapid infiltration of outdoor air and those with little air exchange with the outdoors. Rapid air exchange can be achieved, as at the Southwest Museum, if forced exhaust fans induce a once-through flow of outdoor air. At the other extreme, community galleries operating in converted private mansions with the doors and windows kept closed often experience very slow rates of air exchange with the outdoors.

The Southwest Museum and the Junipero Serra Museum are examples of buildings with rapid air exchange but no air conditioning:

Southwest Museum. This facility is a multistory poured concrete building with an attached tower, built in the early 1900s. High-power fans installed in a former window force about 9400 cubic feet of air per minute (266.2 m^3 /min) out of the building and initiate convection throughout the main portion of the building. Two exhibit rooms are largely unaffected by this continuous flow. Many open windows and doors allow large amounts of circulatory air to pass through the building. A complete air exchange with the outdoors occured about 3.2 to 5.5 times per hour during the period of our tests. The slower air-exchange rate is computed on the basis of the volume of the entire building, while the faster air exchange rate is based on the volume of that portion of the upper floor of the building that is directly aligned with the flow from the open windows to the exhaust fans. The faster air exchange rate applies in the area where our ozone monitor was located.

Junipero Serra Museum, Like the Southwest Museum, the Junipero Serra Museum is a poured concrete Spanish-style building with an attached tower. Open doors and windows, generally large in size and few in number, provide ventilation at this facility. One open door facing the ocean is subjected to a steady breeze.

Ozone concentrations observed inside these buildings were generally quite high, on the order of 70% to 80% of the ozone level in the outdoor air brought into the building (Table 4.3 and Fig.4.6).

Table 4.3. Indoor/outdoor ozone concentration relationships in buildings with a high air exchange rate, but no air conditioning.

Site	Date	Indoor Max. O_3(ppm)	Outdoor Max. O_3(ppm)	Indoor O_3 as Percentage of Outdoor O_3
Southwest Museum	7/11/84	0.090	0.132	69%
Southwest Museum	7/12/84	0.143	0.173	84%
Junipero Serra Museum	8/09/84	0.034	0.049	69%
Junipero Serra Museum	8/10/84	0.022	0.028	79%

Figure 4.6. Indoor/outdoor ozone concentration relationships in the upper floor main gallery of the Southwest Museum, July 1 2, 1984. Model results show indoor O_3 concentrations predicted from the model of Chapter 4 using measured outdoor O_3 concentrations, an outdoor air-exchange rate of 5.5 exchanges per hour, building surface and volume values in the galleries of interest from Table 4.2, and an ozone deposition velocity at surfaces of 0.051 cm sec^{-1} (0.10 ft^3/ft^2-min).

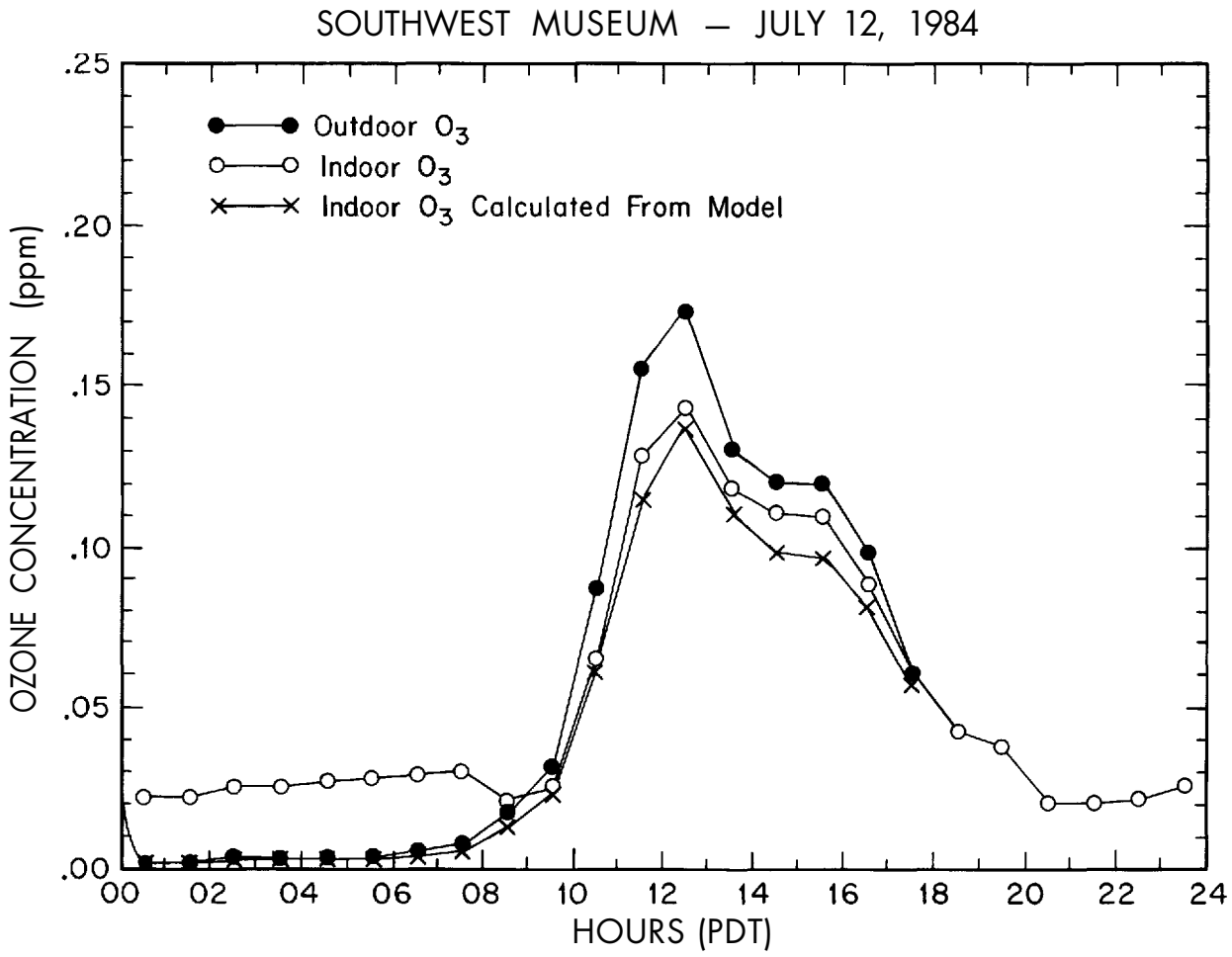

In contrast, museums that lack air conditioning and that have very low air-infiltration rates show some of the lowest indoor O_3 levels observed.

Pasadena Historical Society Museum. This building is a former private mansion converted for use as a museum. A few open windows, mostly on the second floor, provide poor ventilation. Under normal operating conditions, with the front door closed, the building is reasonably well sealed, and outdoor air enters the building at a very slow rate, with an air exchange occurring about once every two hours. An exception occurs when the site is used for luncheons or meetings, and the large front door is left open for the duration of the meeting. Under those conditions, the air-exchange rate is once every 27 minutes.

Lang Gallery. This college art gallery occupies a portion of a modern institutional building. One open window and one door open during public hours provide ventilation at this site. Under those conditions, the air-exchange rate with the outdoors is slightly less than once per hour. The door is closed when the staff leaves for lunch and in the evening. When the building is closed, very little outside air enters the facility. One or two fans circulate the air within the facility, but these fans do not force exchange with the air outdoors.

As seen in Table 4.4, with the exception of the Pasadena Historical Society when doors and windows were left wide open, indoor ozone levels in the above facilities are very low, on the order of 10% to 20% of the outdoor O_3 level. This can be attributed to the very low air-exchange rates (circa once every 1 to 2 hours), which yield long retention times for ozone depletion by reaction with indoor surfaces (Shair and Heitner 1974). Concentrations much lower than this cannot be expected in the absence of a deliberate pollutant removal system. Work at the Lawrence Berkeley Laboratory (Yocom 1982) has shown that even with complete weatherization (i.e., storm doors, indoor insulation, and weatherstripping) indoor/outdoor O_3 ratios range between 0.10 and 0.25, close to those values found at the Pasadena Historical Society mansion when closed over the 4th of July holiday and at the Lang Gallery when it was closed.

Villa Montezuma. This represents an intermediate condition between rapidly ventilated galleries and those that are stagnant and not air conditioned. Villa Montezuma is a Victorian-era mansion of shingled wood frame construction. It is unique in that it is the only building tested in which air circulation is driven by natural convection. A dozen or so open windows and a door provide ventilation, while numerous fans circulate the air within the facility. An up-draft can be felt in the stairwells of this largely vertical building as the warm interior air rises and

is replaced at ground level. Consequently, many of the first floor doors and windows serve as air inlets. The ozone monitor was placed in the main sitting room located on the first floor since many of the major artifacts were located in this area, and ozone concentrations at that location were 33% to 49% of those outside as shown in Table 4.5. The surface-to-volume ratio for this house was very large (0.48 ft^2/ft^3 ; 1.59 m^2/m^3), resulting from its design, which incorporates many small rooms and corridors.

Table 4.4. Indoor/outdoor ozone concentration relationships in buildings with no air conditioning and with a low air-exchange rate.

Site	Date	Indoor Max. O_3 (ppm)	Outdoor Max. O_3 (ppm)	Indoor O_3 as Percentage of Outdoor O_3	Comments
Pasadena Historical Society Museum	7/3/84	0.098	0.166	59%	1
Pasadena Historical Society Museum	7/4/84	0.025	0.155	16%	2
Pasadena Historical Society Museum	7/5/84	0.019	0.133	14%	3
Lang Gallery	8/1/84	0.030	0.140	20%	4
Lang Gallery	8/2/84	0.017	0.168	10%	5

Comments:

1. Worst case. Luncheon held with front door open during peak ozone hours.
2. Building sealed for holiday.
3. Normal operations.
4. Front door open in morning and late afternoon; closed otherwise.
5. Building closed. This is the best case and is observed only when the building is sealed.

Table 4.5. Indoor/outdoor ozone concentration relationships in a building with a natural convection-induced air-exchange system.

Site	Date	Indoor Max. O_3 (ppm)	Outdoor Max. O_3 (ppm)	Indoor O_3 as Percentage of Outdoor O_3	Comments
Villa Montezuma	8/7/84	0.014	0.042	33%	1
Villa Montezuma	8/8/84	0.022	0.045	49%	2

Comments:

1. Normal operations.
2. More windows open than on previous day.

A summary of peak ozone concentrations observed inside museums with conventional air conditioning, but without activated-carbon air filtration, is shown in Table 4.6. Both the Scott Gallery and the Montgomery Gallery are modern structures built specifically to house art collections. Ozone levels in these buildings are lower than at the Southwest Museum because air is recirculated through the cooling zone of the building air conditioning system many times before being exhausted from the building, thus increasing the retention time for ozone loss by reaction with building surfaces. Based on these experiments, one can expect a museum with a typical conventional air conditioning system to experience ozone levels inside the building that are 30% to 40% of those observed outside, with peak indoor concentration lagging behind the outdoor concentration by about one half hour.

Ozone concentrations within museums fitted with activated-carbon air filtration units were generally quite low. Typical O_3-removal efficiencies greater than 90% were observed, and indoor O_3 levels usually were found to be at or below 0.01 ppm (Table 4.7). A typical example of O_3-removal performance by the activated-carbon system at the Huntington Art Gallery is shown as Figure 4.7. Exceptions to this rule were found in certain portions of the J. Paul Getty Museum in Malibu, where the intrusion of untreated outdoor air was observed in ground-floor galleries that were operated with doors left open to the outdoors, and in administrative areas of the museum that are connected to these ground floor galleries via the building's air recirculation system.

Table 4.6. Indoor/outdoor ozone-concentration relationships in buildings with a conventional air conditioning system but with no activated-carbon air filtration.

Site	Date	Indoor Max. O_3 (ppm)	Outdoor Max. O_3 (ppm)	Indoor O_3 as Percentage of Outdoor O_3
Scott Gallery	7/25/84	0.043	0.179	24%
Scott Gallery	7/26/84	0.065	0.221	29%
Montgomery Gallery	7/30/84	0.060	0.150	40%
Montgomery Gallery	7/31/84	0.067	0.171	39%

Table 4.7. Indoor/outdoor ozone-concentration relationships in buildings with an activated-carbon air filtration system.

Site	Date	Indoor Max. O_3 (ppm)	Outdoor Max. O_3(ppm)	Indoor O_3 as Percentage of Outdoor O_3	Comments
Southwest Museum Library	7/13/84	0.026	0.149	17%	
	7/14/84	0.008	0.174	5%	
	7/15/84	0.003	0.116	3%	
Huntington Art Gallery	7/27/84	0.004	0.110	4%	
	7/28/84	0.010	0.172	6%	
Los Angeles County Museum of Art	7/01/85	0.010	0.165	6%	
J. Paul Getty Museum	7/02/85	0.022	0.104	21%	1
	7/08/85	0.009	0.095	9%	2
	7/15/85	0.028	0.075	37%	3

Comments:

1. The administrative area of the museum. Infiltration of untreated outdoor air into the ground-floor galleries also affects the area.
2. Second floor, room 203.
3. Ground floor, room 117. Ground-floor galleries generally have open doors through which untreated outdoor air may enter.

Model Predictions

Having acquired the indoor and outdoor ozone concentrations and data on ventilation system design in a variety of buildings, it becomes possible to explain how the indoor concentrations depend on outdoor ozone levels and on various building parameters. The indoor/outdoor ozone air-quality modeling computer code described earlier in this chapter was used. In the absence of chemical reaction, the calculation reduces to a form equivalent to that of Shair and Heitner (1974), which is the simplest model available that incorporates most of the key features of the problem at hand. Model predictions for the Southwest Museum are shown in Figure 4.6. Figure 4.8 shows results for the Montgomery Gallery with its modern conventional air conditioning system. Generally good agreement between model calculations and indoor measurements also was obtained at sites where unassisted slow air infiltration predominated, as shown for the Pasadena Historical Society Museum (Fig. 4.9).

The generally good agreement between model predictions and observations confirms that the major contributors to the variability of indoor/outdoor ozone relationships between museums can be explained by the combined influence of air-exchange rates, building surface and volume, and pollutant-removal mechanisms. The best comparisons between theory and observation were obtained for buildings—such as the Southwest Museum—with rapid air exchange but no air conditioning or pollutant-removal systems. Model calculations for buildings with a ducted ventilation system typically overpredict indoor concentrations, and this might be because large volumes of air are recirculated through ducts, particulate filtration, and air handlers, resulting in some loss of O_3 to surfaces within the ventilation system that are not represented within the present calculations. Reaction of O_3 with the oxides of nitrogen present in polluted urban air may also act to reduce indoor O_3 concentrations, but the effect of indoor chemical reactions cannot be evaluated during the eleven-site study because data on the co-occurring oxides of nitrogen concentrations were not available during these experiments. In cases where high concentrations of NO or olefinic hydrocarbons are present in indoor or outdoor air, the air-quality model computer code used here can explicitly treat O_3 removal by chemical reaction as explained in Nazaroff and Cass (1988) and Appendix A.

Figure 4.7. O_3-removal performance achieved by the activated-carbon air filtration system at the Huntington Art Gallery.

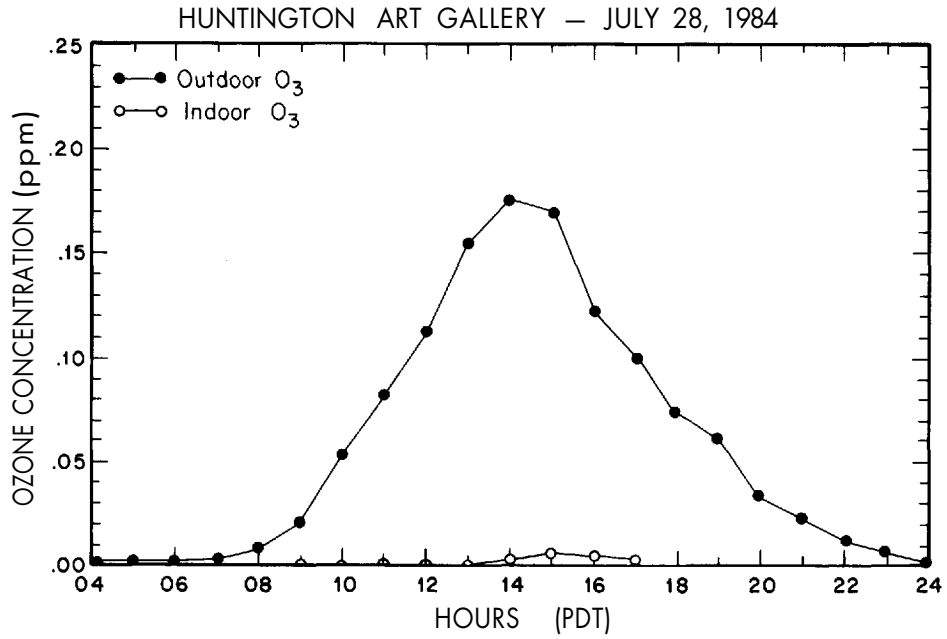

Figure 4.8. Indoor/outdoor ozone concentration relationships in the Montgomery Gallery, which has a modern conventional air conditioning system. Model results show indoor O_3 concentrations predicted from the model of Chapter 4 using measured outdoor O_3 concentrations, an outdoor air-exchange rate of 1.62 exchanges per hour, an internal air recirculation rate of 4.9 exchanges per hour, building surface and volume values from Table 4.2, and an ozone deposition velocity at surfaces of 0.051 cm sec^{-1} (0.10 ft^3/ft^2-min).

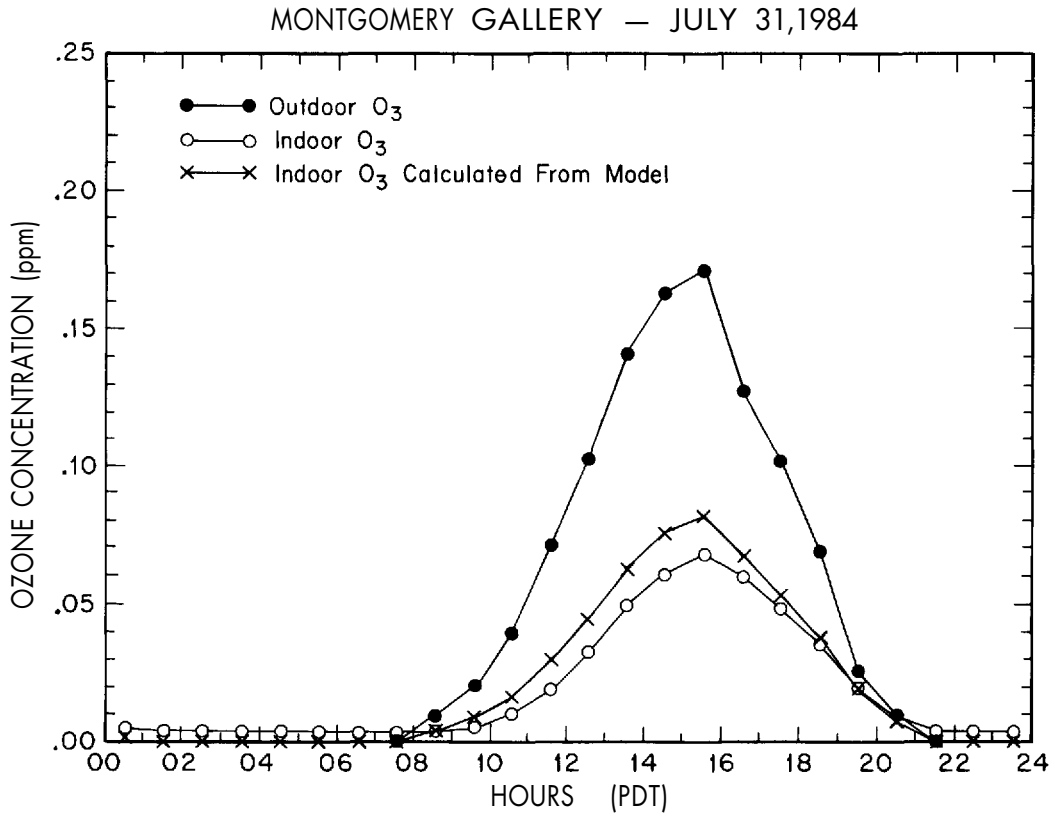

Figure 4.9. Indoor/outdoor ozone concentration relationships in the Pasadena Historical Society Museum, which has no air conditioning system and which has a slow air-exchange rate. Model results show indoor O_3 concentrations predicted from the model of Chapter 4 using measured outdoor O_3 concentrations, an outdoor air-exchange rate of 0.5 exchanges per hour, building surface and volume values from Table 4.2, and an ozone deposition velocity at surfaces of 0.051 cm sec^{-1} (0.10 ft^3/ft^2-min).

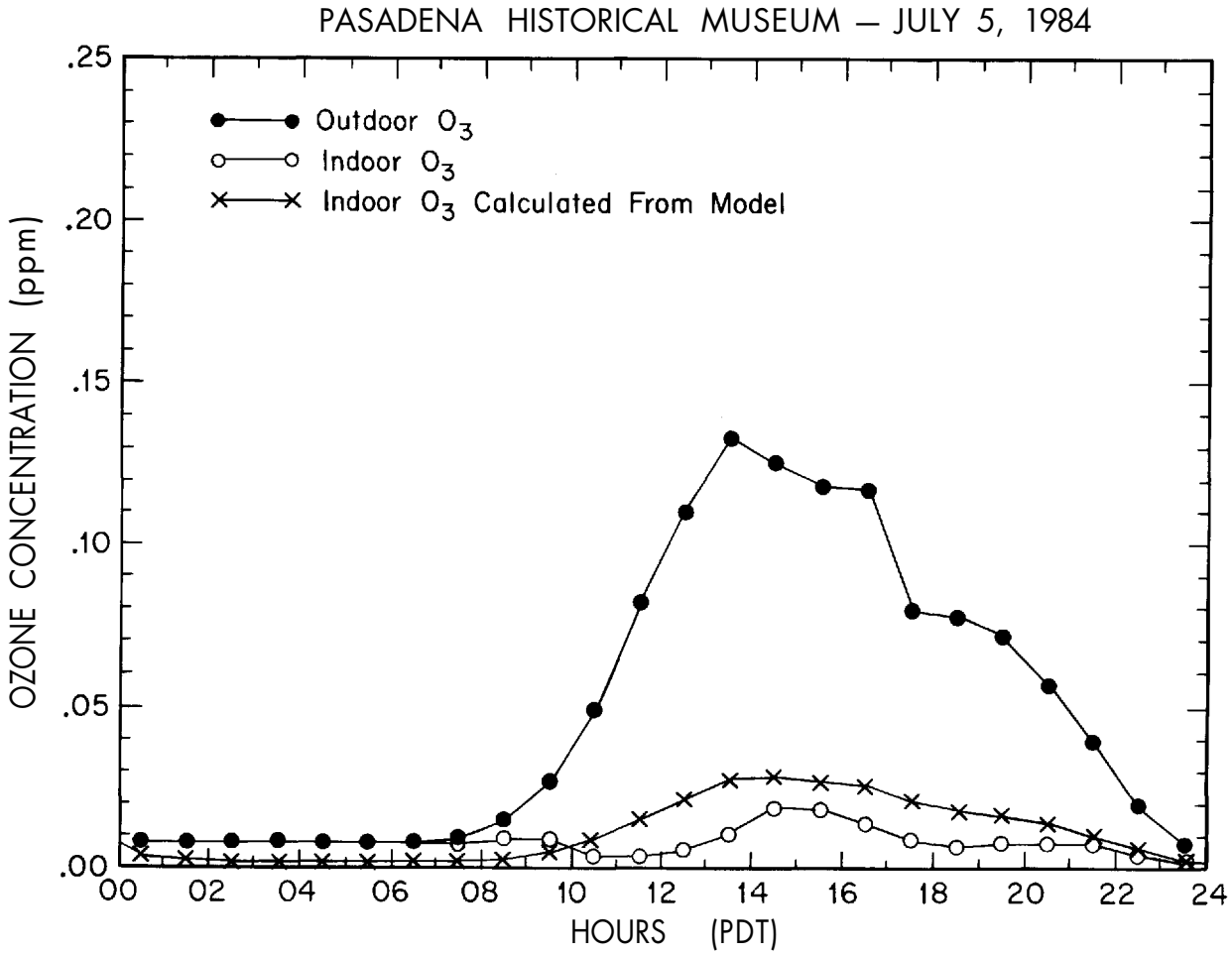

Chapter 5

Protection of Works of Art from Damage Due to Atmospheric Ozone

As ozone damage to materials such as dyed textiles, cellulose, and polymers like those found in rubber and paint binders has been known for many years[1], a variety of recommendations already have been offered concerning acceptable ozone concentrations in the indoor air of museums, libraries, and archives[2]. As seen in Table 5.1, ozone concentration limits that have been suggested range from 0.013 ppm to 0.001 ppm. Most recommendations are that indoor ozone levels in such facilities be limited to about 0.001 ppm.

In contrast, the highest one-hour average outdoor ozone concentration in the air basin that surrounds Los Angeles reached 0.35 ppm during 1986 (California Air Resources Board 1986), and the highest one-hour average ozone concentration during the year, averaged over all ozone monitoring sites in the United States, exceeded 0.12 ppm in the early 1980s (Office of Air Quality Planning and Standards 1983). Ozone concentrations averaged over all hours of the year are lower—in the range 0.02 to 0.054 ppm—across the air-monitoring sites located in the Los Angeles area (California Air Resources Board 1986). Average outdoor ozone concentrations in the range 0.017 to 0.035 ppm are reported widely throughout the world, even at remote locations (Committee on Medical and Biologic Effects of Environmental Pollutants 1977).

The measurement program described in Chapter 4 of this report has demonstrated that high outdoor ozone concentrations can be transferred to the indoor atmosphere of museums. Facilities with a high air exchange with the outdoors and no pollutant-removal system have indoor ozone concentrations more than two-thirds as high as those found outdoors (see Chapter 4). Ozone concentrations as high as 0.143 ppm were measured inside one such museum. In that same survey, it was found that museums with conventional air conditioning systems showed indoor ozone concentrations about 30% to 40% of those outside, while museums with no forced ventilation system, where slow air infiltration provides the only means of air exchange, have indoor ozone levels typically 10% to 20% of those outdoors. Every museum facility studied that lacked an ozone removal system showed indoor ozone concentrations above 0.010 ppm at times. Clearly, there are widespread differences at present between the actual ozone concentration present inside some museums versus the lower concentration limits recommended by many experts, as listed in Table 5.1.

Table 5.1. Suggested ozone concentration limits for art galleries, archives, and libraries (after Baer and Banks 1985).

Authority or Installation	Ozone Concentration Limit (ppm)	Reference
American National Standards Institute (draft)	0.001 ppm	American National Standards Institute (1985)
British Museum Library	0.00 ppm	as cited by Baer and Banks (1985) and by Mathey et al (1983)
Canadian Conservation Institute	0.010 ppm	La Fontaine (1978,1979) as cited by Baer and Banks (1985)
National Bureau of Standards	0.013 ppm	Mathey et al (1983)
National Research Council	0.001 ppm	Committee on Preservation of Historical Records (1986)
Newberry Library Paul N. Banks	0.001 ppm	Banks (1980)
Royal Ontario Museum Workshop	use activated carbon	as cited by Baer and Banks (1985) and by Mathey et al (1983)
G.Thomson	reduce to trace levels (0-0.001 ppm)	Thomson (1978)

The purpose of the present chapter is to examine a variety of methods that can be used to protect museum collections from damage due to atmospheric ozone. Control measures studied include elimination of pollutants from indoor air via ventilation system redesign; construction of display cases to protect works of art; framing of paintings, prints, and watercolors behind glass; selection of ozone-resistant pigments; and application of binders and coatings that protect ozone-sensitive pigments. Each of these ozone damage prevention techniques will be discussed.

Ozone Removal Via Activated Carbon

Activated carbon air filtration systems have been employed for indoor pollutant control in a number of Southern California museums. An activated carbon system was installed at the Huntington Art Gallery on the Huntington Library grounds in the early 1950s. At present, similar systems are employed at the Los Angeles County Museum of Art, the J. Paul Getty Museum, the Norton Simon Museum, and the Southwest Museum Library. The ventilation system at the Virginia Steele Scott Gallery on the Huntington Library grounds recently was outfitted with activated carbon for the purpose of ozone removal following completion of the earlier study reported in Chapter 4 of this research summary.

The single-pass ozone removal efficiency of activated carbon beds in actual use is reported to be as high as 95 $\pm$ 5% when fresh, declining to 50% removal after 3600 hours of use (1000 kg of activated carbon was used to filter 14,000 cfm of air during May-October in Pasadena, California; Shair 1981). The resultant indoor ozone concentrations will depend on the details of how the activated carbon beds are integrated into the building's ventilation system. Referring to the ventilation system schematic shown in Figure 5.1, activated carbon filters could be placed on the outdoor make-up air inlet only (filtering airstream f_{ox}), with no direct treatment of the recirculated air flow. That is the configuration used at the Norton Simon Museum in Pasadena, California. Alternatively, both the outdoor make-up air and the recirculated air flow could be passed through activated carbon filters, as is the case at the new installation at the Scott Gallery. In addition, the ratio of recirculated air to outdoor make-up air can be varied, which will affect the ultimate indoor ozone concentration. To examine the effect of ozone removal efficiency and air recirculation options on indoor ozone concentrations, an indoor air quality simulation model can be used.

Figure 5.1. Schematic representation of a simple building ventilation system.

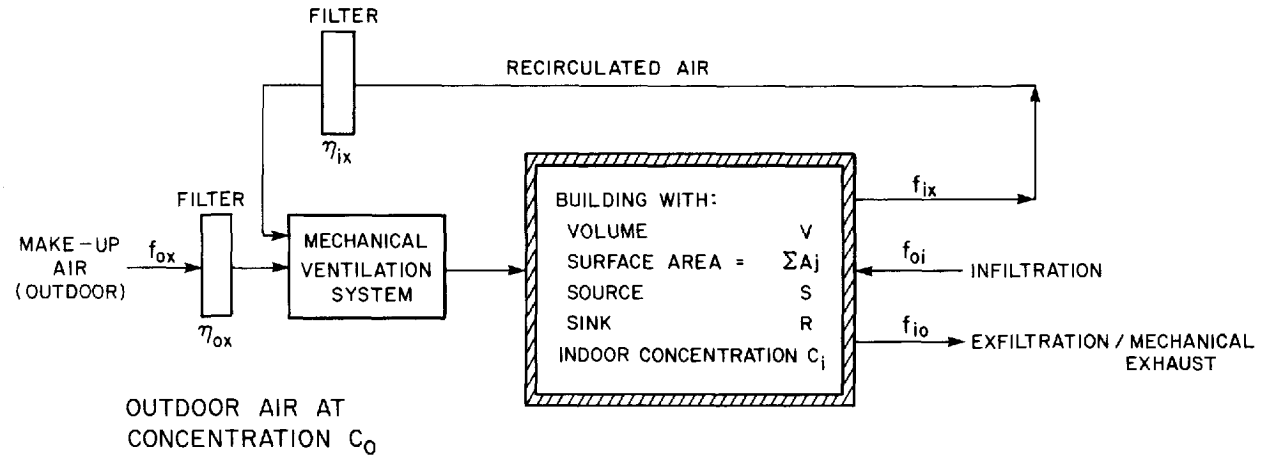

In Chapter 4 and in the Appendix of this work, a computer-based air quality model was developed for predicting the indoor concentrations of photochemically generated air pollutants. A simplified version of that model was then used to confirm that the indoor ozone concentrations observed in several museums were consistent with our present understanding of the effects of ventilation system design and ozone loss rates at interior surfaces (Nazaroff and Cass 1988, Shair and Heitner 1974, Hales et al. 1974).

One of the sites studied was the Montgomery Gallery in Claremont, California, which has a modern air conditioning system but no deliberate ozone removal system. Indoor ozone concentrations in the Montgomery Gallery were predicted, via modeling calculations, to be about 47% as high as the outdoor peak ozone level, which is in close agreement with actual measurements made inside and outside (see Fig. 4.8). In Figure 5.2, the air quality model of Chapter 4 is employed to compute the indoor ozone concentrations that would prevail in the Montgomery Gallery if activated carbon filters were placed on both the outdoor make-up air and on the recirculated air supply (air flows f_{ox} and f_{ix} in Figure 5.1), with no change from the base case air flow rates (6.48 air changes per hour total; 4.86 air changes per hour recirculated air; 1.62 air changes per hour outdoor make-up air). As seen in Figure 5.2, with 95% ozone removal during each pass through an activated carbon filter, peak indoor ozone levels in the Montgomery Gallery would drop to 0.0017 ppm versus a peak of 0.17 ppm outdoors. Greater than 99% removal relative to outdoor ozone concentrations could be achieved in that case by multiple passes of the indoor air through the activated carbon bed combined with ozone loss to interior building surfaces. Even with single pass filtration efficiencies, η_{ox} and η_{ix}, for ozone removal at

Figure 5.2. Air quality model predictions of the effect of activated-carbon air filtration on ozone concentrations inside the Montgomery Gallery, Claremont, California.

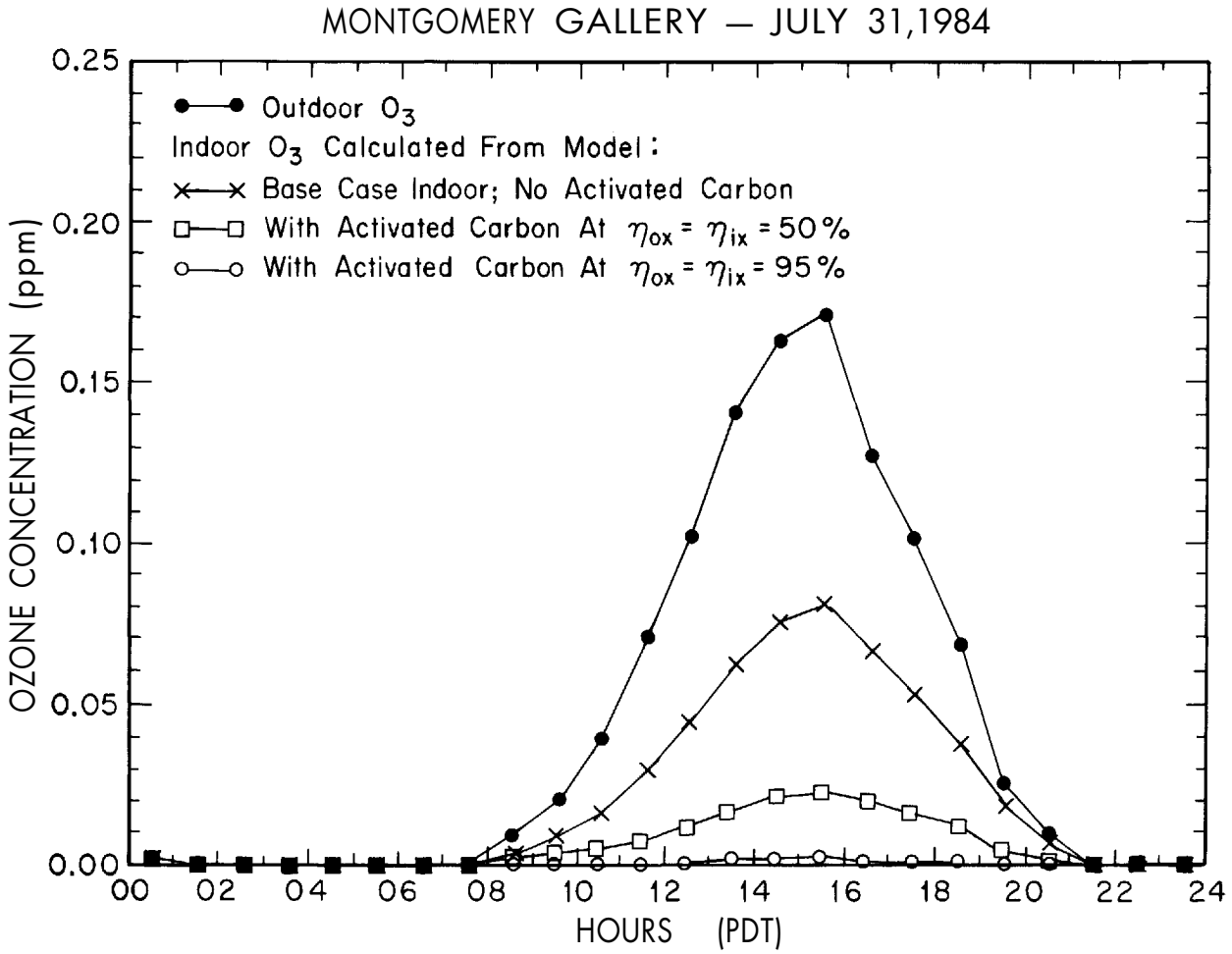

the activated carbon bed of only 50%, the peak ozone concentration would drop from 0.171 ppm outdoors to 0.024 ppm indoors for the air flow conditions observed during our July 31,1984 experiments at the Montgomery Gallery (see Fig. 5.2).

The above analysis indicates that indoor peak ozone concentrations as low as 1% of that outdoors could be achieved at the Montgomery Gallery by addition of activated carbon filters alone under ideal conditions. However, experience gained through indoor measurements at other facilities where activated carbon systems are actually in use at present indicates that indoor ozone concentrations in the range of 3% to 37% of that outdoors are observed in practice (see Chapter 4, Table 4.7). Values at the higher end of this range apparently result from infiltration of untreated air through open doors or windows. When seeking to achieve very low indoor ozone levels, prevention of extraneous infiltration of untreated air becomes a key factor in the overall system performance. If the building is pressurized such that air flows out the doors

when they are opened, then infiltration will be reduced. Careful monitoring of the condition of the activated carbon bed also is required. As seen in Figure 5.2, a decrease in ozone removal efficiency (η_{ox} and η_{ix}) from 95% down to 50% is accompanied by a ten-fold increase in indoor ozone levels. The activated carbon beds must be changed periodically when the ozone removal efficiency of the bed has fallen below design values.

The Effect of Reduced Outdoor Make-up Air

While activated carbon filters clearly can be used for ozone removal, the expense of their installation and maintenance may be beyond the budgets available to many museums. An alternative ozone control procedure for some museums that have a conventional air conditioning system but no deliberate ozone removal system involves careful management of the ratio of recirculated air to outdoor make-up air, flows f_{ox} and f_{ix} in Figure 5.1.

As was discussed in Chapter 4, some of the lowest indoor ozone concentrations observed inside museums occur in private mansions that have been converted to museum use without the installation of a conventional air conditioning system of any kind. These buildings are operated with most doors and windows closed, and slow infiltration of outdoor air provides the only means of penetration of ozone into the building from outdoors. Outdoor air exchange rates from nearly zero up to one air exchange per hour are observed when these buildings are operated with the doors and windows mostly closed (see Chapter 4, Table 4.2, especially note f). Indoor ozone concentrations in the range of 10% to 20% of those outdoors are observed under these conditions (Table 4.4). This is significantly lower than the 30% to 40% ratio of indoor to outdoor ozone levels seen in most museums with conventional air conditioning systems. Careful study of this situation suggests that it may be possible to attain the low indoor ozone levels found in buildings with slow air infiltration without sacrificing the temperature, humidity, and particulate pollutant control afforded by a conventional air conditioning system.

The approach that can be taken to achieve this result involves reducing the outdoor make-up air supply to the building's air conditioning system to the lowest value consistent with recommended ventilation codes, while increasing the recirculated air flow by a comparable amount. This air flow adjustment often can be accomplished by resetting existing mechanical dampers inside the system at no further capital expense. Any adjustment in this direction will reduce indoor ozone levels (in the absence of an indoor ozone source) because less ozone will

be brought into the building from outdoors, while ozone removal at building surfaces will continue to deplete indoor ozone concentrations.

To illustrate the effect of rebalancing the air flows within a museum ventilation system, the indoor air quality model of Chapter 4 will be used in conjunction with data from the Montgomery Gallery experiments. The Montgomery Gallery as tested has an interior volume of 2364 m^3 (83,475 ft^3) and an interior surface area of 2226 m^2 (23,964 ft^2). The total air flow through the ventilation system is 255.4 $m^3\ min^{-1}$ (9019 cfm), with one-fourth of this flow (63.8 $m^3\ min^{-1}$) derived from outdoor air and three-fourths of the air flow taken from recycled indoor air (191.5 $m^3\ min^{-1}$). At those air flow rates, the total air exchange rate for the building is 6.48 air changes per hour, with 1.62 changes per hour due to outdoor air plus 4.86 air changes per hour due to recirculated indoor air. Standards for the minimum amount of make-up outdoor air for use in building ventilation systems are recommended by the American Society of Heating, Refrigerating, and Air-Conditioning Engineers (ASHRAE 1985). The minimum recommended outdoor make-up air flow rate is 8.5 m^3 /hour per person occupying the building (ASHRAE 1985).

Discussions with the Montgomery Gallery personnel suggest that gallery occupancy is highly variable. During the opening reception for a new exhibit, up to 300 persons may be in the building. Design guidelines for libraries (and museums) under normal operating conditions anticipate a design occupancy of 20 persons per 1000 ft^2 of floor space (Wadden and Scheff 1983:143), which for the Montgomery Gallery is about 120 persons. At a design occupancy of 30 persons per 1000 ft^2 of floor area, the occupancy figure would be about 180 persons. However, on most days no more than 50 persons are actually present at the Montgomery Gallery. Much of the summer (the high ozone season), the gallery is closed to the public with only a few staff members present, and occupancy is even lower than 50 persons. At an air exchange rate of 8.5 $m^3\ hr^{-1}$ per person, these alternative occupancy figures for the Montgomery Gallery are translated into required outdoor make-up air flow rates in Table 5.2. The Montgomery Gallery as presently operated is configured to handle the few peak periods of high occupancy during a major reception, with some margin to spare. However, if such a facility were equipped with easily adjustable dampers, the make-up air supply could be cut drastically from present settings during most hours of the year.

Table 5.2. Effect of occupancy on required outdoor make-up air supply at the Montgomery Gallery, Claremont, California.

Occupancy	Outdoor Air Flow (m^3 /min)	Outdoor Air Exchanges per Hour
Base Case (building as tested July 31,1984)	63.8	1.62
300 persons	42.5	1.08
180 persons	25.6	0.65
120 persons	16.9	0.43
50 persons	7.1	0.18

The effect that reduced outdoor make-up air would have on indoor ozone concentrations at the Montgomery Gallery was computed using the air quality model. Outdoor make-up air was reduced to the levels shown in Table 5.2, while recirculated air was increased to keep the total air exchange rate at the observed 6.48 air changes per hour. Calculations were based on the outdoor ozone levels measured during our July 31,1984 experiments at the Montgomery Gallery. The results are shown in Figure 5.3. Under base case conditions, with 1.62 outdoor air exchanges per hour, a peak indoor O_3 concentration of 0.08 ppm is predicted, compared to an outdoor peak one-hour average O_3 concentration of 0.171 ppm. At 1.08, 0.65, 0.43, and 0.18 outdoor exchanges per hour, the peak indoor ozone concentrations would drop to 0.065, 0.046, 0.033, and 0.016 ppm, respectively. If this building's outdoor air dampers were set for an occupancy of 50 persons or less most of the time, indoor ozone concentrations less than 10% of those outdoors could be maintained with little capital investment (as long as precautions are taken to minimize infiltration of outdoor air). Electromechanically driven dampers can be installed that are programmable by time of day and that can be switched manually to a high make-up air flow condition during special events when the museum is unusually crowded.

Reduced make-up air and activated carbon filters, if used separately, will each reduce indoor ozone levels. These ventilation system modifications can also be used simultaneously, for even greater ozone control. Indoor air quality modeling calculations for the Montgomery Gallery showing the effect of using activated carbon with various outdoor air exchange rates are displayed in Figures 5.4 and 5.5. With the outdoor air exchange rate reduced to comfortably accommodate 50 persons within the building (0.18 outdoor exchanges per hour) and with infrequent servicing of the activated carbon bed (50% ozone removal per pass through the activated carbon bed), peak indoor ozone concentra-

tions could be reduced to 0.003 ppm versus 0.171 ppm outdoors, an overall control efficiency of greater than 98%. With fresh activated carbon at a 95% ozone removal efficiency per pass, the same reduced make-up air flow and no infiltration, indoor ozone concentrations would drop to 0.0002 ppm (Fig. 5.5). This is well below the most stringent indoor ozone air quality guideline (see Table 5.1), and would remain so even if outdoor ozone levels were increased to 0.40 ppm, which is approximately the highest outdoor value observed anywhere in the Los Angeles area in recent years.

A note of caution is in order. Reducing the flow of outdoor air will lead to reduced ozone concentrations in those cases where the ozone is supplied solely from outdoor air. It is possible for indoor ozone sources to occur due to the use of electrostatic precipitators for airborne particle removal, or through the use of duplicating machines or electric motors. If indoor sources are present, then reducing the building's outdoor air supply may actually increase indoor ozone concentrations. Finally, any building that contains indoor sources of air pollutants other than ozone (e.g., formaldehyde emitted from particle board) should be analyzed carefully before the outdoor air exchange rate is reduced to ensure that other pollutant control problems are not aggravated.

Figure 5.3. Air quality model predictions of the effect of altered outdoor make-up air flow rates on indoor ozone concentrations at the Montgomery Gallery, Claremont, California.

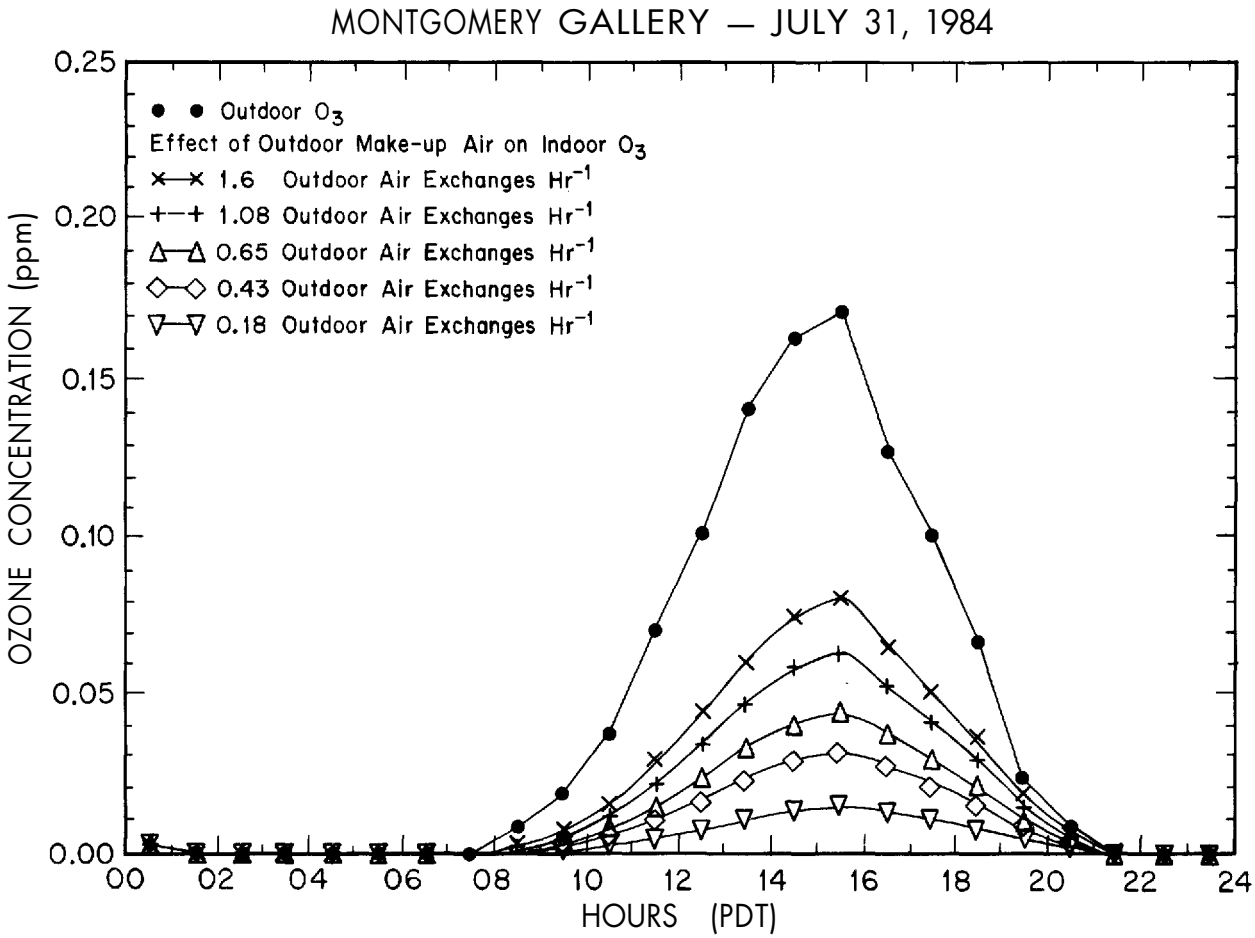

Figure 5.4. Air quality model predictions of the effect of the simultaneous use of activated carbon plus lowered outdoor make-up air on indoor ozone levels at the Montgomery Gallery: Case 1, activated carbon ozone removal efficiency is 50%.

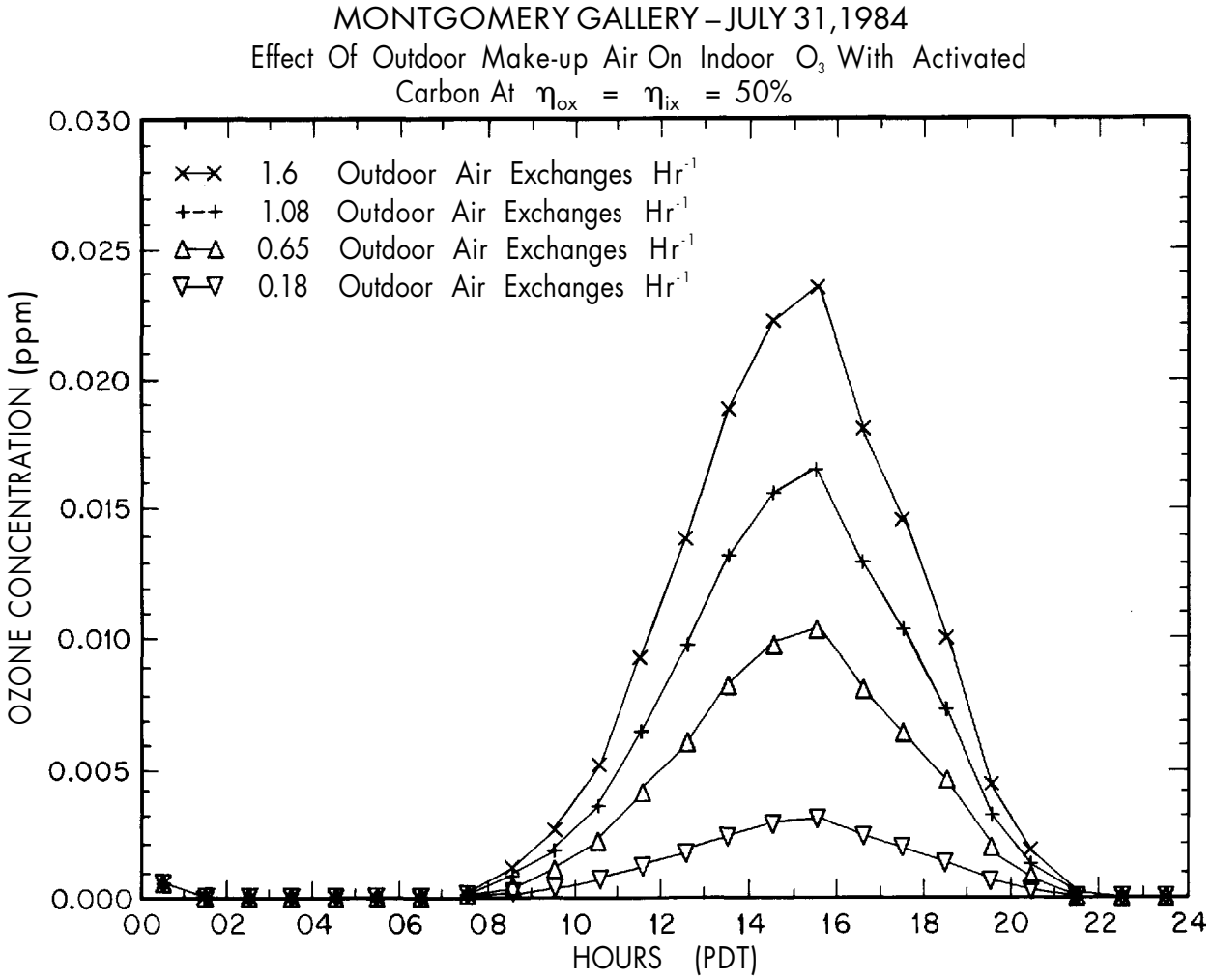

Figure 5.5. Air quality model predictions of the effect of the simultaneous use of activated carbon plus lowered outdoor make-up air on indoor ozone levels at the Montgomery Gallery: Case 2, activated carbon ozone removal efficiency is 95%.

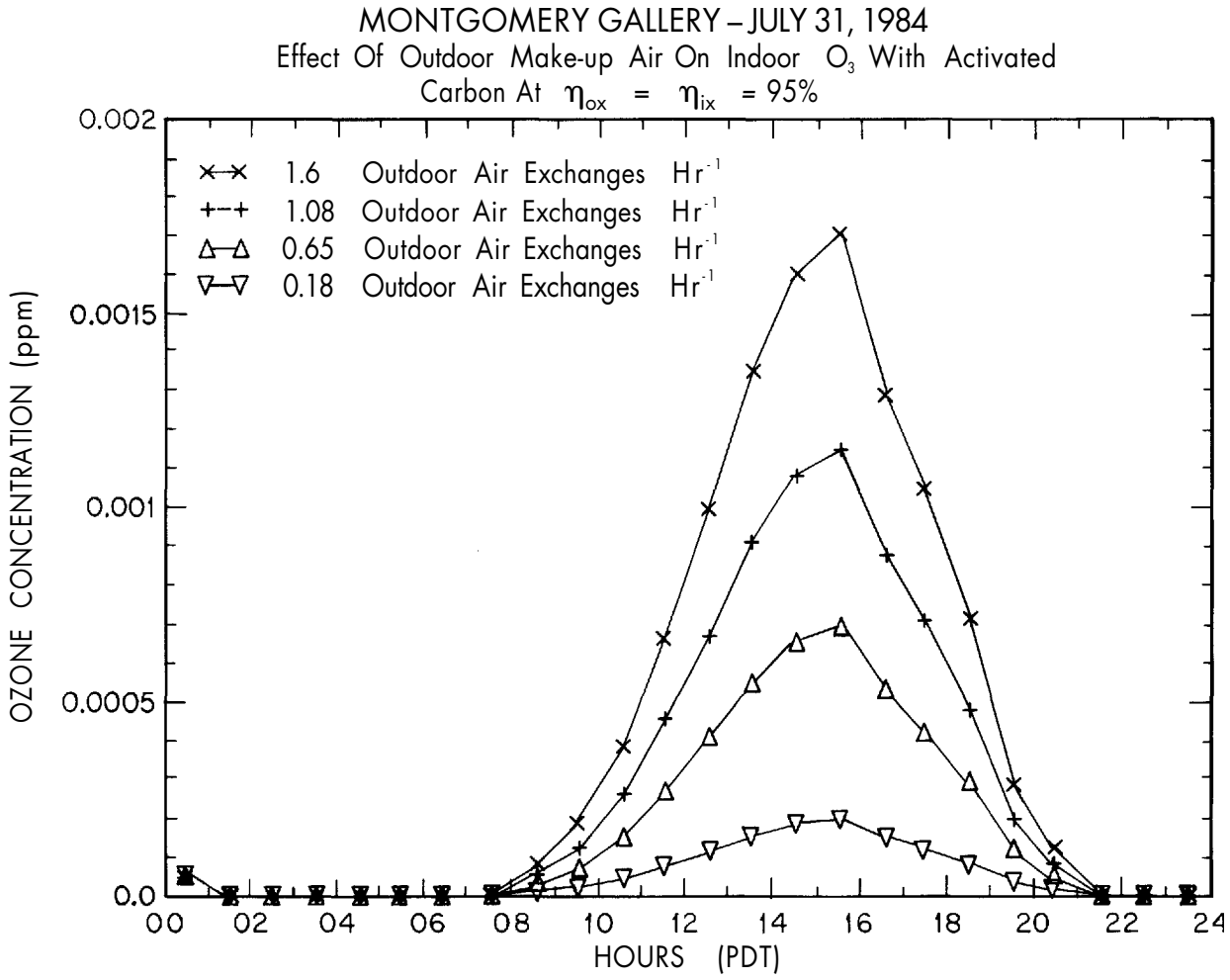

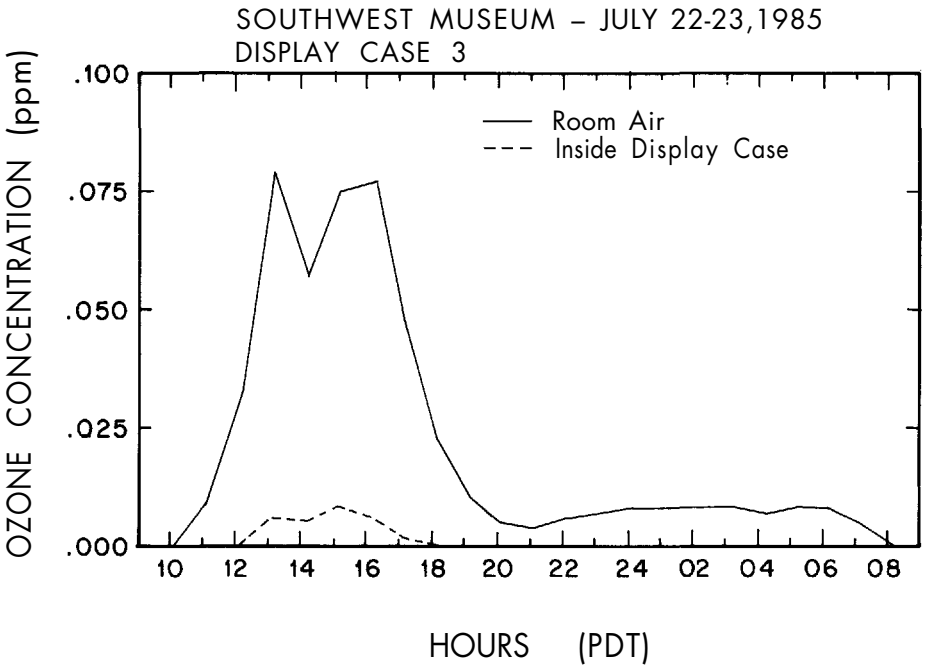

Figure 5.6. Ozone concentrations measured inside Southwest Museum display case 3 and in the surrounding room air, September 22, 1985.

The Effect of Display Cases

In situations where modifications to a museum's ventilation system are not practical, it may be possible to protect ozone-sensitive objects directly through the use of display cases. A display case can be viewed as another means for reducing the effective air exchange rate in the immediate vicinity of the object while allowing an extended time for ozone depletion by reaction with nearby interior surfaces.

Unusually high indoor ozone levels have been noted inside portions of the Southwest Museum, located in Los Angeles, California (see Chapter 4, Table 4.3). Therefore, that museum was chosen as the site for testing the effect of display cases as a barrier between works of art and indoor air.

A procedure for determining the air exchange rate between the room and a loosely fitted display case was developed, based on injection of SF_6 (an inert tracer gas measurable in ultra-low concentrations) into the display case. These display cases selected for study, varying in size and construction, are described in Table 5.3. Approximately 1 cm^3 SF_6 was injected into each display case, and then air samples were withdrawn from the case periodically over a 110 to 140 minute period using plastic syringes. These syringes were capped and later analyzed for the SF_6 concentration in the air sampled by electron capture gas chromatography (Drivas 1974). It was found that the characteristic time for air exchange between display case 3 of Table 5.3 and the surrounding room was 80.4 minutes. Analysis of similar data for display case 2 of Table 5.3

shows a characteristic time for air exchange of 23.1 minutes. In short, these display cases are not tightly sealed.

Accompanying these experiments, ozone concentration measurements were made inside each display case and in the open room air surrounding each case using a matched pair of ultraviolet photometric ozone monitors (Dasibi, models 1003-AH and 1003-PC). Ozone measurements made inside display case 3 and in the surrounding room air on September 22, 1985 are shown in Figure 5.6. While peak one-hour average indoor ozone concentrations reached 0.079 ppm inside the Southwest Museum that day, corresponding ozone levels inside the display case never exceeded 0.008 ppm, lower by a factor often. Display case 2 with its more rapid air-exchange rate showed a peak ozone concentration of 0.009 ppm inside the case on a day with peak ozone concentrations of 0.065 ppm in the surrounding room air, or 14% of the room air ozone concentration found inside the display case.

Table 5.3. Characteristics of three display cases tested for ozone removal at the Southwest Museum.

Display Case	Interior Volume (m^3)	Interior Surface Area (m^2)	Surface Area of Air Gaps (m^2)	Comments
Display case 1	1.36	13.76	0.04	Painted drywall sides; painted wood inserts; track lighting on top of case. The front of the case has sliding glass doors, with an air gap between the doors.
Display case 2	4.75	19.09	0.06	Painted drywall sides; plastic lighting diffuser above; painted wood floor. The front of the case has three sliding glass doors with an air gap between the doors.
Display case 3	5.75	35.17	0.02	Painted drywall sides; painted wood ceiling with lights; painted wood floor and inserts. The front of the case is glass with a very small air gap running along the top edge of the glass front of the case.

It is clear that display cases can be used to greatly reduce the ozone levels in the immediate vicinity of sensitive objects as long as the characteristic time for air exchange between the room and the inside of the display case is sufficiently long.

The Effect of Framing

In the case of watercolors and paintings, the possibility exists to protect works of art from ozone damage by framing under glass. In order to test the protection afforded to an ozone-sensitive material by typical museum framing, a chamber exposure experiment was conducted in the laboratory.

Alizarin crimson pigment is known to be one of the most ozone fugitive colorants typically used by artists (see Drisko et al. 1985/86). Two samples of alizarin crimson (Winsor and Newton n.d.) in methanol suspension were airbrushed onto Arches hot-pressed watercolor paper. Both samples were created at the same depth of shade, about 40% reflectance at the wavelength of maximum absorption. One sample was hinged to 4-ply acid-free mat board and mounted in a window mat (5 cm x 5 cm window). The matted sample was then enclosed in a standard wood frame (15.2 cm x 20.3 cm) with glass glazing, according to recommended practice (Clapp 1978:71-80). The framed and unframed samples then were exposed in the same chamber to 0.40 ppm O_3 at 50% RH, 22 °C in the dark for 7 days according to the procedure described in Chapter 2. The diffuse reflectance spectra of these samples was measured before and after the ozone exposure using a Diano MatchScan II spectrophotometer. Color differences, ΔE, were calculated for CIE Illuminant C using the CIE 1976 L*a*b* formula.

As a result of that ozone exposure, the unframed sample experienced severe fading after 1 week ($\Delta E = 12.3$), while the framed sample was essentially unchanged after exposure ($\Delta E = 0.3$). It is concluded that conventional archival framing can act to provide effective protection of vulnerable materials from ozone exposure (at least in the short term).

Selection of Ozone-Resistant Pigments

Scientific research into the lightfastness of artists' pigments has resulted in permanence ratings that are widely available to the artist, both in standard reference works and in the literature furnished by the suppliers of artists' colors (Levinson 1976, Windsor and Newton n.d.). In a similar fashion, protection against ozone-induced fading can be ensured for works of art that are yet to be created by selection of pigments that resist oxidation by ozone.

A large number of modern inorganic and organic artists' watercolors (Shaver et al. 1983, Drisko et al. 1985/86) and traditional organic pigments (Whitmore et al. 1987, Whitmore and Cass 1988) have been tested for fading in the presence of atmospheric ozone. These experi-

ments involved exposure to 0.3 to 0.4 ppm O_3 in the dark for three months at circa 22 °C and 50% RH. That exposure (ozone concentration times duration) is roughly equivalent to a 6 to 8 year period inside a museum in the Los Angeles area that has conventional air conditioning but no pollutant removal system. Of the inorganic pigments tested, only the arsenic sulfides (e.g., orpiment) showed any definite color change due to ozone exposure (when judged by human observer Munsell color matches). Most of the traditional natural organic colorants tested show measurable fading when exposed to ozone. However, many of the modern synthetic organic colorants examined are relatively stable toward ozone exposure. Watercolors in the Winsor and Newton line composed of quinacridone (PV 19), BON arylamide red (PR 10), chlorinated para red (PR 4, not lightfast), arylamide yellow (PY 1), and chlorinated copper phthalocyanine (PG 7) showed essentially no change in color before and after ozone exposure when judged by human observer Munsell color matches (Drisko et al. 1985/86). While most organic colorants can be expected to react with ozone at some rate, modern synthetics can be found that react so slowly that their use should be considered as an alternative to the ozone-fugitive traditional organic colorants, like the alizarin lakes.

The Effect of Binders and Coatings

Binders and coatings were examined that might be used to protect ozone-sensitive pigments from oxidation by ozone or its reaction products. Binders studied included linseed oil, egg tempera, casein, beeswax, dammar, alkyd enamel, acrylic polymer emulsions, and solvent-based acrylics, shellac, and Ethulose (a consolidant). It was found that most of the binders and coatings studied provided considerable protection from ozone-induced fading in systems containing alizarin crimson as an example of an ozone-fugitive pigment. Important exceptions to this observation were noted, however. Alizarin crimson prepared as a paint in several acrylic binders faded severely as did alizarin crimson dry pigment samples coated with some acrylic polymer emulsions. A change in the physical properties of dammar varnish was noted upon ozone exposure. For selection of binder and coating systems that will protect ozone-sensitive pigments from fading, the interested reader should refer to the tables in Wittman et al. (1989) or in the complete project final report (Cass et al. 1988).

Notes

1. Baer and Banks 1985; Belvin 1973; Campbell et al. 1974; Haylock and Rush 1976; Jaffe 1967; Katai et al. 1966; Kerr et al. 1969; Lebensaft and Salvin 1972; Newton 1945; Rowe and Chamberlain 1937; Salvin 1969; Salvin and Walker 1955; Salvin et al. 1952.

2. American National Standards Institute 1985; Baer and Banks 1985; Banks 1980; Committee on Preservation of Historical Records 1986; Lafontaine 1978, 1979; National Bureau of Standards 1983; Thomson 1978.

Appendix

Mathematical Modeling of Chemically Reactive Pollutants in Indoor Air

Introduction

The existence of a fading hazard to works of art posed by photochemical oxidants depends in part on whether the high ozone and NO_2 concentrations found in outdoor urban air are transferred to the indoor atmospheres of museums. In this appendix, a computer-based mathematical model for predicting the indoor concentrations of photochemically related air pollutants is developed and tested. The model is designed for subsequent use as a tool for diagnosing the causes of the high indoor pollutant levels that are found in certain buildings. The model also may be used by architects and engineers to test the likely performance of air-handling and purification systems of buildings in advance of their construction.

Considerable progress has been made recently in developing mathematical models for predicting pollutant concentrations in outdoor ambient air. In modeling urban air basins, state-of-the-art approaches utilize a spatially resolved grid with explicit treatment of advective transport, photochemical reactions, deposition to the earth's surface, and pollutant emissions (McRae et al. 1982a, McRae and Seinfeld 1983). Regional models, used in the study of acid deposition, incorporate many of the above features plus transformation processes involving pollutant reaction within aqueous droplets (Ruff et al. 1985).

By comparison, most approaches to modeling pollutant concentrations in indoor air have been relatively primitive, treating pollutant species as chemically independent and assuming the building interior to constitute a single, well-mixed volume (e.g., see Shair and Heitner 1974, Traynor et al. 1982a, Yamanaka 1984, Fisk 1984). Extended developments have included multichamber formulations (Hernandez and Ring 1982, Özkaynak et al. 1982), a model for predicting radon progeny concentrations that incorporated a description of natural convection (Schiller 1984), and explicit treatment of the kinetics of the primary photolytic cycle (Özkaynak et al. 1982). To date, however, there has not been an indoor air pollution model with the capability of explicitly treating an arbitrary chemical kinetic mechanism.

Despite the moderate success of the models cited above, there are many reasons that argue for the development of a model for indoor air pollution that explicitly incorporates reactive chemistry. Data on indoor pollutant concentrations suggest that chemical reactions may

proceed at rates comparable to, or even much greater than, the ventilation rate (for example, $NO + O_3$ and $NO_2 + O_3$). A major element of the mass-balance models cited above—the "reactivity (Traynor et al. 1982a) or "indoor sinks" (Shair and Heitner 1974)—is not well understood, and there are discrepancies between the wall-loss rates determined in chamber studies and field experiments (Sabersky et al. 1973, Shair 1981). Some secondary pollutants produced, for example, in photochemical smog may not be well determined by the simple mass-balance approach. And finally, it is becoming increasingly apparent that many indoor environments are as complex in their constitution—if not more so—than polluted outdoor environments (e.g., see Berglund et al. 1984). It is reasonable to expect, given the wide range of pollutants that may be emitted directly indoors, the introduction of pollutants from outdoor air via the ventilation system, and the wide range of indoor lighting levels (and hence varied photolytic reaction rates), that there are numerous circumstances in which a chemically explicit model is needed to accurately predict concentrations of indoor pollutants.

In this appendix, a general mathematical model is formulated that describes the time dependence of indoor air pollutants in a chemically reacting system. An important contribution of this formulation over previous work is its explicit treatment of gas-phase photolytic and thermal reactions. The model is also formulated to compute for each species the production rates associated with ventilation, chemical reaction, and direct emission, and to compute the removal rates associated with ventilation, chemical reaction, filtration, and wall loss. As a partial validation of the model, a case is simulated in which outdoor air, containing photochemically reactive air pollutants, is introduced into a museum gallery. The simulated indoor concentrations of ozone, nitric oxide and NO_x-NO are compared with measured data during a two-day period in November 1984. Several interesting perturbations from this base case are considered in studying the likely effects of pollutant sources and altered building materials on indoor air chemistry.

Model Formulation

Two fundamental postulates form the basis of the model:

1. The building can be represented as a set of chambers, with the air flow rate from each chamber to all others known as a function of time. Each chamber is visualized as a room or group of rooms. The core of each chamber is considered to be well mixed and separated from the building surfaces by a thin concentration boundary layer. The details of the boundary layer affect the rate of pollutant removal

at fixed surfaces, but may otherwise be neglected in determining pollutant concentrations.

2. Within each chamber, the rate of change of the concentration of each chemical species may be described by an equation of the form

$$\frac{dC}{dt} = S - LC \tag{A.1}$$

where *S* represents the sum of all sources: direct emission, advective transport from other chambers (including the mechanical ventilation system and outdoors), and production by chemical reaction; L represents the sum of all sinks: loss by homogeneous chemical reaction, transformation and removal processes occurring on surfaces, and removal by transport from the chamber. *S* and *L* are, in general, functions of time and of the concentrations of all pollutant species in all chambers.

Table A.1. Kinetic Mechanism

	Reaction[d]	Rate Constant (ppm min K units)
1	$NO_2 + h\nu \rightarrow NO + O(^3P)$	a
2	$O(^3P) + O_2 + M \rightarrow O_3 + M$	$0.346\ T^{-2}\ \exp(510/T)$
3	$O_3 + NO \rightarrow NO_2 + O_2$	$9.245 \times 10^5\ T^{-1}\ \exp(-1450/T)$
4	$NO_2 + O(^3P) \rightarrow NO + O_2$	$3.99 \times 10^6\ T^{-1}$
5	$NO + O(^3P) \rightarrow NO_2$	$1.67 \times 10^5\ T^{-1}\ \exp(584/T)$
6	$NO_2 + O(^3P) \rightarrow NO_3$	$8.81 \times 10^5\ T^{-1}$
7	$O_3 + NO_2 \rightarrow NO_3 + O_2$	$5.19 \times 10^4\ T^{-1}\ \exp(-2450/T)$
8	$NO_3 + NO \rightarrow 2\ NO_2$	$8.81 \times 10^6\ T^{-1}$
9	$NO + OH \rightarrow HNO_2$	$5.07 \times 10^6\ T^{-1}$
10	$HNO_2 + hn \rightarrow NO + OH$	a
11	$HO_2 + NO_2 \rightarrow HNO_2 + O_2$	$17.3\ T^{-1}\ \exp(1006/T)$
12	$HNO_2 + OH \rightarrow H_2O + NO_2$	$2.91 \times 10^6\ T^{-1}$
13	$NO_2 + HO_2 \rightarrow HNO_4$	$1.73 \times 10^4\ T^{-1}\ \exp(1006/T)$
14	$HNO_4 \rightarrow HO_2 + NO_2$	$1.80 \times 10^{15}\ \exp(-9950/T)$
15	$HO_2 + NO \rightarrow NO_2 + OH$	$3.58 \times 10^6\ T^{-1}$
16	$RO_2 + NO \rightarrow NO_2 + RO$	$3.58 \times 10^6\ T^{-1}$
17	$RCO_3 + NO\ (+O_2) \rightarrow NO_2 + RO_2 + CO_2$	$1.13 \times 10^6\ T^{-1}$
18	$NO_2 + OH \rightarrow HNO_3$	$4.401 \times 10^{17}\ T^{-1}\ (280/T)^{1/2}\ 10^{-(11.6T/(17.4+T))}$
19	$CO + OH\ (+ O_2) \rightarrow HO_2 + CO_2$	$1.31 \times 10^5\ T^{-1}$
20	$O_3 + h\nu \rightarrow O(^3P) + O_2$	a
21	$HCHO + h\nu\ (+ 2\ O_2) \rightarrow 2\ HO_2 + CO$	a
22	$HCHO + h\nu \rightarrow H_2 + CO$	a
23	$HCHO + OH\ (+O_2) \rightarrow HO_2 + H_2O + CO$	13890
24	$RCHO + h\nu \rightarrow HO_2 + RO_2 + CO$	a
25	$RCHO + OH\ (+ O_2) \rightarrow RCO_3 + H_2O$	25680

Table A.1. (Cont.)

	Reaction[d]	Rate Constant (ppm min K units)
26	$C_2H_4 + OH \rightarrow RO_2$	11660
27	$C_2H_4 + O(^3P) \rightarrow HO_2 + RO_2$	1219
28	$OLE + OH \rightarrow RO_2$	89142
29	$OLE + O(^3P) \rightarrow RO_2 + RCO_3$	22118
30	$OLE + O_3 \rightarrow 0.5\ RCHO + 0.5\ HCHO + 0.3\ HO_2 + 0.31\ RO_2 + 0.14\ OH + 0.03\ RO$	0.136
31	$ALK + OH \rightarrow RO_2$	4700
32	$ALK + O(^3P) \rightarrow RO_2 + OH$	99.8
33	$ARO + OH \rightarrow RO_2 + RCHO$	16112
34	$RO \rightarrow HO_2 + 0.5\ HCHO + RCHO$	2.0×10^5
35	$RONO + h\nu \rightarrow RO + NO$	a
36	$RO + NO \rightarrow RONO$	$4.38 \times 10^6\ T^{-1}$
37	$RO + NO_2 \rightarrow RNO_3$	$2.19 \times 10^6\ T^{-1}$
38	$RO + NO_2 \rightarrow RCHO + HNO_2$	$1.91 \times 10^5\ T^{-1}$
39	$NO_2 + RO_2 \rightarrow RNO_4$	$1.64 \times 10^6\ T^{-1}$
40	b	
41	$RNO_4 \rightarrow NO_2 + RO_2$	$1.80 \times 10^{15}\ exp(-9950/T)$
42	$RCO_3 + NO_2 \rightarrow PAN$	$6.17 \times 10^5\ T^{-1}$
43	$PAN \rightarrow RCO_3 + NO_2$	$4.77 \times 10^{16}\ exp(-12516/T)$
44	$NO_2 + NO_3 \rightarrow N_2O_5$	$7.48 \times 10^5\ T^{-1}$
45	$N_2O_5 \rightarrow NO_2 + NO_3$	$4.07 \times 10^{16}\ exp(-11080/T)$
46	$H_2O + N_2O_5 \rightarrow 2\ HNO_3$	$5.66 \times 10^{-4}\ T^{-1}$
47	$O_3 + OH \rightarrow HO_2 + O_2$	$6.62 \times 10^5\ T^{-1}\ exp(-1000/T)$
48	$O_3 + HO_2 \rightarrow OH + 2\ O_2$	$4.85 \times 10^3\ T^{-1}\ exp(-580/T)$
49	$NO_3 + h\nu \rightarrow NO + O_2$	a
50	$HO_2 + HO_2 \rightarrow H_2O_2 + O_2$	$3.4 \times 10^4\ T^{-1}\ exp(1100/T) + 5.8 \times 10^{-5}\ T^{-2}\ exp(5800/T)\ [H_2O]$ [c]
51	$H_2O_2 + h\nu \rightarrow 2\ OH$	a
52	$RO_2 + RO_2 \rightarrow 2\ RO + O_2$	$2.04 \times 10^4\ T^{-1}\ exp(223/T)$
53	$NO_3 + HCHO\ (+ O_2) \rightarrow HNO_3 + HO_2 + CO$	0.86
54	$NO_3 + RCHO\ (+ O_2) \rightarrow HNO_3 + RCO_3$	3.6
55	$NO_3 + h\nu \rightarrow NO_2 + O(^3P)$	a
56	$NO_3 + OLE \rightarrow RPN$[d]	$3288\ T^{-1}$
57	$NO_2 + NO_3 \rightarrow NO_2 + NO + O_2$	$175\ T^{-1}$

a. Rate depends on photon flux; see Table A.2.

b. Reaction in earlier mechanisms that was subsequently eliminated.

c. $[H_2O]$ is water vapor concentration in ppm.

d. In the chemical mechanism, groups of similar organic compounds are lumped together, weighted according to their reactivity. The symbols for these lumped organics are as follows: ALK stands for alkanes; ARO stands for aromatics; OLE stands for olefins; R stands for any organic functional group (i.e., RCHO indicates aldehydes that are more complex than formaldehyde); RPN stands for nitroxyperoxyalkyl nitrates and dinitrates.

Figure A.1. Schematic representation of the ventilation components of the multichamber indoor air quality model.

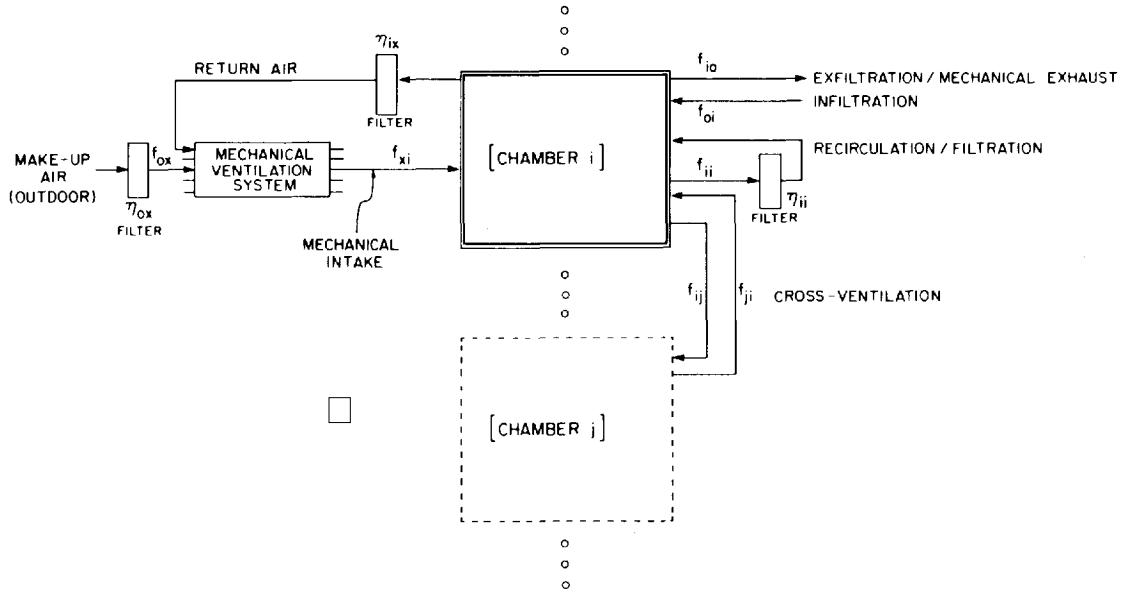

Ventilation

The treatment of ventilation is an extension of the formulation of Shair and Heitner (1974) to incorporate an arbitrary number of chambers. A schematic illustration of the approach is presented in Figure A.1. For each chamber, air may enter directly from outside (infiltration), from the mechanical ventilation system (supply), and from each of the other chambers (cross-ventilation). Air may be removed to the outside (exfiltration or exhaust), to the mechanical ventilation system (return), and to each of the other chambers. The mechanical ventilation system is treated as a special chamber having zero volume. In addition to the return air from each chamber, air from outdoors (make-up) may be supplied directly to the mechanical ventilation system. Pollutant removal devices ("filters") may be specified for each return-air line and for the make-up air line. Also, within each chamber, air may be recirculated through a filter. For each pollutant species, the filtration efficiency may be specified by the user.

Mathematically, if we consider a chemically inert compound, the effects of the ventilation system may be represented as follows:

$$\frac{dC_i}{dt} = \sum_{j=0}^{n} \left[\frac{f_{ji}C_j - f_{ij}C_i}{V_i} \right] + \left[\frac{f_{xi}C_x - f_{ix}C_i}{V_i} \right] - \frac{\eta_{ii} f_{ii} C_i}{V_i} \quad \text{(A.2)}$$

and

$$C_x = \frac{\sum_{j=0}^{n} (1 - \eta_{jx}) f_{jx} C_j}{\sum_{j=0}^{n} f_{xj}} \quad \text{(A.3)}$$

where C_i = the concentration of the compound in chamber i, V_i = the volume of chamber i, f_{ij} = the volume flow rate from chamber i to chamber j, η_{ij} = the efficiency of removal of the compound by the filter located in the air stream connecting chamber i to chamber j, and subscripts x and 0 refer, respectively, to the mechanical ventilation system and to outdoor air. Equation A.2 can readily be converted into the form of Equation A.1.

Ventilation data for a specific building can be obtained in several ways. Tracer gas experiments may be used to determine flow rates between pairs of chambers (Sinden 1978). Under the uniform-mixing assumption, flow rate measurements in ventilation system ducts may be used to provide the necessary data. In buildings without mechanical ventilation systems, such as many residences, simple models may be used to predict infiltration (Sherman 1980).

Table A.2. Coefficients used to determine photolysis rates (Baulch et al. 1982, McRae 1982).

	Reaction	$h_{uv}(10^{-20}cm^2)$	$h_{vis}(10^{-20}cm^2)$
1	$NO_2 + h\nu \rightarrow NO + O(^3P)$	39.4	0.95
10	$HNO_2 + h\nu \rightarrow NO + OH$	8.1	0
20	$O_3 + h\nu \rightarrow O(^3P) + O_2$	0.16	0.21
21	$HCHO + h\nu \ (+ 2\ O_2) \rightarrow 2\ HO_2 + CO$	0.58	0
22	$HCHO + h\nu \rightarrow H_2 + CO$	0.43	0
24	$RCHO + h\nu \ (+ 2\ O_2) \rightarrow HO_2 + RO_2 + CO$	0.56	0
35	$RONO + h\nu \rightarrow RO + NO$	8.7	0.21
49	$NO_3 + h\nu \rightarrow NO + O_2$	0	11.5
51	$H_2O_2 + h\nu \rightarrow 2\ OH$	0.13	0
55	$NO_3 + h\nu \rightarrow NO_2 + O(^3P)$	0	99.1

Chemical Kinetics

The model can be adapted to incorporate any of the kinetic mechanisms commonly employed in outdoor photochemical air quality models and can be modified to explicitly treat special problems occurring from the indoor emission of unusual chemical substances. For the examples illustrated in the present appendix, a modified version of the Falls and Seinfeld chemical mechanism is employed (McRae et al. 1982a, McRae and Seinfeld 1983, Hecht and Seinfeld 1972, Hecht et al. 1974, Falls and Seinfeld 1978, Russell et al. 1985). More than 50 simultaneous chemical reactions are considered. Because the current form of the mechanism is not available in a single reference, it is presented in Table A.1 of this appendix.

Photolysis Rates

A number of important atmospheric chemical reactions are photolytic in nature. Rates of such reactions depend on the spherically integrated photon flux and are commonly expressed as

$$k_p = \int_0^\infty \sigma\,[\lambda]\ \varphi\,[\lambda]\ I\,[\lambda,t]\ d\lambda \tag{A.4}$$

where $\sigma[\lambda]$ is the absorption cross-section of the molecule (cm^2), ($\varphi[\lambda]$ is the quantum yield, $I\,[\lambda,t]$ is the photon flux density (photons $cm^{-3}\ s^{-1}$), and λ is the wavelength of light (cm).

The most accurate calculation of photolysis rates within a given building requires data on the spectral, spatial, and temporal distribution of the ambient lighting, and the model is capable of handling information provided at that level of detail. However, in many cases lighting levels indoors are so much lower than those outdoors that many otherwise important photolytic reactions proceed at small or even negligible rates. For such cases an approximate approach is provided.

In the approximate case, light is treated as having two components, ultraviolet (300-400 nm) and visible (400-760 nm). Within each component, the spectral distribution is assumed to be flat. Consequently,

$$k_p = h_{uv} I_{uv} + h_{vis} I_{vis} \tag{A.5}$$

$$h_{uv} = (100\ \text{nm})^{-1} \int_{300\text{nm}}^{400\text{nm}} \sigma\varphi\, d\lambda \tag{A.6}$$

$$h_{vis} = (360\ \text{nm})^{-1} \int_{400\text{nm}}^{760\text{nm}} \sigma\varphi\, d\lambda \tag{A.7}$$

In Equation A.5, I_{uv}, and I_{vis} represent the spherically integrated (spatially averaged) photon flux (photons $cm^{-2}\ s^{-1}$) in the ultraviolet and visible bands, respectively. The constants, h_{uv} and h_{vis}, are determined from published data (Baulch et al. 1982, McRae 1982) and are presented in Table A.2.

In the model, the ultraviolet and visible fluxes are each assumed to have two components, one due to artificial lighting, the other due to sunlight entering through windows or skylights. For the former, hourly values of the photon flux are specified in each band. For the latter, hourly values of ultraviolet and visible attenuation factors are specified. These factors are then applied to the outdoor photon fluxes determined using a solar simulator (McRae 1982).

For calculations of outdoor radical concentrations, outdoor photolysis rates are required. Here, the approach of McRae (1982) is followed without modification.

Data on indoor light levels sufficient to exercise the model for a specific building may be obtained with a radiometer and ultraviolet light meter (Hall 1967:151-157, Thompson 1967) as described elsewhere in this paper. Ultraviolet photon flux also may be inferred by measuring the photolysis rate of NO_2 (Jackson et al. 1975).

Treatment of Highly Reactive Species

In the indoor model calculations, the pseudo-steady-state approximation (PSSA; Seinfeld 1986) is applied for O, OH, and RO. The PSSA is also employed to determine the outdoor concentrations of these three species and HNO_4, HO_2, NO_3, N_2O_5, RCO_3, RNO_4, and RO_2 as has been done in simulating outdoor air pollution (McRae et al. 1982b).

Heterogeneous Reactions

In addition to photolytic and thermal reactions occurring in the gas phase, important processes may occur on fixed surfaces such as the floor, walls, and ceiling, and on or within airborne particles. Considerable evidence demonstrates that such processes have substantial impact on both outdoor (e.g., see Russell et al. 1985) and indoor (e.g., see Shair and Heitner 1974) pollutant concentrations.

In previous indoor air pollution models, these processes have been lumped into a first-order decomposition rate, k_s, often assumed to take place entirely on fixed surfaces. An alternative, but nearly equivalent, formulation is in terms of deposition velocity, v_g, which is defined as the ratio of the pollutant flux to a surface to the free-stream concentration. The rate of change of pollutant concentration due to this process alone is then given by

$$\frac{dC}{dt} = -k_s C = -v_g \left(\frac{A}{V}\right) C \qquad \text{(A.8)}$$

where A / V represents the superficial surface-to-volume ratio of the room.

This approach is far from ideal. Processes such as the catalytic conversion of one pollutant species to another and adsorption followed a substantial time later by desorption are not accommodated by this

approach. Yet recent evidence suggests that NO_2 may be converted to NO on walls (Yamanaka 1984) and that, in the presence of NO_2, nitrous acid is formed at substantial rates by heterogeneous reaction (Pitts et al. 1985b, Besemer and Nieboer 1985). At present too little is known to incorporate an explicit description of important surface reactions other than unimolecular decomposition and irreversible adsorption.

Measurements of heterogeneous reaction rate or deposition velocity have been reported for several species, as summarized in Table A.3.

The loss rate depends, in general, on not only the combined reactivity of the compound and the surface, but also on the degree of air movement. Since direct evidence on surface-loss rates of some highly reactive species in the model do not exist (e.g., for HNO_3), it is appropriate that evidence pertaining to the transport-limited deposition velocity be considered.

Although seldom realized in rooms, the case of perfectly still air represents the lower boundary on the transport-limited deposition velocity. Here, the deposition velocity is of the order of 10^{-3} cm s^{-1}, determined by the molecular diffusion coefficient divided by a characteristic dimension of the room.

Table A.3 Measurements of indoor deposition velocity.

Species	Deposition Velocity (cm s^{-1})	Notes
O_3	0.036 ± 0.021	24 measurements in 13 buildings; one excluded due to suspected NO source (Shair and Heitner 1974).
	0.02-0.07	Inferred from measurements of ozone loss rate in a single residence (Sabersky et al. 1973).
	0.001-0.11 (New) 0.0005-0.015 (Aged)	For various materials exposed in a chamber study (Sabersky et al. 1973).
	0.027[a] (Aluminum) 0.015 (Stainless Steel) 0.036 (Office) 0.061 (Bedroom)	Inferred from measurements of ozone loss rate in experimental chambers and rooms (Mueller et al. 1973).
	0.001-0.20	For various typical indoor materials exposed in a test room (Sutton et al. 1976).
NO	-0.0001 ± 0.001	Decay rate, in a house, of emissions from gas-fired range; assumed A/V = 2 m^{-1} (Traynor et al. 1982b).
	0.0008	Decay rate, in a house, of emissions from gas-fired range; assumed A/V = 2 m^{-1} (Wade et al. 1975).
	0.0017 ± 0.0014	Analysis of data from gas-stove emissions experiment using simplified kinetic model; assumed A/V = 2 m^{-1} (Özkaynak et al. 1982).
	0.0000-0.003	For various indoor surface materials, measured in test chamber, 20-26 °C, 40-60% RH (Miyazaki 1984).
NO_2	0.018 ± 0.009	Concentration decay rate from gas-stove emission experiment in test room; 11 runs; includes homogeneous reactions; assumed A/V = 2 m^{-1} (Traynor et al. 1982a).
	0.011	Decay rate, in a house, of emissions from gas-fired range; assumed A/V = 2 m-1 (Wade et al. 1975).
	0.006 (50% RH) 0.011 (60% RH) 0.017 (70% RH)	Analysis of decay rates from emissions due to gas- and kerosene-fired unvented heaters; attempt to exclude homogeneous reactions (Yamanaka 1984).
	0.0003-0.12	For various indoor surface materials, measured in test chamber, 20-26 °C, 40-60% RH (Miyazaki 1984).
HCHO	0.005 ± 0.003	Analysis of concentration decay rate from gas-stove emission experiment in test room; 5 runs; includes homogeneous reactions; assumed A/V = 2 m^{-1} (Traynor et al. 1982a).

a. Data show strong positive correlation with relative humidity, varying from 0.0007 cm/s at 5% RH to 0.028 cm/s at 87% RH.

For rooms in which the air is not still, the analogy between heat and mass transfer can be used to obtain estimates of the transport-limited deposition velocity. Gadgil (1980) developed a model to predict the rate of heat transfer from room walls due to natural convection. In simulating a 3 x 3 x 3 m enclosure with one wall maintained at 4.5 °C higher than the other surfaces, he found an average Nusselt number of 145 for the hot wall. For a compound with a diffusion coefficient of 0.2 $cm^2\ s^{-1}$, the transport-limited deposition velocity to this wall would be 0.1 $cm\ s^{-1}$. This compares well to the deposition velocity of 0.13 $cm^2\ s^{-1}$, obtained by applying the Von Karman integral momentum balance to a 3-meter long, vertically oriented plate heated to 4.5 °C above the free-stream air (Eckert and Drake 1972:528). Wilson (1968) measured the relaxation time for air temperature in a suddenly cooled room. His results suggest a transport-limited deposition velocity of 0.07 $cm\ s^{-1}$ for natural convection and 0.18 $cm\ s^{-1}$ for stirred air, again assuming a diffusion coefficient of 0.2 $cm^2\ s^{-1}$.

Somewhat higher values are indicated by experimental studies of the behavior of unattached decay products of radon in rooms. The deposition velocity for these species, which are believed to be removed at surfaces at the transport-limited rate, have been found to be 0.06-0.6 $cm\ s^{-1}$, with the consensus value of 0.2 $cm\ s^{-1}$ (Knutson 1988). The diffusion coefficient of these species is approximately 0.05 $cm^2\ s^{-1}$, smaller than that for gaseous pollutants with lower molecular weights.

The results from Wilson and from the theoretical heat-transfer studies suggest that for circumstances in which room air is not highly stirred, the average transport-limited deposition velocity is within 50% of 0.07 $cm\ s^{-1}$. Further research is needed to resolve the discrepancy with studies of radon decay-product removal at surfaces.

Outdoor Concentrations

With the current chemical mechanism, the model requires as input the hourly averaged outdoor concentration of 15 species or groups of species. These data may be obtained by direct outdoor measurement or from a photochemical air quality model that describes the chemical evolution of the outdoor air over time (McRae et al. 1982a, Russell et al. 1985). For the application reported in this paper, an approach was used which combines outdoor monitoring data with inferences based on detailed experimental and modeling studies.

Initial Conditions

The initial indoor pollutant concentrations are treated in the same way as the outdoor concentrations: concentrations of 15 species are specified and the remaining 10 are computed assuming that steady-state conditions prevail. For most buildings, simulation results are relatively insensitive to changes in the initial conditions: the limiting characteristic

time associated with a perturbed initial condition is given by the inverse air-exchange rate which in many cases is less than 1 hour.

Direct Emissions

The model accepts as input the direct indoor emission of any species other than O, OH, and RO. As currently formulated, hourly averaged values are specified, and linear-interpolation is used to obtain the emission rate at any instant during the simulation. This rate is added directly to the source term *S* in Equation A.1.

Numerical Solution Technique

The procedure used for solving the system of coupled differential equations that constitutes the model is known as the asymptotic integration method (Young and Boris 1977). The implementation used in the present model was slightly modified from that established by McRae et al. (1982b). The program is written in Vax-11 Fortran and is run on a Vax-11 /750. A 24-hour simulation of a single chamber with an average integration time step of 10 seconds requires approximately 8 minutes of CPU time.

Model Application: Virginia Steele Scott Gallery

Introduction

Control of indoor pollutants is sought not only to prevent adverse health effects but also to limit the rate of materials damage. Some of the most stringent standards for indoor air quality are specified for museums, archives, and rare book libraries. Since these collections must be preserved indefinitely, even very slow rates of deterioration could lead to unacceptable accumulated damage. Recommended objectives for indoor SO_2, NO_x, and O_3 concentrations in such facilities are a few parts per billion (Baer and Banks 1985). Strong acids (e.g., HCl), organic acids (e.g., acetic acid), and formaldehyde are to be controlled to the lowest possible levels (Mathey et al. 1983).

Analytical tools are needed both to predict the levels of chemically complex mixtures that will occur in new buildings prior to their construction and to diagnose the source of pollutants present in existing facilities. Surface loss of pollutants is particularly important in museums as it indicates the dose delivered to the collection. In the present chapter, simulations are conducted of pollutant levels in a newly constructed museum, based on data taken for this purpose at the Virginia Steele Scott Gallery on the Huntington Library grounds in San Marino, California. First, the model is exercised to verify that it correctly represents indoor pollutant levels in this building as it was constructed. Next, the effect of a series of hypothetical perturbations on that building's design are analyzed. These cases illustrate circumstances in which

homogeneous chemistry in indoor air assumes added significance in determining the concentrations of photochemically reactive pollutants.

Description of the Site

Figure A.2 shows a floor plan of the west gallery at the Scott building and the ventilation flow rates, taken from the architectural plans and engineering specifications. The conditioned volume of the west gallery is 2530 m^3 and the superficial surface area is 3060 m^2. In the gallery areas, rooms 101 and 102, which constitute 86% of the conditioned volume, the floors are oak plank, and the walls are painted plaster and plywood. The ceiling consists of plaster-veneer coffered beams and plastic diffusers. Above room 101 are skylights; fluorescent lamps behind the diffusers provide background lighting to room 102. The lighting in both rooms is supplemented by track lamps. Floor coverings in the other rooms are granite or ceramic tile, or linoleum-type flooring. Walls and ceilings are, for the most part, gypsum dry-wall.

The ventilation system is designed to maintain a temperature of 70 ± 1 °F and a relative humidity of 50 ± 3% in the galleries. The only pollutant removal devices in the ventilation system at the time of our tests were strainer mat-type filters (U.L. Class 2, Farr 30/30), designed to remove coarse particulate matter. When the internal recirculation fan is on, the total air-flow rate through the mechanical ventilation system is 345 $m^3\ min^{-1}$. The outdoor make-up air-flow rate assumes two values: 85 $m^3\ min^{-1}$ during the day and 14 $m^3\ min^{-1}$ at night. The daytime setting was maintained from approximately 7 a.m. to 6 p.m. during the study period. In each room, supply and return registers are located on the ceiling raising the possibility of ventilation "short-circuiting," which would lead to a smaller effective ventilation exchange rate (0.3–2.0 h^{-1}) and the absence of rapid fluctuations in monitored pollutant concentrations, combined with the relatively large recirculation rate (8 h^{-1}), suggests that convection was sufficient to effect rapid mixing during the daytime. On the other hand, the indoor data show fluctuations in pollutant concentrations at night that could be due to incomplete mixing.

Monitoring Experiment

For a ten-day period beginning on October 30, 1984, O_3, NO, and NO_2 concentrations were monitored inside and outside the Scott Gallery. Ozone concentrations were measured with a pair of UV photometric ozone monitors (Dasibi models 1003-AH and 1003-PC). A pair of chemiluminescent NO_x monitors (Thermo Electron Corporation, model 14B/E) was used to measure NO and NO_2. NO_2 values measured by this method include contributions from other nitrogen-containing species such as HNO_3 and PAN (Winer et al. 1974). The symbol NO_{2*} will be used to signify measurement data for this group of species, determined as NO_x-NO by the monitors. The NO_x monitors were calibrated daily

against zero air and a known supply of 0.4 ppm NO in nitrogen. Data from all instruments were continuously registered on strip-chart recorders. Pollutant concentration values averaged over 12-minute intervals throughout the experiment were extracted from the strip-chart records.

On two days during the monitoring period, November 4—5, peak outdoor O_3 concentrations exceeded 120 ppb in the presence of NO_x levels in excess of 200 ppb. Because of the relatively high pollution levels, model validation efforts were focused on these days.

Input Data for the Validation

Because of the large recirculation rate and the large fractional volume in room 101, the Scott Gallery was initially modeled as a single chamber. Ventilation rates were those indicated in the architectural specifications. Filter efficiency was assumed to be zero for all gaseous species.

Ultraviolet and visible photon fluxes were computed from data taken both in room 101 and outdoors with a radiometer equipped with a UV cutoff filter (Eppley model PSP; filter GG 395) and a spot meter (UVC meter) designed to measure the ratio of radiance in the ultraviolet to the total illuminance (Grosjean et al. 1988a, Grosjean et al. 1988b). From these measurements the skylights were estimated to transfer a photon flux equal to 0.7% of the visible light and 0.15% of the ultraviolet falling on the roof of the building outdoors. Artificial lighting was estimated to contribute flux densities of 0.7×10^{15} and 2.3×10^{13} photons cm^{-2} s^{-1} in the visible and ultraviolet, respectively, between 9 a.m. and 6 p.m.

For the "base case" simulation, deposition velocities reported in the literature for NO, NO_2, O_3, and HCNO have been used (see Table A.4). Higher aldehydes were assumed to have the same surface removal characteristics as formaldehyde. Removal of highly reactive species (H_2O_2, PAN, HNO_2, RNO_2, RNO_4, HNO_3, N_2O_5, NO_3, HO_2, RO_2, HNO_4, and RCO_3) was taken to proceed at a transport-limited rate, based principally on Wilson's experiments. Other species (e.g., CO) are assumed to be sufficiently inert that their removal rates at building surfaces are negligible.

Data on outdoor concentrations of the 15 pollutants required by the model were specified by the following approach.

The outdoor monitoring data on O_3, NO, and NO_2* collected on-site were used. Based on the results of monitoring studies (Hanst et al. 1982, Tuazon et al. 1981) outdoor HNO_3 and PAN concentrations in ppb were estimated as 10% and 5%, respectively, of the outdoor ozone concentration in ppb. The concentrations of HNO_3 and PAN were subtracted from the measured NO_x-NO concentration to correct for interfer-

ence in determining the NO_2 values used in the validation study (Winer et al. 1974).

The outdoor data taken at the Scott Gallery were compared with NO, NO_x-NO, and O_3 measurements reported for the same time interval by the South Coast Air Quality Management District's (SCAQMD) monitoring station in Pasadena, located within 1.5 km of the Scott Gallery. Good agreement between these two data sets was found. Having established the close correspondence between these two monitoring sites, data for CO from the Pasadena station of the SCAQMD were used.

Figure A.2. Floor plan of the west wing of the Virginia Steele Scott Gallery, San Marino, California. Daytime/(nighttime) ventilation flow rates are given in units of m^3 min^{-1}. Air sampling locations for the validation experiment are indicated by "x."

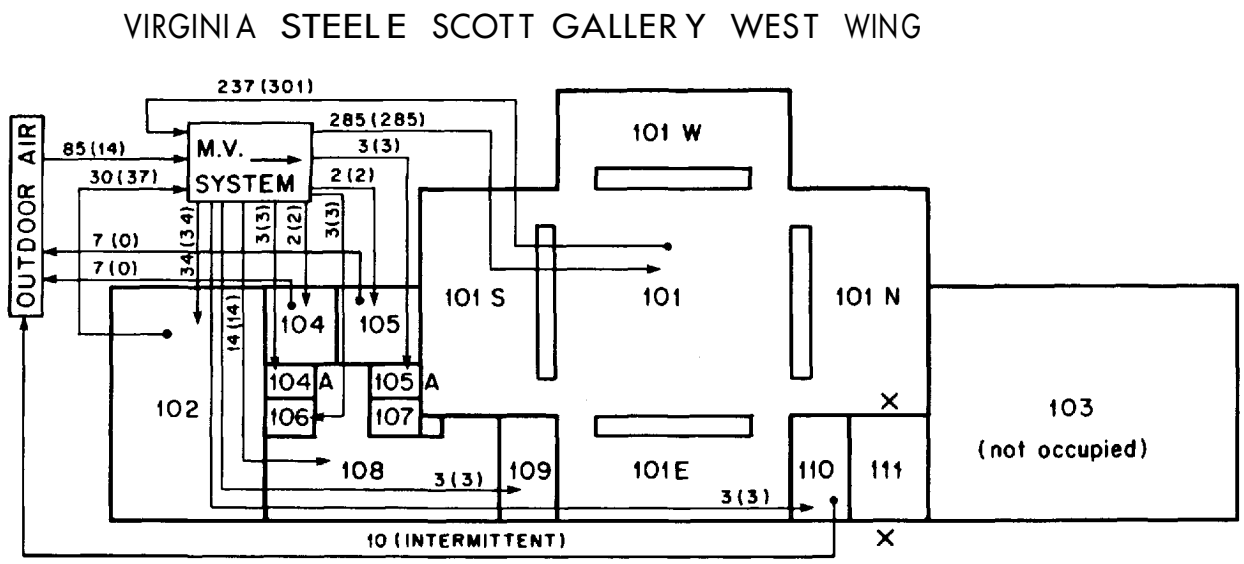

Hourly data on total hydrocarbons are measured by the SCAQMD at Azusa, California. These total hydrocarbon data were subdivided into formaldehyde, higher aldehydes, olefins, alkanes, aromatics, and ethylene using the splitting factors determined by Russell and Cass (1986) on the basis of detailed analysis of the composition of morning air in Los Angeles reported by Grosjean and Fung (1984).

Input data for concentrations of the remaining species in outdoor air (H_2O_2, HNO_2, and RNO_2) were determined from general experience in modeling ambient air pollution in the Los Angeles basin (Russell 1985). The hydrogen peroxide concentration was assumed to be 5% of the outdoor ozone concentration. Nitrous acid concentration was assumed to peak at 1.5 ppb during the hour after sunrise, falling to zero linearly over an hour on either side of the peak. The outdoor concentration of RNO_2 was assumed to be zero.

The initial indoor concentrations of NO, NO_2, and O_3 were specified based on values measured inside the Scott Gallery. For all other species, the initial concentration was computed by bringing the model to its steady-state value based on the initial outdoor concentration, the air-exchange rate, the wall loss rate, and assuming no homogeneous chemical reaction. Since there are no known direct emissions of pollutants within the Scott Gallery, indoor pollutant source strengths were set to zero for the base case model calculations.

Perturbations of the Model Parameters

Six simulations in addition to the base case were run to examine the response of the model to changes in some of the input parameters (see Table A.4). Three of these cases were run to examine the sensitivity of the results to assumptions about the input data. In particular, the "low NO_2 wall loss" case was run because indoor and outdoor monitoring data showed that the average total NO_x levels inside the Scott Gallery were very close to those outside. The case with "no explicit chemistry" was run to compare the predictions of previous model formulations with the present work. The "multichamber" case addresses the magnitude of errors resulting from assuming that this building may be represented as a single well-mixed chamber.

The three remaining cases were selected to examine how changes in building design or operation could influence indoor pollutant concentrations through chemical reaction. The case with an "indoor hydrocarbon source" could represent a situation in which fumes from an underground parking garage enter the building, or a case in which solvents are used within the building. The "indoor oxides of nitrogen source" considers the effect of operating combustion appliances. The "glass-walled building" case considers the effects of increased photolytic reaction rates and reduced wall loss rates associated with glass.

Results

A comparison of measured and simulated ozone concentrations is presented in Figure A.3. Model results are shown for both the base-case and the no-chemistry case. The full kinetic model is slightly better in predicting indoor ozone concentrations, particularly during the morning hours when the presence of a significant nitric oxide concentration constitutes a substantial sink for ozone by reaction 3. As indicated in Table A.5, the heterogeneous wall loss rate is the dominant factor in accounting for the difference between indoor and outdoor ozone concentrations within this particular building. Chemical reaction is, however, a significant net sink.

Table A.4. Simulation input parameters.

Base Case

Deposition Velocity (cm s^{-1}):

O_3	0.036
NO_2	0.006
HCHO,RCHO	0.005
PAN	0.035
HNO_2, HNO_3, HNO_4, HO_2, H_2O_2, NO_3, N_2O_5, RCO_3, RNO_4, RONO, RO_2	0.07
NO, ALK, ARO, CO, C_2H_4, OLE	0.0

All other input parameters discussed in text.

Low NO_2 Wall Loss (WL)

Same as base case except deposition velocity for NO_2 changed to 0.0.

No Explicit Chemistry (No Chem)

Same as base case except rates of all reactions in kinetic mechanism set to 0.0.

Multichamber Case

Same as base case except building treated as four chambers:

Chamber 1	Rooms 101, 101E, 101W, 101N, 101S
Chamber 2	Room 102
Chamber 3	Rooms 104, 104A, 105, 105A, 106, 107, 108, 109
Chamber 4	Rooms 110, 111

Mechanical ventilation rates determined from architectural specifications (see Fig. A.2). Cross-ventilation flow rates taken as minimum necessary to balance air flows. Artificial lighting assumed same for each chamber. Day light only in chamber 1.

Indoor Hydrocarbon Source (HC Source)

Same as base case with added continuous indoor emission of hydrocarbons at following rates (ppb min^{-1}):

Alkanes	46.7
Aromatics	9.6
Olefins	9.6

This corresponds approximately to evaporation of 10 cm^3 h^{-1} of gasoline (McRae 1982) and is taken as a model either of the use of a naptha-based solvent as may occur in a preservation lab, or of the presence of an underground garage.

Indoor Oxides of Nitrogen Source (NO_x Source)

Same as base case with added emission of combustion-generated pollutants during the hours 0700-1 300 at following rates (ppb min^{-1}):

Nitrogen dioxide	2.5
Nitric oxide	2.5
Carbon monoxide	64.4
Formaldehyde	0.6

Simulates the emissions due to gas-fired cooking equipment such as might be present in a cafeteria. Emissions data from Traynor et al. (1982a). Assumes 10 range-top burners and 5 ovens (residential size) in continuous use during 6-hour cooking period. Range hoods assumed to reduce emissions into the main volume to 40% of the total (Revzan 1984).

Glass-Walled Building (Glass-Walled)

Changes from base case: (1) all deposition velocities reduced to 5% of base case values (based on chamber measurements of deposition rates on glass surfaces (Sabersky et al. 1973, Miyazaki 1984); (2) indoor photolysis rates computed assuming that indoor photon flux in visible range is 50% of that outdoors and that ultraviolet light is further attenuated according to the transmissivity data for window glass given in Summer (1962).

Figure A.3. Comparison of modeled and measured ozone concentrations for a two-day period.

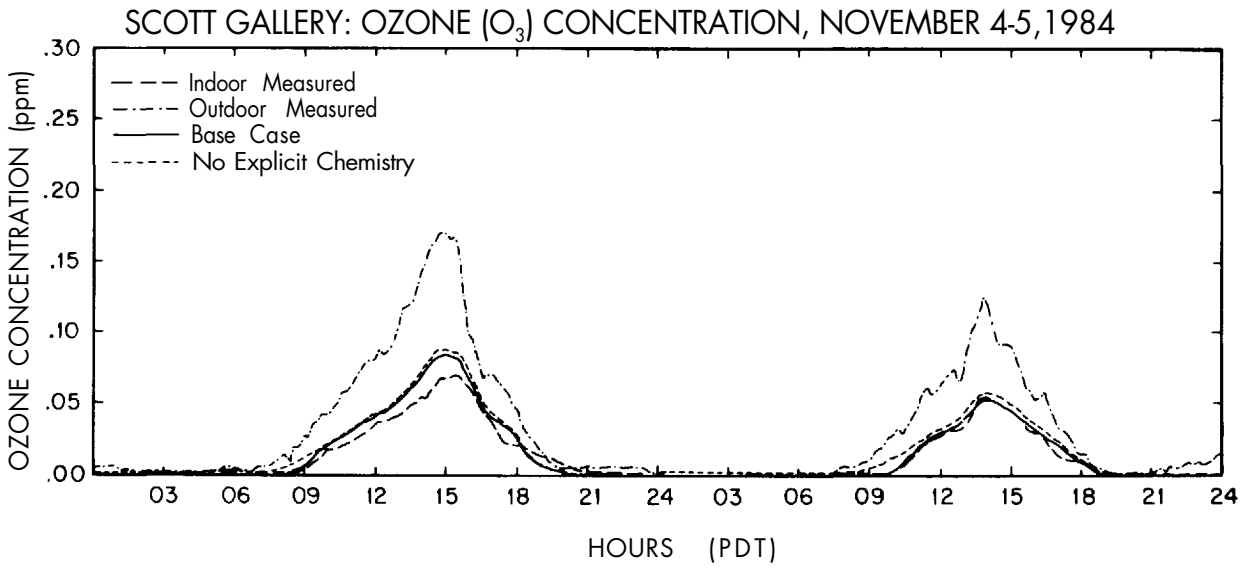

Comparisons between measurements and simulations for oxides of nitrogen are presented in Figure A.4. At most times the measured NO_x and NO_2* concentrations are seen to lie between the results for the base case and "low NO_2 wall loss" simulations. The nitric oxide concentration, on the other hand, is underpredicted at most times by both simulations, supporting Yamanaka's (1984) inference that NO_2 is converted to NO at indoor surfaces. The "low NO_2 wall loss" case predicts a total NO_x concentration that is closer to the measured value (5% high) than is the result for the base case simulation (14% low).

Tables A.5 and A.6 summarize the simulation results, giving average source and sink rates and average concentrations, respectively. Figure A.5 presents average concentrations for selected species. Several of the findings are noteworthy.

Comparing the average concentrations for the base case and no-chemistry simulations, we see that several nitrogen-containing species—HNO_2, HNO_3, HNO_4, NO_3 and N_2O_5—are produced at substantial net rates by chemical reaction indoors. For the latter two species, indoor concentrations exceed those outdoors. In a conventionally lit building, formation of these species may occur indoors during the day by reaction pathways normally associated with nighttime chemistry outdoors (Russell et al. 1985). N_2O_5 recently has been implicated in the production of mutagenic compounds in outdoor air (Pitts et al. 1985a); the possibility that N_2O_5 is present at elevated levels indoors should be further studied.

Figure A.4. Comparison of modeled and measured concentrations of (a) nitric oxide, (b) nitrogen dioxide (NO_2*, measured as NO_x-NO), and (c) total oxides of nitrogen for a two-day period. In the case of nitric oxide, the "base case" and "low (NO_2) wall loss" simulations produce essentially equivalent results.

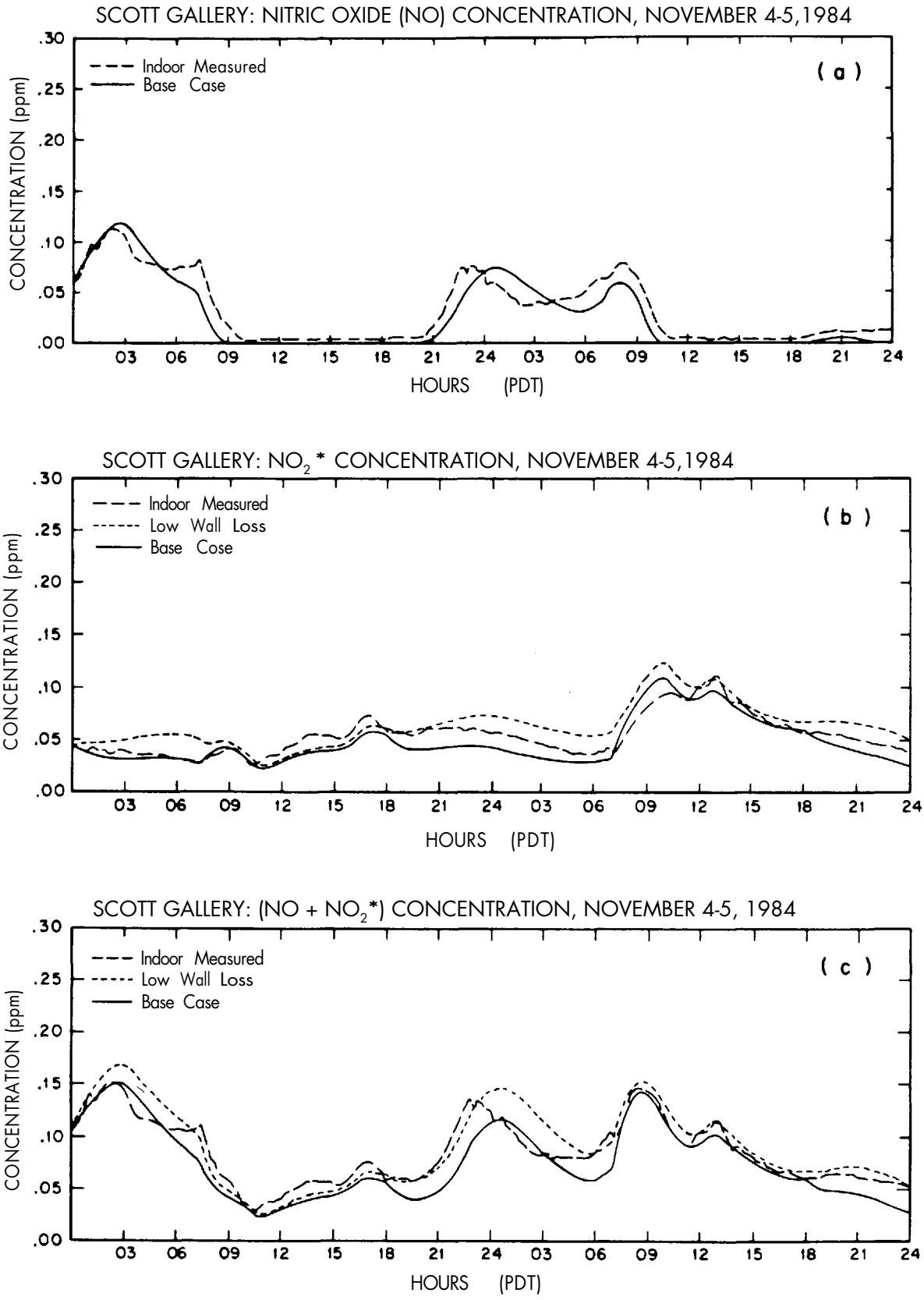

Pitts et al. (1985b) experimentally demonstrated the production of nitrous acid in an indoor environment with elevated levels of NO_2 and inferred from their data a steady-state average ratio of HNO_2 to NO_2 of 15×10^{-3}. The base-case indoor simulation also indicates that HNO_2 is formed indoors, but the HNO_2 to NO_2 ratio due to homogeneous gas-phase chemistry alone is lower, 0.4×10^{-3}. This discrepancy supports the hypothesis that heterogeneous reactions (e.g., on building surfaces) may play an important role in nitrous acid production.

Information on the flux of reactive species to interior surfaces may be useful in assessing the potential for damage to materials displayed in museums. Under the assumptions of the base case simulation, the average fluxes of O_3 and HNO_3 to the walls during this 2-day period were 38.4 and 8.8 $\mu g\ m^{-2}\ h^{-1}$, respectively.

The results of the multichamber simulation indicate that the treatment of this building as a single chamber is a reasonable approximation. Concentration variations among chambers are approximately 10% or less, due to the relatively high rate of recirculation through the mechanical ventilation system.

The two cases for which an indoor pollutant source is postulated show that such sources may either increase or decrease the concentration of species not directly emitted. For example, the hydrocarbon source leads to substantial reduction in the indoor concentration of O_3 and NO, but markedly increased concentrations of HNO_2, HNO_4, HCHO, and H_2O_2, among others. The indoor combustion source likewise leads to a consumption of O_3, but increased production of HNO_2 and HNO_3.

In the case of the glass-walled building, indoor concentrations of several key species—including O_3, HNO_2, HNO_3, PAN, and H_2O_2—are increased markedly over the base-case values, and in fact are seen to exceed the outdoor levels. In this case, homogeneous chemical reactions are greatly enhanced by the combined effects of increased lighting, leading to higher photolysis rates and reduced wall loss, leading to higher concentrations of reactive species.

Table A.5. Source and sink rates (ppb h^{-1}) in Scott Gallery for selected species and simulations: average for November 4 and 5, 1984.

Simulation:		Base Case		HC Source		NO_x Source		Glass-Walled Bldg.	
Species	Process	Source	Sink	Source	Sink	Source	Sink	Source	Sink
NO	Ventilation	17.6	15.0	17.6	8.6	17.6	36.2	17.6	16.6
	Chemical Rxn	1.6	5.7	1.4	11.8	3.4	24.1	129	131
	Emission	0		0		38		0	
	Wall Loss		0		0		0		0
NO_2	Ventilation	69	58	69	54	69	99	69	67
	Chemical Rxn	172	172	666	666	154	136	418	418
	Emission	0		0		38		0	
	Wall Loss		12		13		19		1
O_3	Ventilation	58	29	58	20	58	21	58	65
	Chemical Rxn	2	8	1	25	3	23	131	123
	Emission	0		0		0		0	
	Wall Loss		23		15		17		3
HNO_2	Ventilation	0.029	0.025	0.029	0.064	0.029	0.046	0.029	0.134
	Chemical Rxn	0.051	0.0001	0.161	0.0004	0.104	0.0003	0.175	0.049
	Emission	0		0		0		0	
	Wall Loss		0.055		0.125		0.086		0.019
HNO_3	Ventilation	5.8	2.6	5.8	2.4	5.8	2.7	5.8	7.4
	Chemical Rxn	0.8	0	0.4	0	1.1	0	2.4	0
	Emission	0		0		0		0	
	Wall Loss		4.1		3.8		4.3		0.8
NO_3	Ventilation	0.007	0.008	0.007	0.004	0.007	0.005	0.007	0.007
	Chemical Rxn	29.6	29.6	12.8	12.8	24.7	24.7	43.1	43.1
	Emission	0		0		0		0	
	Wall Loss		0.013		0.007		0.009		0.001
N_2O_5	Ventilation	0.4	0.5	0.4	0.2	0.4	0.4	0.4	0.5
	Chemical Rxn	29.1	28.1	12.2	12.1	23.8	23.1	38.8	38.6
	Emission	0		0		0		0	
	Wall Loss		0.8		0.4		0.7		0.1
PAN	Ventilation	2.9	1.6	2.9	1.7	2.9	1.6	2.9	3.4
	Chemical Rxn	0.8	0.8	0.9	0.8	0.8	0.8	2.6	1.9
	Emission	0		0		0		0	
	Wall Loss		1.3		1.3		1.3		0.1
HCHO	Ventilation	14.3	13.1	14.3	23.9	14.3	21.2	14.3	18.1
	Chemical Rxn	1.0	0.03	13.7	0.06	1.1	0.1	4.3	0.5
	Emission	0		0		8.9		0	
	Wall Loss		2.2		4.0		3.1		0.2
RCHO	Ventilation	12.8	12.0	12.8	25.6	12.8	12.7	12.8	20.6
	Chemical Rxn	1.3	0.05	17.5	0.1	2.0	0.1	8.8	0.9
	Emission	0		0		0		0	
	Wall Loss		2.0		4.5		2.1		0.2
H_2O_2	Ventilation	2.9	1.2	2.9	2.0	2.9	1.1	2.9	2.9
	Chemical Rxn	0.1	0.0001	2.2	0.0002	0.1	0.0001	0.2	0.003
	Emission	0		0		0		0	
	Wall Loss		1.9		3.1		1.8		0.2

Figure A.5. Average measured and modeled pollutant concentrations for the Scott Gallery, November 4-5, 1984.

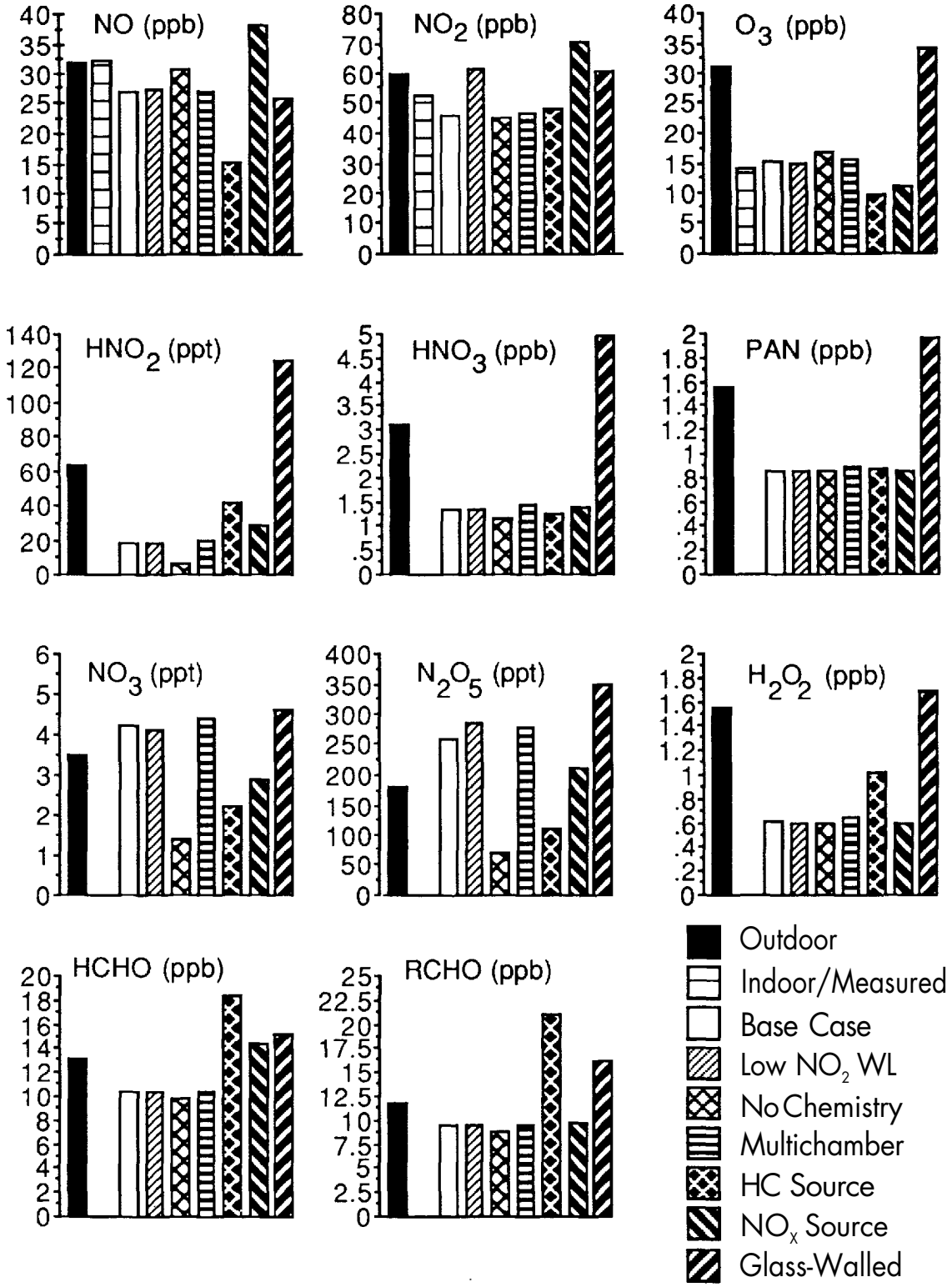

Table A.6. Species concentrations (ppb) in Scott Gallery: Average for November 4 and 5, 1984.

Spec.	Outdoor	Indoor	Indoor Simulations						
	Meas/Sim.[a]	Measured	Base Case	Low NO_2 WL	No Chem	Multichamber[b]	HC Source	NO_x Source	Glass-Walled
NO	31.8	32.3	27.2	27.5	30.7	27.2	15.2	38.1	26.0
NO_2	59.8[c]	52.4[c]	45.9	61.6	45.0	46.5	48.5	70.4	61.0
O_3	31.2	14.0	15.1	14.9	16.8	15.5	9.8	11.1	34.1
HNO_2	0.063		0.018	0.018	0.007	0.019	0.041	0.028	0.124
HNO_3	3.12		1.35	1.36	1.17	1.43	1.25	1.39	4.96
HNO_4	0.343		0.176	0.181	0.133	0.184	0.646	0.135	0.304
NO_3	0.0035		0.0042	0.0041	0.0014	0.0044	0.0022	0.0029	0.0046
N_2O_5	0.181		0.258	0.285	0.072	0.277	0.110	0.211	0.350
PAN	1.56		0.86	0.86	0.85	0.89	0.87	0.85	1.96
RNO_4	0.87		0.44	0.44	0.34	0.47	2.21	0.34	0.78
RONO	0.0		0.00007	0.00006	0.0	0.00007	0.00205	0.00043	0.00107
HCHO	13.2		10.3	10.3	9.8	10.4	18.3	14.5	15.1
RCHO	11.7		9.5	9.5	8.8	9.6	21.0	9.8	16.3
HO_2	0.0151		0.0079	0.0072	0.0060	0.0082	0.0400	0.0049	0.0123
H_2O_2	1.56		0.61	0.60	0.59	0.64	1.02	0.59	1.69
O	1.31 E-06		6.21 E-09	6.92 E-09	0.0	6.24 E-09	5.10E-09	12.0 E-09	4.62 E-07
OH	2.80 E-03		0.22 E-05	0.21 E-05	0.0	0.23 E-05	0.22 E-05	0.40 E-05	2.41 E-05
RCO_3	0.00042		0.00017	0.00015	0.00016	0.00018	0.00030	0.00011	0.00043
RO	6.03 E-07		0.37 E-07	0.35 E-07	0.0	0.38 E-07	4.62 E-07	1.08 E-07	5.10 E-07
RO_2	0.0146		0.0071	0.0063	0.0058	0.0074	0.0584	0.0044	0.0104

a. Outdoor average concentrations for species not listed: ALK - 241 ppb, ARO - 63 ppb, C - 3.04 ppm, C_2H_4 - 22 ppb, OLE - 15 ppb.

b. Volume-weighted average for four chambers.

c. Quantitative interference from HNO_3 and PAN assumed and subtracted from measured NO_x-NO. For indoor value, results from base-case simulation used.

Discussion

The results of this study identify those cases where homogeneous chemistry is important as a pollutant transformation process in indoor atmospheres. Concentrations of many species (e.g., O_3) are significantly perturbed by chemical reaction, especially when outdoor air pollutants are combined with direct indoor emissions. For other species (e.g., N_2O_5) an accounting of the effect of homogeneous chemical reactions is essential because the rates of chemical production in indoor air dominate other source terms.

The results of the present work—the reasonable agreement between measured and simulated pollutant concentrations, and the minor effect of treating the Scott Gallery as a four-chamber rather than a one-chamber building—indicate that the assumption that each chamber in the model is well mixed did not interfere with obtaining accurate results. Additional work to relax the uniform mixing hypothesis is warranted. Efforts to determine the rates of mixing in indoor air and to examine the effect of poor mixing on the apparent rates of chemical reaction are recommended. One approach to relaxing the uniform-mixing assumption is to use the atmospheric diffusion equation (Seinfeld 1986) in place of Equation A.1 to describe the time-rate-of-change of pollutant concentrations. To solve the problem using this approach, one requires information on localized indoor air velocities and eddy diffusivities. The basis for describing indoor air motion is partially established in numerical codes for natural convection in enclosures (Gadgil 1980). A model that employs an explicit description of air motion at scales smaller than the dimension of the rooms would be considerably more difficult to validate and costly to apply than the present approach. Nevertheless, it could prove quite useful in examining the validity of the uniformly mixed model and in treating the mass-transport aspects of surface reaction on a more fundamental basis.

The present model is also restricted in the scope of the transformation processes considered. The explicit description is limited to gaseous pollutants and gas-phase chemistry. The approach taken to account for pollutant interactions at fixed surfaces is a simplified one and possible interactions of gaseous pollutants with suspended particulate matter are not considered at all. The results reported here indicate that a dominant route for removal of highly reactive pollutants is deposition on walls (see Table A.5). Also, as discussed above, there are indications that nitrogen-containing species may be chemically transformed rather than simply removed at surfaces. Further research is needed to improve the understanding of these heterogeneous processes. Such work should include carefully designed experiments that account for both mass transport and surface-reaction kinetics.

The model as presently formulated has a number of important applications in addition to those discussed in this appendix. It may be used to assess the effects of filtration of selected compounds, to design indoor air quality control strategies based on ventilation scheduling, and to simulate specialized cases where unusual chemicals are present. The model is formulated to be a general tool for studying chemically reactive air pollution systems. Within limits, one can specify an arbitrary chemical mechanism, modify the computer code in a straightforward manner, and simulate an indoor environment in which homogeneous chemical reactions play an important role in determining pollutant concentrations.

References

American National Standards Institute
1985 American National Standard Practice for Storage of Paper-Based Library and Archival Documents—Draft 4. New York.

American Society of Heating, Refrigerating and Air Conditioning Engineers
1985 *ASHRAE Handbook-1985 Fundamentals*. Atlanta.

American Society for Testing and Materials
1980 Standard Method of Specifying Color by the Munsell System, Designation D 1535-80. Philadelphia.

Baer, N.S., and P.N. Banks
1985 Indoor Air Pollution: Effects on Cultural and Historic Materials. *The International Journal of Museum Management and Curatorship* 4:9-20.

Banks, P.N.
1980 *Addendum to Planning Report 7: Preliminary Statement on Environmental Standards for Storage of Books and Manuscripts.* Chicago: The Newberry Library.

Baulch, D.L., R.A. Cox, P.J. Crutzen, R.F. Hampson, Jr., J.A. Kerr, J. Troe, and R.T. Watson
1982 Evaluated Kinetic and Photochemical Data for Atmospheric Chemistry: Supplement I. *Journal of Physical Chemistry, Reference Data* 11:327-496.

Beloin, N.J.
1973 Fading of Dyed Fabrics Exposed to Air Pollutants. *Textile Chemist and Colourist* 5:128-133.

Berglund, B., T. Lindvall, and J. Sundell, eds.
1984 *Indoor Air*. 5 vols. Stockholm: Swedish Council for Building Research.

Besemer, A.C., and H. Nieboer
1985 The Wall as a Source of Hydroxyl Radicals in Smog Chambers. *Atmospheric Environment* 19:507—513.

Billmeyer, F.W., Jr. and M. Saltzman
1981 *Principles of Color Technology.* 2nd ed. New York: John Wiley & Sons.

Brommelle, N.S.
1964 The Russell and Abney Report on the Action of Light on Watercolors. *Studies in Conservation* 9:140-152.

California Air Resources Board
1986 California Air Quality Data-Summary of 1986 Air Quality Data. Sacramento.

Campbell, G.G., G.G. Schurr, D.E. Slawikowski, and J.W. Spence
1974 Assessing Air Pollution Damage to Coatings. *Journal of Paint Technology* 46:59-71.

Cass, G.R., J.R. Druzik, D. Grosjean, W.W. Nazaroff, P.M. Whitmore, and C.L. Wittman
1988 Protection of Works of Art from Photochemical Smog. *Environmental Quality Laboratory Report* 28. Pasadena: California Institute of Technology.

Cass, G.R., W.W. Nazaroff, C. Tiller, and P.M. Whitmore
n.d. Protection of Works of Art from Atmospheric Ozone. To be submitted for publication.

Clapp, A.F.
1978 *Curatorial Care of Works of Art on Paper.* Oberlin: Intermuseum Conservation Association.

Committee on Medical and Biologic Effects of Environmental Pollutants, National Academy of Sciences
1977 Ozone and Other Photochemical Oxidants. Washington, D.C.

Committee on Preservation of Historical Records, National Research Council
1986 *Preservation of Historical Records.* Washington, D.C.: National Academy Press.

Davidson, C.L, J.F. Osborn, and R.C. Fortmann
1984 Modeling and Measurement of Pollutants Inside Houses in Pittsburg, Pennsylvania. In *Indoor Air: Chemical Characterization and Personal Exposure* 4:69-74. B. Berglund, T. Lindvall, and J. Sundell, eds. Stockholm: Swedish Council for Building Research.

Drisko, K, G.R. Cass, P.M. Whitmore, and J.R. Druzik
1985/86 Fading of Artists' Pigments due to Atmospheric Ozone. In *Wiener Berichte Über Naturwissenschaft in Der Kunst* 2/3. A. Vendl, B. Pichler, and J. Weber, eds. Vienna: Verlag ORAC.

Drivas, P.J.
1974 Investigation of Atmospheric Dispersion Problems by Means of a Tracer Technique. Ph.D. diss., California Institute of Technology.

Druzik, J.R., M.S. Adams, C. Tiller, and G.R. Cass
n.d. The Measurement and Model Predictions of Indoor Ozone Concentrations in Museums. *Atmospheric Environment.* In press.

Eckert, E.R.G., and R.M. Drake, Jr.
1972 *Analysis of Heat and Mass Transfer.* New York: McGraw-Hill.

Falls, A.H., and J.H. Seinfeld
1978 Continued Development of a Kinetic Mechanism for Photochemical Smog. *Environmental Science and Technology* 12:1398-1406.

Fisk, W.J.
1984 Ventilation for Control of Indoor Air Quality. In *Indoor Air: Building Ventilation and Thermal Climate* 5:187-192. B. Berglund, T. Lindvall, and J. Sundell, eds. Stockholm: Swedish Council for Building Research.

Gadgil, A.J.
1980 On Convective Heat Transfer in Building Energy Analysis. Ph.D. diss., University of California, Berkeley.

Grosjean, D., and K. Fung
1984 Hydrocarbons and Carbonyls in Los Angeles Air. *Journal of the Air Pollution Control Association* 34:537-543.

Grosjean, D., P.M. Whitmore, C.P. De Moor, G.R. Cass, and J.R. Druzik
1987 Fading of Alizarin and Related Artists' Pigments by Atmospheric Ozone: Reaction Products and Mechanisms. *Environmental Science and Technology* 21:635-643.

Grosjean, D., P.M. Whitmore, G.R. Cass, and J.R. Druzik
1988a Ozone Fading of Natural Organic Colorants: Mechanisms and Products of the Reaction of Ozone with Indigos. *Environmental Science and Technology* 22:292-298.

Grosjean, D., P.M. Whitmore, C.P. De Moor, G.R. Cass, and J.R. Druzik
1988b Ozone Fading of Organic Colorants: Products and Mechanism of the Reaction of Ozone with Curcumin. *Environmental Science and Technology* 22:1357-1361.

Grosjean, D., P.M. Whitmore, G.R. Cass, and J.R. Druzik
n.d. Ozone Fading of Triphenylmethane Colorants: Reaction Products and Mechanisms. *Environmental Science and Technology.* In press.

Hales, C.H., A.M. Rollenson, and F.H. Shair
1974 Experimental Verification of Linear Combination Model for Relating Indoor-Outdoor Pollutant Concentrations. *Environmental Science and Technology* 8:452-453.

Hall, E.T.
1967 Design of a UV Light Meter. In *London Conference on Museum Climatology.* London: International Institute for Conservation (IIC).

Hanst, P.L., N.W. Wong, and J. Bragin
1982 A Long-Path Infra-Red Study of Los Angeles Smog. *Atmospheric Environment* 16:969-981.

Haylock, J.C., and J.L. Rush
1976 Studies on the Ozone Fading of Anthraquinone Dyes on Nylon Fibers. *Textile Research Journal* 46:1-8.

Hecht, T.A., and J.H. Seinfeld
1972 Development and Validation of a Generalized Mechanism for Photochemical Smog. *Environmental Science and Technology* 6:47-57.

Hecht, T.A., J.H. Seinfeld, and M.C. Dodge.
1974 Further Development of Generalized Kinetic Mechanism for Photochemical Smog. *Environmental Science and Technology* 8:327-339.

Hernandez, T.L., and J.W. Ring
1982 Indoor Radon Source Fluxes: Experimental Tests of a Two-Chamber Model. *Environment International* 8:45-57.

Hibbert, E.
1927 *Journal of the Society of Dyers and Colourists* 43:292-294.

Jackson, J.O., D.H. Stedman, R.G. Smith, L.H. Hecker, and P.O. Warner
1975 Direct NO_2 Photolysis Rate Monitor. *Review of Scientific Instruments* 46:376-378.

Jaffe, L.S.
1967 The Effects of Photochemical Oxidants on Materials. *Journal of the Air Pollution Control Association* 17:375-378.

Katai, A.A., and C. Schuerch
1966 Mechanism of Ozone Attack on α-methyl Glucoside and Cellulosic Materials. *Journal of Polymer Science* 4(A-1):2683-2703.

Kerr, N., M.A. Morris, and S.H. Zeronian
1969 The Effect of Ozone and Laundering on a Vat-Dyed Cotton Fabric. *American Dyestuff Reporter* 58:34-36.

Knutson, E.O.
1988 Modeling Indoor Concentrations of Radon and its Decay Products. In *Radon and Its Decay Products in Indoor Air,* W.W. Nazaroff and A.V. Nero, eds. New York: J. Wiley & Sons.

Lafontaine, R.H.
1978 Recommended Environmental Monitors for Museums, Archives and Art Galleries. *Technical Bulletin* (Canadian Conservation Institute) 3:1-22.

Lafontaine, R.H.
1979 Environmental Norms for Canadian Museums, Art Galleries and Archives. *Technical Bulletin* (Canadian Conservation Institute) 5:1-4.

Lebensaft, W.W., and V.S. Salvin
1972 Ozone Fading of Anthraquinone Dyes on Nylon and Acetate. *Textile Chemist and Colourist* 4:182-186.

Levinson, H.W.
1976 *Artists' Pigments—Lightfastness Tests and Ratings.* Hallandale, Fla.: Colorlab.

Mathey, R.G., T.K. Faison, S. Silberstein, J.E. Woods, W.B. Johnson, W.P. Lull, C.A. Madson, A. Turk, K.L. Westlin, and P.N. Banks
1983 Air Quality Criteria for Storage of Paper-Based Archival Records. *NBSIR* 83-2795. Washington, D.C.: National Bureau of Standards.

McRae, G.J.
1982 Mathematical Modeling of Photochemical Air Pollution. Ph.D. diss., California Institute of Technology.

McRae, G.J., W.R. Goodin, and J.H. Seinfeld
1982a Development of a Second-Generation Mathematical Model for Urban Air Pollution–I: Model Formulation. *Atmospheric Environment* 16:679-696.

McRae, G.J., W.R. Goodin, and J.H. Seinfeld
1982b Numerical Solution of the Atmospheric Diffusion Equation for Chemically Reacting Flows. *Journal of Computational Physics* 45:1-42.

McRae, G.J., and J.H. Seinfeld
1983 Development of a Second-Generation Mathematical Model for Urban Air Pollution–II: Evaluation of Model Performance. *Atmospheric Environment* 17:501-522.

Miyazaki, T.
1984 Adsorption Characteristics of NO_x by Several Kinds of Interior Materials. In *Indoor Air: Chemical Characterization and Personal Exposure* 4:103-110. B. Berglund, T. Lindvall, and J. Sundell, eds. Stockholm: Swedish Council for Building Research.

Mueller, F.X., L. Loeb, and W.H. Mapes
1973 Decomposition Rates of Ozone in Living Areas. *Environmental Science and Technology* 7:342-346.

Nazaroff, W.W., and G.R. Cass
1988 Mathematical Modeling of Chemically Reactive Pollutants in Indoor Air. *Environmental Science and Technology* 20:924-934.

Newton, R.G.
1945 Mechanism of Exposure Cracking of Rubber with a Review of the Influence of Ozone. *Journal of Rubber Research* 14:27-39.

Office of Air Quality Planning and Standards, U.S. Environmental Protection Agency
1983 National Air Quality and Emissions Trends Report, 1981, EPA-450/4-83-011. Research Triangle Park, N.C.

Özkaynak, H., P.B. Ryan, G.A. Alien, and W.A. Turner
1982 Indoor Air Quality Modeling: Compartmental Approach with Reactive Chemistry. *Environment International* 8:461-471.

Pitts, Jr., J.N., J.A. Sweetman, B. Zielinska, R. Atkinson, A.M. Winer, and W.P. Harger
1985a Formation of Nitroarenes from the Reaction of Polycyclic Aromatic Hydrocarbons with Dinitrogen Pentoxide. *Environmental Science and Technology* 19:1115-1121.

Pitts, J.N., Jr., T.J. Wallington, H.W. Biermann, and A.M. Winer
1985b Identification and Measurement of Nitrous Acid in an Indoor Environment. *Atmospheric Environment* 19:763-767.

Revzan, K.L.
1984 Effectiveness of Local Ventilation in Removing Simulated Pollution from Point Sources. In *Indoor Air: Building Ventilation and Thermal Climate* 5:65-72. B. Berglund, T. Lindvall, and J. Sundell, eds. Stockholm: Swedish Council for Building Research.

Ruff, R.E., K.C. Nitz, F.L. Ludwig, C.M. Bhumralkar, J.D. Shannon, C.M. Sheih, I.Y. Lee, R. Kumar, and D.J. McNaughton
1985 Evaluation of Three Regional Air Quality Models. *Atmospheric Environment* 19:1103-1115.

Russell, A.G.
1985 Carnegie-Mellon University, personal communication.

Russell, A.G. and G.R. Cass
1986 Verification of a Mathematical Model for Aerosol Nitrate and Nitric Acid Formation and Its Use for Control Measure Evaluation. *Atmospheric Environment* 20:2011-2025.

Russell, A.G., G.J. McRae, and G.R. Cass
1985 The Dynamics of Nitric Acid Production and the Fate of Nitrogen Oxides. *Atmospheric Environment* 19:893-903.

Sabersky, R.H., Sinema, D.A., and Shair, F.H.
1973 Concentrations, Decay Rates and Removal of Ozone and Their Relation to Establishing Clean Indoor Air. *Environmental Science and Technology* 7:347-353.

Salvin, V.S.
1969 Ozone Fading of Dyes. *Textile Chemist and Colourist* 1:245-251.

Salvin, V.S., and R.A. Walker
1955 Service Fading of Disperse Dyestuffs by Chemical Agents Other than the Oxides of Nitrogen. *Textile Research Journal* 25:571-585.

Schiller, G.E.
1984 A Theoretical Convective-Transport Model of Indoor Radon Decay Products. Ph.D. diss., University of California, Berkeley.

Seinfeld, J.H.
1975 *Air Pollution: Physical and Chemical Fundamentals.* New York: McGraw-Hill.

Seinfeld, J.H.
1986 *Atmospheric Chemistry and Physics of Air Pollution.* New York: J. Wiley & Sons.

Shair, F.H.
1981 Relating Indoor Pollutant Concentrations of Ozone and Sulfur Dioxide to Those Outside: Economic Reduction of Indoor Ozone through Selective Filtration of the Make-up Air. *ASHRAE Transactions* 87(1):116-139.

Shair, F.H., and K.L. Heitner
1974 Theoretical Model for Relating Indoor Pollutant Concentrations to Those Outside. *Environmental Science and Technology* 8:444-451.

Shaver, C.L., G.R. Cass, and J.R. Druzik
1983 Ozone and the Deterioration of Works of Art. *Environmental Science and Technology* 17:748-752.

Sherman, M.H.
1980 Air Infiltration in Buildings. Ph.D. diss., University of California, Berkeley.

Sinden, F.W.
1978 Multichamber Theory of Air Infiltration. *Building and Environment* 13:21-28.

Summer, W.
1962 *Ultraviolet and Infra-Red Engineering.* New York: Interscience Publishers.

Button, D.J., KM. Nodolf, and K.K. Makino
1976 Predicting Ozone Concentrations in Residential Structures. *ASHRAE Journal* 18(9):21-26.

Thomson, G.
1967 Calibration and Use of a UV Monitor. In *London Conference on Museum Climatology.* London: International Institute for Conservation (IIC).

Thomson, G.
1978 *The Museum Environment.* London: Butterworths.

Traynor, G.W., D.W. Anthon, and C.D. Hollowell
1982a Technique for Determining Pollutant Emissions from a Gas-Fired Range. *Atmospheric Environment* 16:2979-2987.

Traynor, G.W., M.G. Apte, J.F. Dillworth, C.D. Hollowell, and E.M. Sterling
1982b The Effects of Ventilation on Residential Air Pollution Due to Emissions from a Gas-Fired Range. *Environment International* 8:447-452.

Tuazon, E.C., A.M. Winer, and J.N. Pitts, Jr.
1981 Trace Pollutant Concentrations in a Multiday Smog Episode in the California South Coast Air Basin by Long Path Length Fourier Transform Infrared Spectroscopy. *Environmental Science and Technology* 15:1232-1237.

Wadden, R.A. and P.A. Scheff
1983 *Indoor Air Pollution.* New York: Wiley-Interscience.

Wade, W.A., III, W.A. Cote, and J.E. Yocum
1975 A Study of Indoor Air Quality. *Journal of the Air Pollution Control Association* 25:933-939.

Weber, A.E.
1933 *American Dyestuff Reporter* 22:157-161.

Whitmore, P.M., and G.R. Cass
1988 The Ozone Fading of Traditional Japanese Colorants. *Studies in Conservation* 33:29-40.

Whitmore, P.M., and G.R. Cass
1989 The Fading of Artists' Colorants by Exposure to Atmospheric Nitrogen Dioxide. *Studies in Conservation* 34:85-97.

Whitmore, P.M., G.R. Cass, and J.R. Druzik
1987 Ozone Fading of Traditional Natural Organic Colorants on Paper. *Journal of the American Institute for Conservation* 21:45-58.

Wilson, M.J.G.
1968 Indoor Air Pollution. *Proceedings of the Royal Society of London* A307:215-221.

Winer, A.M., J.W. Peters, J.P. Smith, and J.N. Pitts, Jr.
1974 Response of Commercial Chemiluminescent NO-NO_2 Analyzers to Other Nitrogen-Containing Compounds. *Environmental Science and Technology* 8:1118-1121.

Winsor and Newton
n.d. Notes on the Composition and Permanence of Artists' Colours. Middlesex, England: Winsor and Newton.

Wittman, C.L., P.M. Whitmore, and G.R. Cass
n.d. The Ozone Fading of Artists' Pigments: An Evaluation of the Effect of Binders and Coatings. Submitted to the *Journal of the American Institute for Conservation.*

Yamanaka, S.
1984 Decay Rates of Nitrogen Dioxide in a Typical Japanese Living Room. *Environmental Science and Technology* 18:566-570.

Yocom, J.E.
1982 Indoor-Outdoor Air Quality Relationships: A Critical Review. *Journal of the Air Pollution Control Association* 32:500-520.

Young, T.R., and J.P. Boris
1977 A Numerical Technique for Solving Stiff Ordinary Differential Equations Associated with the Chemical Kinetics of Reactive-Flow Problems. *Journal of Physical Chemistry* 81:2424-2427.

The Getty Conservation Institute
4503 Glencoe Avenue
Marina del Rey, California 90292-6537
USA

Telephone: 213 822-2299

ISBN 0-89236-126-3